Strain and bioprocess development for enhanced docosahexaenoic acid production in recombinant *Yarrowia lipolytica*

Dissertation

zur Erlangung des Grades

des Doktors der Ingenieurwissenschaften

der Naturwissenschaftlich-Technischen Fakultät

der Universität des Saarlandes

von

Demian Dietrich

Saarbrücken

2023

Tag des Kolloquiums: 13.10.2023

Dekan: Prof. Dr. Ludger Santen

Berichterstatter 1: Prof. Dr. Christoph Wittmann

Berichterstatter 2: PD Dr. Frank Breinig

Vorsitz: Prof. Dr. Uli Kazmaier

Akad. Mitarbeiter: Dr. Mark Lommel

Publications

Partial results of this work have been published previously. This was authorized by the Institute of Systems Biotechnology, represented by Prof. Dr. Christoph Wittmann.

Peer-reviewed articles:

Dietrich D, Jovanovic S, Cao P, Kohlstedt M, Wittmann C; 2023: Refactoring the genetic architecture of a myxobacterial polyketide gene cluster enables advanced heterologous docosahexaenoic acid production in *Yarrowia lipolytica.* Submitted.

Jovanovic S, **Dietrich D**, Becker J, Kohlstedt M, Wittmann C; 2021: Microbial production of polyunsaturated fatty acids — high-value ingredients for aquafeed, superfoods, and pharmaceuticals. *Current opinion in biotechnology, 69*, 199-211. doi: 10.1016/j.copbio.2021.01.009

Gemperlein K, **Dietrich D**, Kohlstedt M, Zipf G, Bernauer HS, Wittmann C, Müller R; 2019: Polyunsaturated fatty acid production by *Yarrowia lipolytica* employing designed myxobacterial PUFA synthases. *Nature Communications, 10*(1), 4055. doi: 10.1038/s41467-019-12025-8

The following article was published in the time of this work, but is not part of the thesis:

Jovanovic S, **Dietrich D**, Gläser L, Cao P, Kohlstedt M, Wittmann C; 2023: Multiomics view of recombinant *Yarrowia lipolytica*: Enhanced ketogenic amino acid catabolism increases polyketide-synthase-driven docosahexaenoic production to high selectivity at the gram scale. Submitted.

Conference contributions

Dietrich D, Gemperlein K, Wenzel S, Kohlstedt M, Müller D, Müller R and Wittmann C, 2019: Polyunsaturated fatty acid production by *Yarrowia lipolytica* employing designed myxobacterial PUFA synthases, PhD day Faculty NT, Saarland University, Saarbrücken, Germany

Dietrich D, Gemperlein K, Wenzel S, Kohlstedt M, Müller D, Müller R and Wittmann C, 2019: Optimized bioprocess for production of high-value omega-3 fatty acids in recombinant *Yarrowia lipolytica,* HIPS Symposium 2019, Saarbrücken, Germany.

Dietrich D, Jovanovic S, Gemperlein K, Kohlstedt M, Müller D, Zipf G, Bernauer HS, Müller R, Wenzel S and Wittmann C, 2020: Optimized bioprocess for production of high value omega-3 fatty acids in recombinant *Yarrowia lipolytica*, 6th Joint Conference of the DGHM & VAAM, Leipzig, Germany.

Dietrich D, Gemperlein K, Wenzel S, Kohlstedt M, Müller D, Müller R and Wittmann C, 2022: Production of high-value omega-3 fatty acids in recombinant *Yarrowia lipolytica*, Yeast lipid conference (YLC), Gothenburg, Sweden.

Danksagung

An erster Stelle möchte ich Prof. Dr. Christoph Wittmann für die Aufnahme am Institut für Systembiotechnologie und die Bereitstellung des Themas im MYXO4PUFA-Projekts danken. Ich möchte dir von ganzem Herzen für deine Rolle bei der Entwicklung meiner persönlichen und beruflichen Fähigkeiten danken. Deine vertrauensvolle Betreuung schaffte Raum für meine Eigenmotivation und Ideen, in Balance mit unentbehrlicher Leitung.

PD Dr. Frank Breinig möchte ich für die Übernahme des Zweitgutachtens danken.

Dem Gesamten Team von MYXO4PUFA Projekt möchte ich für eine tolle Zusammenarbeit danken. My special thanks goes to Sofija. Having someone to fight and tame our diva *Yarrowia*, was indispensable. *Jeb'o si ježa u leđa,* but we made it.

Mein besonderer Dank gilt Dr. Michael Kohlstedt für die wissenschaftliche Unterstützung und Zusammenarbeit, besonders für die Korrekturlesung meiner Dissertationsschrift. Danke für tägliche Mittagspausen, die wir zusammen mit dem besten Mensa-Essen Deutschlands, prägende Diskussionen über das Weltgeschehen bis hin zu Mittagspausen beendende Gespräche Richtung Gürtellinie verbracht haben.

Dem gesamten iSBio Team möchte ich für ein tolles Arbeitsumfeld und stete Hilfsbereitschaft danken. Mein Dank geht besonders an Dr. Gideon Gießelmann, der mein Potential für schlechte Wortwitze (Apple Bottom Jeans) schon früh erkannt hat und mich ans iSBio akquiriert hat. Zusammen mit Dr. Lars Gläser und Dr. Martin Kuhl wart ihr ein essenzieller Teil meiner Promotion. Stuckateurmeister Quartett 4 life. Dr. Judith Becker gilt mein Dank als Vorbild als Wissenschaftlerin. Deine immer ehrlichen Worte prägten mich als Wissenschaftler und Mensch.

Viktoria, kein Absatz würde meiner Dankbarkeit für dich gerecht werden. Seit Tag eins hast du mich in der Promotion als Freundin und Partnerin bedingungslos begleitet. Du warst ein unersetzlicher Gesprächspartner, als ausgezeichnete Wissenschaftlerin und quietschendes Emotionswölkchen. Vielen Dank für deine Unterstützung, Geduld und vor allem Verständnis. Deine herzliche und lebensfrohe Art macht jeden Tag besser, auch an Tagen, an denen nichts geklappt hat, hast du es geschafft mir ein *happy place* zu schenken. Ich hab dich noch lieb.

Ich möchte meiner geliebten Familie und meinen Freunden, die mir auf dem beschwerlichen Weg dieser Dissertation zur Seite gestanden haben, von ganzem Herzen danken. Ihre unerschütterliche Unterstützung, ihr Zuspruch und ihr Verständnis haben mir sehr viel bedeutet.

Table of contents

I Summary

Engineered strains of the oleaginous yeast *Y. lipolytica* produce commercially attractive polyunsaturated fatty acids (PUFAs). In a pioneering study, strain Af4 was shown to produce docosahexaenoic acid (DHA), a major industrial PUFA, through expression of a myxobacterial PUFA synthase. This work aimed to increase the production of DHA in *Y. lipolytica* Po1h::Af4. In the first part, the impact of nutrients on the complex fermentation process was studied, resulting in different types of nutrient setups to trigger DHA production, including the comparison of different C-sources. In shake flask cultures, an improoved medium allowed to produce DHA up to a selectivity of 17% of TFAs. The second part tackled DHA overproduction on the genetic level by optimizing the expression of the PUFA cluster. A basic design, based on the commonly used *pTEF*, was sufficient to drive DHA production. Beneficially, the incorporation of the late-phase *pminLEU2* plus additional genetic elements, such as UAS1B4 sequences, 5' introns, and intergenic spacers, DHA production increased up to 16-fold. The control elements acted synergistically, whereby the UAS1B4 elements generally increased expression, while the intron caused gene-specific effects. The synthetic producer strains were found genetically stable over 185 h of cultivation. A fed-batch fermentation, using the improved nutrient set-up with glucose as the carbon source yielded a DHA titer of 350 mg L^{-1} and a selectivity of 11% of DHA among TFAs.

II Zusammenfassung

Gentechnisch veränderte Stämme der ölhaltigen Hefe *Y. lipolytica* produzieren kommerziell attraktive mehrfach ungesättigte Fettsäuren (PUFAs). In einer innovativen Studie wurde gezeigt, dass der Stamm *Y. lipolytica* Po1h::Af4 durch Expression einer myxobakteriellen PUFA-Synthase Docosahexaensäure (DHA), eine wichtige PUFA, produzieren kann. Ziel dieser Arbeit war es, die Produktion von DHA in *Y. lipolytica* zu steigern. Im ersten Teil wurde der Einfluss von Nährstoffen auf den komplexen Fermentationsprozess untersucht, was zu verschiedenen Arten von Medienkonfigurationen zur Auslösung der DHA-Produktion führte, einschließlich des Vergleichs verschiedener C-Quellen. Dies ermöglichte ein optimales Medium und die Produktion von DHA bis zu einer Selektivität von 17%. Der zweite Teil befasste sich mit der DHA-Überproduktion auf genetischer Ebene, indem die Expression des PUFA-Clusters optimiert wurde. Die Verwendung des *minLEU2*-Promotors und Einbau von UAS1B4-Sequenzen, 5'-Introns und intergenen *Spacern* konnte die DHA-Produktion um 16-fache im Vergleich zum Basisstamm gesteigert werden. Die genetischen Elemente wirkten synergistisch, wobei die UAS1B-Elemente die Expression generell erhöhten, während das Intron genspezifische Effekte verursachte. Die Produzenten blieben über 185 h Kultivierung genetisch stabil. Eine optimierte Fermentation unter Verwendung des verbesserten Mediums ergab einen DHA-Titer von 350 mg L^{-1} und eine Selektivität von 11% DHA anteilig am Gesamtlipids.

1 Introduction

1.1 General introduction

The oleaginous yeast *Yarrowia lipolytica*, which was identified in 1972 by David Yarrow (Yarrow, 1972), is found in diverse environments, has a broad substrate spectrum, and shows great versatility in growth conditions (Mamaev & Zvyagilskaya, 2021). Due to its remarkable adaptability, *Y. lipolytica* has gained significant interest in both research and industry. Additionally, advancements in the genetic toolbox have expanded the possibilities for strain modification (Bankar et al., 2009; Larroude et al., 2018). *Y. lipolytica* has various potential applications, ranging from direct use as a feedstock to functioning as a cell factory for producing bio-based chemicals, particularly in the field of lipids (Jach & Malm, 2022; Miller & Alper, 2019). Lipids include various molecules that are essential components of our diet and body, with long-chain polyunsaturated fatty acids (LC-PUFAs) like eicosapentaenoic acid (EPA) and docosahexaenoic acid (DHA) being particularly beneficial (Calder, 2018). Since LC-PUFAs cannot be sufficiently synthesized by the human body, they must be obtained from the diet (Das, 2006). Insufficient levels can disrupt cellular functions and play a crucial role in eye health, cardiovascular health, inflammation response, and mental health (Del Gobbo et al., 2016; Seddon et al., 2006; Zárate et al., 2017).

There are two distinct routes for the biosynthesis of LC-PUFAs: The aerobic and anaerobic synthesis (Gurr et al., 2002). The aerobic pathway employs fatty acid synthase (FAS) enzymes, while the anaerobic pathway utilizes polyketide synthases (PKS) (Metz et al., 2001). In the widespread aerobic pathway saturated fatty acid are synthesized, then elongated and reduced by additional enzymes to generate LC-PUFAs. In contrast, anaerobic PKS-based systems keep and rearrange the existing double bonds in the iterative chain elongation, thus synthesize LC-PUFAs directly without the need of extra elongases and desaturases (Metz et al., 2001). Only a small fraction of organisms in the biosphere has the ability to produce EPA and DHA *de novo*, with organisms from marine environments being the primary source (Sayanova & Napier, 2004; Uttaro, 2006). Among these organisms, species of the Thraustochytrids genus (e.g. *Schizochytrium* sp.) are known to be able to accumulate the highest

amounts of LC-PUFAs (Gladyshev et al., 2013), while terrestrial organisms contribute negligibly to global production (Kaštovská et al., 2007). Despite substantial production of LC-PUFAs in marine organisms, only a small percentage (0.2%) is transferred to the terrestrial ecosystem and humans face a deficiency in these health-promoting molecules (Gladyshev et al., 2009a). Obtaining sufficient LC-PUFAs through fish, as the main source in the human diet, poses risks due to anthropogenic pollution (Gladyshev et al., 2012). Moreover, overfishing and climate change impact fish populations and reduce the concentration of LC-PUFAs, posing a risk of insufficient supply for the majority of the human population (Colombo et al., 2020; FAO, 2022). Therefore, relying primarily on fish from marine source or aquaculture is unsustainable, highlighting the need to explore alternative sources (Sijtsma & de Swaaf, 2004).

A production of high LC-PUFA-containing microorganisms as a nutrient source for aquaculture or human nutrition could offer a more sustainable solution. Microbial production allows for targeted production of specific fatty acids from renewable resources. Single cell oils (SCO) extracted from microbial sources offer advantages over fish oils, although challenges remain in terms of cost-effectiveness due to product recovery, downstream processing, and purification (Ochsenreither et al., 2016). While natural producers of LC-PUFAs, like microalgae, have been utilized for commercial production, issues arise with photosynthesis-based systems such as open-pond cultivation, which have low cell densities, slow growth rates, sterility and scalability concerns (Gu et al., 2022; Khozin-Goldberg et al., 2011). Heterotrophic microalgae have been commercially utilized for the production of DHA (Fedorova-Dahms et al., 2014), and efforts have been made to produce LC-PUFAs heterologously in organisms such as *Escherichia coli*, lactic acid bacteria, and *Pseudomonas putida* (Amiri-Jami & Griffiths, 2010; Amiri-Jami et al., 2014; Gemperlein et al., 2016). These biotechnological workhorses potentially offer advantages for large-scale production (Nielsen, 2019). In the search for potential LC-PUFA producers, several organisms from the fungi kingdom have been investigated (Guo et al., 2019; Johansson et al., 2016). Among them, oleaginous yeast *Rhodosporidium toruloides* and *Yarrowia lipolytica* are promising candidates and have been engineered to produce LC-PUFAs (Arbter et al., 2019; Xue et al., 2013b). *Y. lipolytica*, in particular, has shown great potential for lipid production, with the

ability to accumulate lipids up to 30-50% of its cell dry mass (90% for GMOs) and proved to be a robust workhorse (Beopoulos et al., 2009a; Beopoulos et al., 2009b; Blazeck et al., 2014; Qiao et al., 2015). Research efforts have focused on establishing *Y. lipolytica* as a platform for producing fatty acids with tailored chain lengths and variations in saturation levels (Wang et al., 2022). Genetically modified strains have been developed by DuPont to produce EPA-enriched SCOs for feed and food applications (Xue et al., 2013). Recent studies have explored the incorporation of myxobacterial PKS-based PUFA synthases in *Y. lipolytica*, resulting in various strains with distinct LC-PUFA profiles (Gemperlein et al., 2019). This innovative approach holds promise for manufacturing customized fatty acids mixtures or specific valuable fatty acids. Importantly, compared to the DuPont process, significantly less NADPH is needed, and fewer genetic modifications are required.

1.2 Main objectives

The present work aimed at the enhanced DHA production with the oleaginous yeast *Yarrowia lipolytica* by bioprocess and strain development. In a first part, the medium was subject of optimization. The previously used medium should be analyzed first in regards of general cultivation characteristics and adapted to gain stable conditions. Here, pH buffer systems should be tested for growth characteristics, pH stability, as well as the influence on DHA production. Based on the stable base medium, an advanced medium should be evaluated, aiming at the identification of the most influential media components and concentrations onto DHA productivity in *Y. lipolytica* Po1h::Af4. Here, the carbon and nitrogen source, as well as concentrations of media components were subject of the analysis. The transition from shake flask to a fed-batch fermentation should be evaluated to gain insights for the optimization of an industrial relevant process design.

In the second part, the genetic architecture of the mxyobacterial PUFA cluster from *Y. lipolytica* Po1h::Af4 was targeted to gain insights of the different genetic parts of the cluster onto the DHA productivity. For this purpose, two promoters, different tandem repeats of UAS1B, the use of an intron and the influence of the spacer sequence should be tested. The resulting cluster version are then evaluated for expression levels, genetic stability, levels of DHA and its precursors. Finally, a fed-batch fermentation should be conducted, using the insights of the media development onto a bioreactor-based production process.

2 Theoretical background

2.1 *Yarrowia lipolytica* and its applications

The oleaginous yeast *Yarrowia lipolytica* was identified in 1972 by David Yarrow from the Delft Microbiology Laboratory (Yarrow, 1972) and named in 1980 from von Arx and van der Walt (van der Walt & von Arx, 1980), whereas *lipolytica* refers to the ability to hydrolyze lipids. With its outstanding lipolytic and proteolytic activities *Y. lipolytica* can be found ubiquitously in lipid or protein-rich environments and was previously isolated from dairy and meat products or oil-polluted waters, but can also be found in sea water and soils (Fröhlich-Wyder et al., 2019; Groenewald et al., 2014; Mamaev & Zvyagilskaya, 2021). The ability to grow in such diverse environments results from *Yarrowias'* broad substrate spectrum (Figure 1), making use of both hydrophilic (e.g., D-glucose, glycerol, D-fructose) and hydrophobic carbon sources such as fatty acids, alkanes, or triglycerides. In addition, it is able to use organic acids and alcohols in some extent. Current research is constantly expanding the substrate range by testing complex mixtures from industry (e.g. olive oil mill waste or animal fats) and metabolically engineering the cells catabolism (Ledesma-Amaro & Nicaud, 2016; Madzak, 2021; Spagnuolo et al., 2018). Besides the broad substrate spectrum *Y. lipolytica* is capable to survive and grow under various growth and stress conditions. The pH range is reported to be from 3.5 - 8 for most strains and extends to an even broader pH range of 2 - 9.3 for others (Sutherland et al., 2014). In terms of temperature *Yarrowia lipolytica* grows from 4 - 37 °C, with an optimum between 25 and 30 °C (Sutherland et al., 2014). Additionally, *Y. lipolytica* is able to tolerate osmotically challenging salt concentrations of 7.5% NaCl, and in certain specific strains, this tolerance has been even reported to be twice as high (Sutherland et al., 2014). With these outstanding versatility, *Y. lipolytica* constantly gains interest in research and industry (Figure 2) and is the most studied unicellular fungus after *Saccharomyces cerevisiae* (Bankar et al., 2009). Consequently, the genetic toolbox to modify and optimize the strains expanded over time. Multiple DNA assembly techniques such as Golden Gate, Gateway or Gibson assembly have been successfully applied in *Yarrowia* research.

The genetic parts for the construction of an expression cassette, such as promoter, terminators or selection markers have been extensively studied, giving access to a broad library for each genetic element to choose from (Larroude et al., 2018).

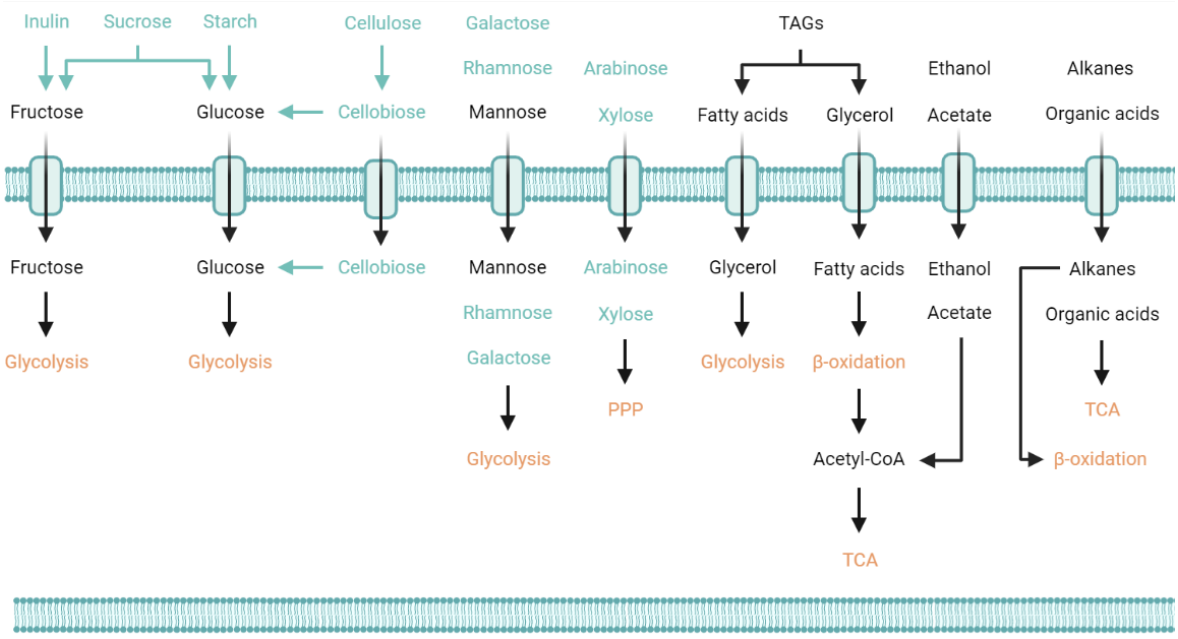

Figure 1: Substrate spectrum and assimilation pathways of *Y. lipolytica*.
Cyan: Substrates enabled by genetic engineering; Black: Natural substrates; Orange: Assimilation pathways. Adapted from Ma et al. (2020)

Since its discovery the number of publications related to *Y. lipolytica* steadily increased until today (Figure 2). On one hand its regarded as model organism for non-conventional yeast in which several cellular mechanisms like protein secretion, dimorphism, lipid body biogenesis or lipid homeostasis have been investigated (Nicaud, 2012). On the other hand, it has been widely used in biotechnological applications due to its ability to assimilate and produce hydrophobic substances, especially fatty acids (Liu et al., 2015). Moreover, it has been described as cell factory for a broad range of bio-based chemicals like carotenoids, polyketides, polymers, terpenes, nanoparticles or proteins (Miller & Alper, 2019).

Lipids and their derivatives (8.8%) are the second-most patented product group synthesized with *Y. lipolytica* after peptides and proteins (65.1%) (Park & Ledesma-Amaro, 2022). Due to its natural protein content of ~50%, its outstanding nutritional values and vitamin content, *Y. lipolytica* is proposed to

serve as food supplement not only as feed stock for animals but for human nutrition as well (Jach & Malm, 2022). Skotan SA established a process to produce single-cell protein (SCP) for human and animal consumption and registered it for the distribution in the EU (Bornscheuer, 2018; Groenewald et al., 2014). *Y. lipolytica* wildtype strains naturally secrete high amounts of lipases, proteases, phosphatases, and RNases to degrade extracellular resources, facilitating their transport across the cell membrane. (Barth & Gaillardin, 1996). Consequently, the protein secretion machinery as well as post-translational modification pathways, high secretion rates and low over-glycosylation (Belo, 2010) facilitate the production of industrial proteins in *Yarrowia*.

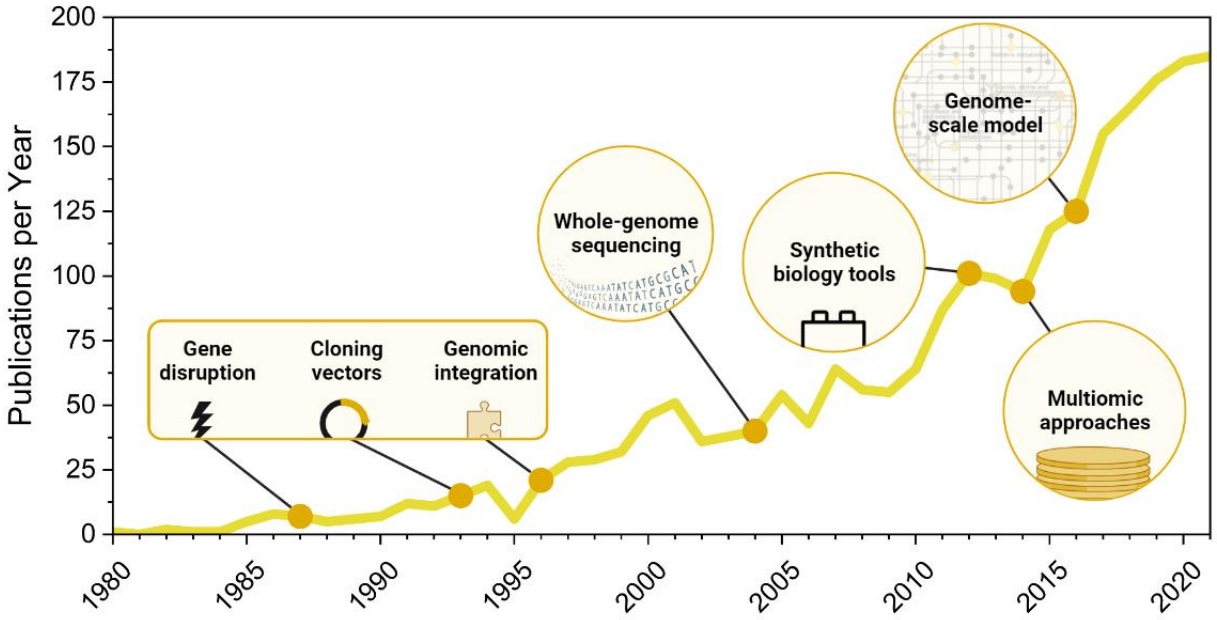

Figure 2: Publications and milestones associated with *Yarrowia lipolytica*.

Numbers of publications per year, results from PubMed with "*Yarrowia lipolytica*" as search term on the 21.09.2022. Milestones are marked as an orange dot in the year of discovery/development; taken from Park and Ledesma-Amaro (2022).

2.2 Metabolic engineering of *Yarrowia lipolytica*

Genetic engineering is often a crucial step to unlock the full potential of a microorganism. Generally, two methods to achieve such a genetic modification can be distinguished: episomal vectors and chromosomal integration. Episomal plasmids do not occur naturally in *Y. lipolytica* (Larroude et al., 2018), thus researchers have to mimic a chromosome by integrating at least an autonomously replicating sequence (ARS) and a centromere sequence on the shuttle vector (Fournier et al., 1993; Matsuoka et al., 1993). These systems are constantly improving (Cui et al., 2021a; Guo et al., 2020), however the use is limited due to low-copy numbers of ARS-based plasmids (1 - 3 plasmids per cell), a high loss frequency and the need for selection pressure to maintain the plasmid (Madzak et al., 2004; Vernis et al., 1997). The preferred method to engineer *Y. lipolytica*, especially in industrial settings is therefore the manipulation of the chromosome, opening the possibility to extend, alter and delete existing DNA loci, offering high stability and reproducibility. Integrative vectors in *Y. lipolytica* are inserted by homologous recombination (HR), which requires flanking regions of 0.5-1 kb to insert exogenous DNA into the desired region with an efficiency of 0-36% (Schwartz et al., 2017). However, most of the exogenous DNA is integrated randomly through non-homologous end joining (NHEJ). The microbe prefers this method to cope with double-strand breaks instead of HR (Richard et al., 2005). This eases the way of random chromosomal integration, but renders the commonly favored targeted integration more difficult. To increase the HR rate the gene *ku70*, which encodes for the enzyme responsible for double-strand repair in NHEJ was deleted (Lustig, 1999). This deletion drastically improves the HR efficiency, even with HR regions as low as 50 bp (Verbeke et al., 2013). When combined with hydroxyurea treatment, the efficiency is further increased (Jang et al., 2018). Apart from classical HR approaches, CRISPR/Cas9-based methods have been established to rationally design the integration site, rather than relying on random DNA double-strand breaks at the targeted integration site (Holkenbrink et al., 2018a). Here, targeted integration techniques have reached an efficiency that enables the omission of a selection marker, resulting in a reduction of time required metabolic engineering of *Y. lipolytica* since there is no need for a second HR, Cre/loxP system based excision (Zhou et al., 2021), or other techniques such as 5-

fluoroorotic acid treatment to remove the marker gene afterwards (Widlund & Davis, 2005).

Overall, the integration site of exogenous DNA significantly impacts its expression and integration efficiency. Holkenbrink et al. (2018b) investigated several integration sites and evaluated their integration efficiency, expression strength, and their impact on cell viability. The tested integration sites facilitate a useful base for integrating synthetic genes or clusters without the need for extensive screening, as previously done by Gemperlein et al. (2019).

To efficiently express (heterologous) genes in a microorganism, a thorough understanding of the mechanics of the individual genetic components is necessary. *Y. lipolytica*, being an eukaryotic organism, has complex and multi-level regulatory mechanisms, that start from transcriptional regulation by DNA packaging, core promoter, as well as distal and proximal enhancing or silencing sequences, and extend to post-processing and post-translational regulatory features (Le Hir et al., 2003a). Until today the influence of each component is not fully understood. In metabolic engineering, the genetic architecture of the gene cassette is a critical component of the design process. Common designs for *Y. lipolytica* often consist of a core or minimal promoter, an upstream activating sequence (UAS) located upstream of the open reading frame (ORF), as well as a terminator sequence located downstream of the ORF (Figure 3).

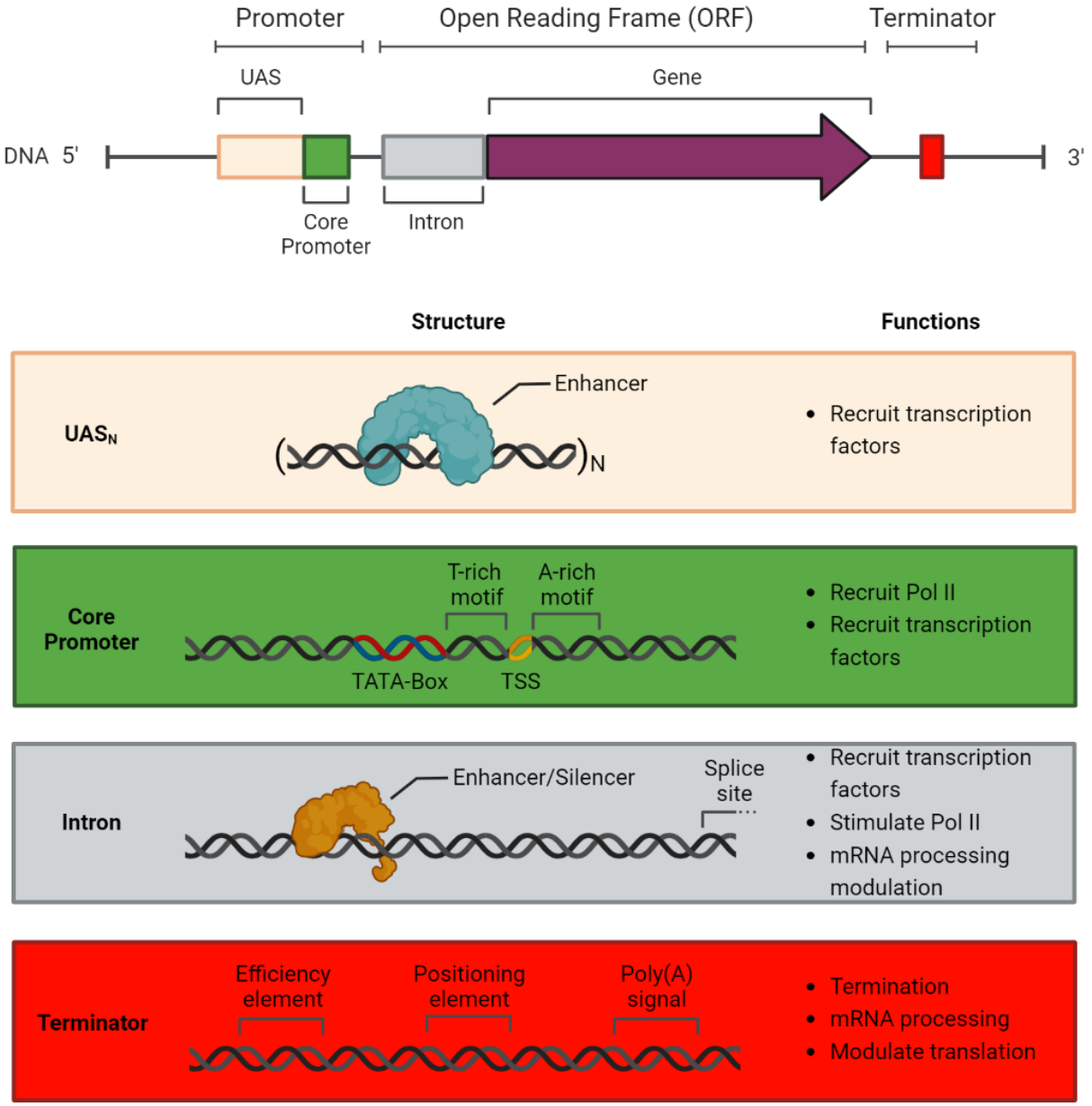

Figure 3: Genetic architecture of a gene cassette and their functions in yeast.

Each gene cassette consists of a promoter region upstream of the open reading frame, consisting of upstream activating sequences (UAS; optional) and a core promoter. UAS recruit enhancer proteins (transcription factors), whereas the core promoter mainly recruits RNA polymerase II. Introns can contain several regulatory elements such as enhancer and silencer binding sites and modulate multiple gene expression mechanisms (Le Hir et al., 2003b). The terminator contains an efficiency and positioning element, as well as the poly(A) signal. ORF: open reading frame; UAS: upstream activating sequence; TSS: transcription start site; Pol II: RNA polymerase II.

The selection of a suitable promoter is a critical part of the genetic design process. In *Y. lipolytica*, several core promoters, either constitutive or inducible, have been tested and utilized (Larroude et al., 2018). The most prominent ones are the constitutive promoters of the translation elongation factor-1 gene *tef (pTEF,* (Müller et al., 1998)) and the extracellular protease encoding *xpr* gene (*pXPR2*). Due to the complexity of eukaryotic transcriptional regulation, endogenous promoters are commonly implemented for heterologous gene expression. Effects of sequence alterations are difficult to predict in eukaryotic organisms (Lubliner et al., 2013; Weingarten-Gabbay & Segal, 2014) and until today the exact functioning of core promoter elements is not fully understood (Erb & van Nimwegen, 2011). Studies in *Saccharomyces cerevisiae* as budding yeast model indicated that the highest promoter activity is achieved with an overall low GC-content, T-rich motifs upstream, and A-rich motifs downstream from the transcription start site (TSS) (Lubliner et al., 2013). Furthermore, the TATA-box modulates the expression strength in *Y. lipolytica*, as demonstrated in a core promoter architecture optimization by synthetic hybrid promoter designs (Shabbir Hussain et al., 2016).

Upstream activating sequences in yeast are similar to enhancer sequences in multicellular eukaryotes, as they are *cis*-acting regulatory sequences that bind transcription factors and directly affect gene expression (Webster et al., 1988). In *Y. lipolytica,* the UAS2 sequence of the pXPR2 for example dependents on carbon or nitrogen source as well as the pH (Madzak et al., 1999). On the other hand, UAS1B from the pXPR2 promoter, corresponding to the position -805 to -776 in the promoter pXPR2 was originally demonstrated to drive expression in various media, insensitive of pH, carbon, and nitrogen source (Madzak et al., 1999). Over the years, UAS1B has become one of the most common UAS in genetic engineering of *Y. lipolytica* (Blazeck et al., 2013; Gemperlein et al., 2019; Shabbir Hussain et al., 2016; Tai & Stephanopoulos, 2013). Up to 32 UAS1B sequences can be fused to further modulate expression strength (Blazeck et al., 2011b; Madzak et al., 2000).

In a hybrid promoter design Madzak and colleagues generated a set of promoters consisting of the minimal LEU2 promoter and 1 to 4 copies of the UAS1B taken from pXPR2 promoter (Madzak et al., 2000). These hybrid promoters have been

widely utilized in biotechnological applications, since their expression is highest in stationary phase, thus not interfering with growth.

In yeast, the terminator sequence is not only required for efficient termination of expression but affects mRNA stability and modulates overall protein levels (Geisberg et al., 2014; Mischo & Proudfoot, 2013). The terminator consists of an efficiency element, enhancing the efficiency of a second element, the positioning element, which itself provides the information to the poly(A) polymerase where to position the poly(A) tail determined by the poly(A) signal sequence. Terminators have recently gained more attention, as optimized synthetic terminators enabled increased mRNA levels (4.4-fold) and protein levels (3.7-fold) in *Y. lipolytica* (Curran et al., 2015). Furthermore, terminators act as insulators by binding RNA polymerase II at the efficiency element, thus competing with downstream promoter sequences, making them important engineering factors, especially in heterologous gene clusters (Song et al., 2016).

Introns play a unique role in gene expression regulation as they are not directly part of the regulatory system. However, introns have been indicated to have significant effects on gene expression at multiple levels. Firstly, introns influence transcription by serving as repositories for enhancer/silencer sequences or by modulating nucleosome positioning (Le Hir et al., 2003b). Additionally, splicing signals within introns potentially stimulate RNA polymerase II, particularly promoter-proximal introns, which have been shown to enhance transcription initiation in yeast and mammalian cells (Furger et al., 2002; Kwek et al., 2002). On the level of mRNA processing, an intron might improve mRNA stability by enhancing polyadenylation, due to direct contacts between the spliceosome and the poly(A) machinery. In addition, splicing has been associated with mRNA export, localization, and translation (Le Hir et al., 2003b). In *Y. lipolytica,* 16% of all genes contain introns, making it the intron-richest hemiascomycete currently known (Gaillardin et al., 2013). The high level of introns and their multidimensional impact on protein expression underline the importance to test and implement them in heterologous gene expression. As a particular example given, the first intron of the *tef* gene in combination with multiple promoters leads to significant positive effects on transcription and protein levels (Cui et al., 2021b; Tai & Stephanopoulos, 2013).

2.3 Long-chain polyunsaturated fatty acids and their role in human health

Lipids are a crucial component of our diet, serving as a source of energy through β-oxidation, as well as being a substantial component in our body. Lipids encompass a diverse range of molecules, including fatty acids (FAs) as the basic component and all derivatives of FA, as well as associated biosynthetic derivatives. FAs are aliphatic hydrocarbon chains ranging from C14 to C22 with a terminal carboxyl group. They rarely occur outside this range (C2 to C36) or with an odd-numbered chain length (Christie & Han, 2012). FAs occur either saturated, i.e. without double bonds, or unsaturated, i.e. with one or more double bonds (in *cis* or *trans* configuration). Double bonds are commonly methylene-interrupted but occasionally occur in conjugated configuration. The position of the last double bond is denoted according to the position relative to the last C-atom - labeled as ω in the aliphatic chain. The chain length acts as the main classification, dividing them in short (C2-C6), medium (C7-C12), long (C13-C22), very long (C23+).

Thereby, the group of long-chain polyunsaturated fatty acids (LC-PUFAs) are of special interest in human nutrition and health. Here, the molecules eicosapentaenoic acid (EPA; C20:5, ω*3*) and docosahexaenoic acid (DHA; C22:6, ω*3*) are considered most beneficial (Calder, 2018). Health organizations all over the world recommend the integration of these substances in the daily diet to maintain good health (Li et al., 2021a). Humans are unable to *de novo* synthesize LC-PUFAs, since they are metabolically incapable to introduce a double bond beyond carbons 9 and 10 in a FA. This means that the molecules linoleic acid (LA; 18:2, ω*6*) and the α-linolenic acid (ALA; 18:3, ω*3*) are essential fatty acids (EFAs), which need to be taken up, whereas oleic acid (OL; C18:1, ω9) is none (Das, 2006). Starting from ALA, the human body is able to build longer fatty acids with different degree of saturation, however, it is controversial that the conversion rates towards LC-PUFAs such as EPA and DHA are insufficiently low (Metherel & Bazinet, 2019). It is therefore widely recommended to ingest a certain amount with the diet. The optimal dosage of EPA and DHA varies among health organizations, considering factors such as age and health status. For instance, the U.S. Food and Drug Administration (FDA) recommends a daily intake of 500 mg of EPA and DHA (Hussein et al., 2005; Li et al., 2021a).

Insufficient levels of ω3-LC-PUFAs result in a change in the *ω6/3* ratio, which in turn lead to an imbalanced synthesis of eicosanoids - signaling molecules disrupting cellular functions and other metabolic processes (Wijendran & Hayes, 2004). The recommended optimal ratio to maintain a healthy diet is 2:1 (Simopoulos et al., 2000) and should not exceed 10:1 for infants (Gerster, 1998).

LC-PUFAs are an important building block of most biological membranes, constituting 10-15% of all FAs, and are responsible for both their functioning and structure. LC-PUFAs serve as modulators for optimal membrane fluidity, as well as for the integration of membrane enzymes, channels, and other vital components (Koletzko et al., 2009). DHA is particularly abundant in the retina and in the brain. In fact, the brain's gray matter contains a high concentration of DHA, accounting for 18% of its total lipid content (Skinner et al., 1993) and 12% in the retina (Makrides et al., 1994). Studies have demonstrated that supplementation with *ω3* LC-PUFAs positively affects eye health, particularly in protection against age-related macular degeneration (Seddon et al., 2006).

Further potential health benefits of LC-PUFAs are extensive and include the prevention of a wide range of diseases. In terms of cardiovascular health (CVH) - specifically coronary heart disease (CHD) - recent research has linked adequate concentrations of EPA and DHA in blood plasma, serum, erythrocytes, and adipose tissue with favorable CVH outcomes (Del Gobbo et al., 2016). This effect is explained by the reduction of several risk factors, including concentrations of triglycerides (TAGs), blood pressure, thrombosis, and inflammation, as well as the improvement of cardiac and vascular function (Breslow, 2006; Calder, 2004; Harris, 1996; Kris-Etherton et al., 2002; Leslie et al., 2015; Saravanan et al., 2010). Interestingly, research investigating the dietary habits of various nations has revealed an association between high consumption of LC-PUFAs from marine sources and improved CVH, such as in Alaska (Newman et al., 1993), Greenland (Bjerregaard & Dyerberg, 1988), Northern Canada (Dyerberg et al., 1978) or Japan (Kris-Etherton et al., 2002).

EPA and DHA serve as precursors for numerous bioactive lipid mediators, although the functions of many remain poorly understood. However, a significant proportion of these mediators are known to play a role in inflammation and infection response (Zárate et al., 2017). In addition to their function as precursors for a range of bioactive substances, EPA and DHA exhibit anti-inflammatory

effects, in particular therapeutic benefits for inflammatory diseases such as rheumatoid arthritis (Miles & Calder, 2012), inflammatory bowel disease (Calder, 2009) and asthma (Calder, 2006). Additionally, research has linked LC-PUFA consumption during early childhood and pregnancy to a reduced risk of developing autoimmune diseases. Given that allergic tendencies often develop during infancy, a sufficient LC-PUFA supply during this critical period will lower the risk factors for allergies over the whole life span (Reynolds & Finlay, 2017). The supply of LC-PUFAs during pregnancy and infancy has further positive effects. Harris et al. (2015) reported a significant reduction in the risk of preterm birth from 5.7% to 1.7% in subjects who received DHA supplementation. Similarly, a meta-analysis of studies examining the effects of LC-PUFA supplementation during pregnancy even found a 17% reduction in preterm birth risk. (Kar et al., 2016). Given the importance of LC-PUFAs as building blocks, particularly for the brain and eye, it is not surprising that ensuring adequate supply during fetal development is highly recommended. Fetal brain development in particular, requires an even higher amount of DHA since approximately 50% of the brain's DHA is accumulated during pregnancy. This underscores the importance of meeting a 5-fold increased DHA requirement compared to that of an adult brain during this critical period of development (Haag, 2003). Furthermore, DHA supplementation was positively associated with general physical and mental development as for example improved eye-hand coordination (Dunstan et al., 2008), problem-solving skills (Drover et al., 2009), and general cognitive abilities could be improved (Drover et al., 2011).

Mental health problems are becoming more prevalent in modern society (Kieling et al., 2011). Interestingly, LC-PUFAs have been found to have positive effects on mental health, including mitigation of depression symptoms, impulsivity, and suicidal intent. Garland et al. (2007) found EFA levels in patients inversely correlated with depression and impulsivity scores. Especially low DHA levels were associated with elevated susceptibility for depression (Sublette et al., 2006). The risk of suffering from mental disorders is largely determined in the early stages of life, with about 50% of patients experiencing disorders before the age of 15 (Kessler et al., 2005). Studies have investigated the use of LC-PUFAs in the treatment of mental health problems, reducing suicidal behavior and improve well-being after 12 weeks of LC-PUFA supplementation. (Hallahan et al., 2007).

2.4 Biosynthesis of LC-PUFAs

Until today two routes for the biosynthesis of PUFAs can be distinguished, an aerobic and an anaerobic synthesis. The most common aerobic pathway is based on the ubiquitous fatty acid synthase (FAS) pathway, in which saturated fatty acids are assembled up to a certain chain length (Figure 4). FAS are divided in Type I and Type II synthases, consisting of a multienzyme complex or separate enzymes, respectively. FASI occurs in animals, bacteria, and yeast, whereas FASII occurs in bacteria and plants. Additionally, FASIII commonly referred to as elongases complement FASI and FASII systems ubiquitously (Gurr et al., 2002). The product of FAS varies between organisms and FAS types. However, hexadecanoic acid (C16:0) is the major product of most FAS systems (Vagelos, 1974). The biosynthesis starts with the condensation of acyl carrier protein (ACP)-bound acetyl-CoA as a primer molecule with malonyl-ACP to form a β-ketoacyl-ACP intermediate, followed by a reduction and subsequent dehydration. In the final step the double bond is reduced to gain butyryl-ACP, which elongated subsequently with malonyl-CoA. This cycle is repeated until the targeted saturated fatty acid (SFA) is synthesized. From this SFA base molecule most other FAs are derivatized by elongases (FASIII) and desaturases to gain longer and more desaturated FAs. Since elongases are specific to the molecule and position of the intended double bound, numerous enzymes are needed to synthesize LC-PUFAs via the aerobic pathway. For example: in order to synthesize DHA, approximately 30 different enzymes and 70 reactions are needed (Metz et al., 2001), making it a highly complex synthesis. Looking at the energy balance, the aerobic PUFA synthesis is inefficient since the needed double bonds are initially oxidized consuming one NADPH and later incorporated again in the desaturation step at the expense of another NADPH. Despite its inefficiency, the aerobic way is the most widespread in eukaryotes and most prokaryotes.

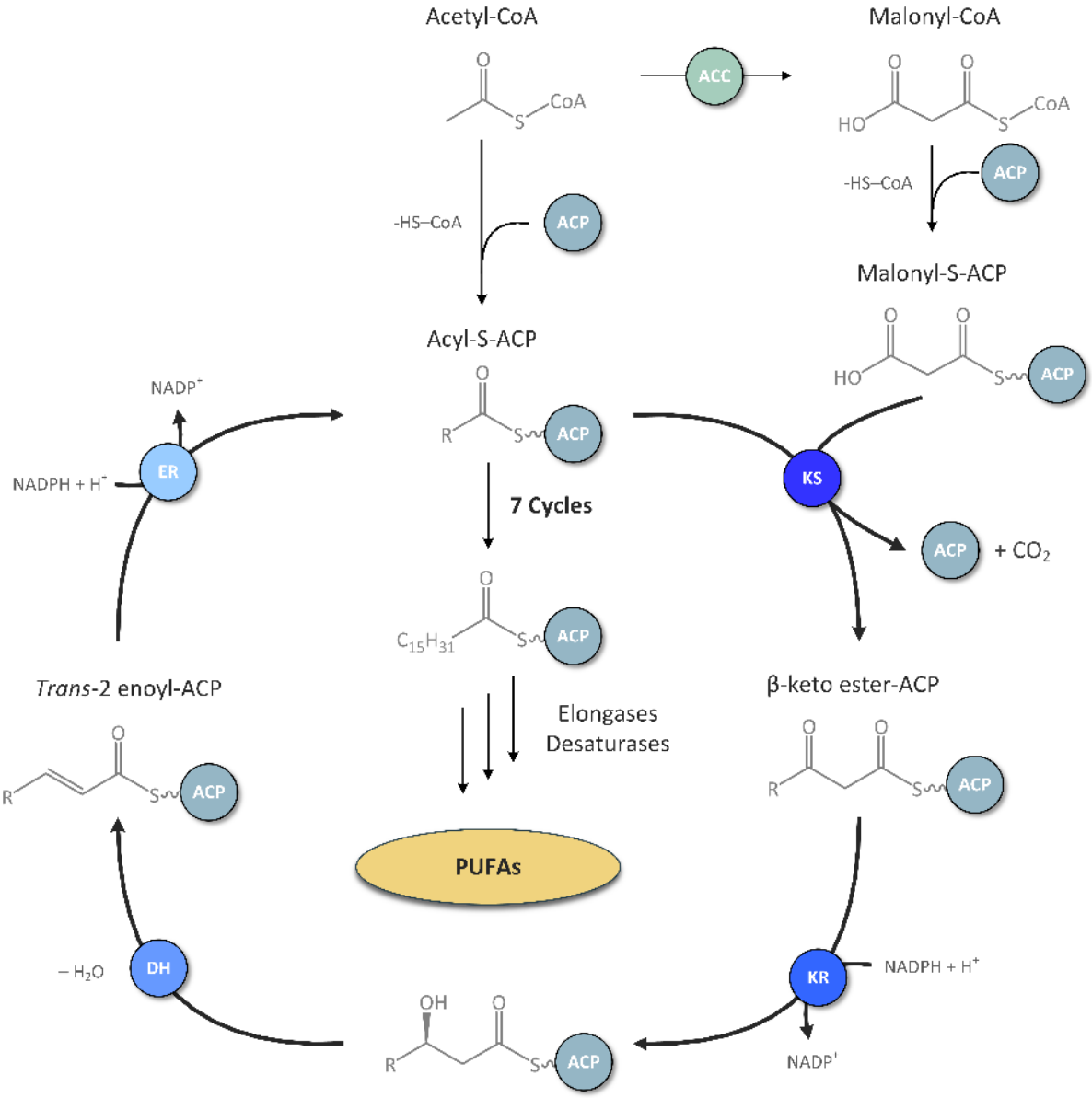

Figure 4: Aerobic fatty acid synthesis by FAS system.

Aerobic pathway representation by the FAS system in *E. coli*. In the first cycle acetyl-CoA is used as a primer molecule, thus the residual R of the Acyl-S-ACP is a methyl group (CH_3), whereas in every subsequent cycle it is prolonged by an aliphatic C_2 unit. Elongase and desaturase reaction is optional and specific to the organism. ACC: acetyl-CoA carboxylase, ACP: acyl carrier protein, KS: keto synthase, KR: keto reductase, DH: dehydrogenase, ER: enoyl reductase, PUFAs: poly-unsaturated fatty acids.

Initially, it was hypothesized that organisms which synthesize high levels of LC-PUFAs would primarily use the aerobic FAS-based pathway (Watanabe et al., 1997). Later, Metz et al. (2001) proposed an alternative pathway which involves polyketide synthases (PKS) and is today referred to as the anaerobic LC-PUFA synthesis pathway (Figure 5).

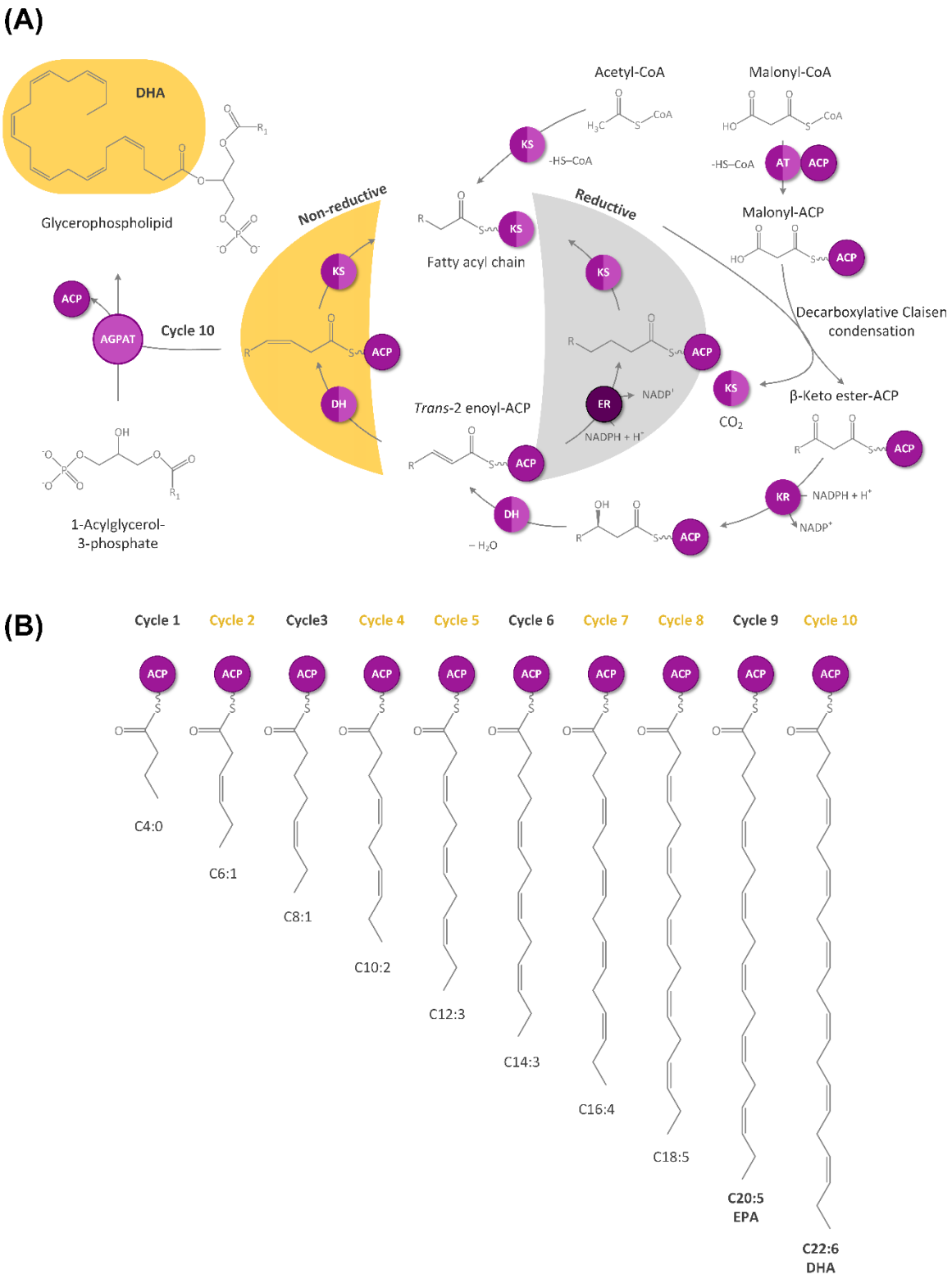

Figure 5: Anaerobic fatty acid synthesis by PKS-like PUFA synthases.

Anaerobic PKS-like PUFA synthesis pathway representation in *Aetherobacter* spp. (A) Acetyl-CoA is used as a primer molecule, thus the residual R of the Acyl-S-ACP is a hydrogen molecule (H), whereas in every following cycle it is prolonged by an aliphatic C_2 unit. Following the elongation and dehydratase reaction, the double bond is either reduced or isomerized into a *cis*-bond. The final product is determined by the enzyme complex. (B) Fatty acid intermediates after each cycle during the synthesis of DHA (Adapted from Ye et al. (2015). Yellow: Non-reductive cycle; Grey: Reductive cycle; ACP: acyl carrier protein, acyl transferase, KS: keto synthase, KR: keto reductase, DH: dehydratase/isomerase, ER: enoyl reductase, AGPAT: 1-acylglycerol-3-phosphate-O-acyltransferase.

As FAS and PKS systems are generally similar in their structure and enzyme complex, also the synthetic steps are rather similar. This includes the acetyl- and malonyl-ACP condensation (Figure 6A), followed by the reduction of the ketone group and the hydratase reaction. However, unlike FAS systems PKS-like systems comprise a reductive and a non-reductive route. The reductive route is chemically identical with the reaction in FAS-based systems (Figure 6B), whereas in the non-reductive route the generated double bond is not reduced but isomerized directly in the iterative process of chain elongation, which saves reducing equivalents in form of NADPH both in the oxidation and later reduction step (Figure 6C). The double bond is isomerized depending on the configuration as the *trans*-double bond is converted to a *cis*-double bond. Additionally, the double bond is shifted from the α,β-position to either the β,γ- or γ,δ-position, generating a methylene-interrupted polyene (Ye et al., 2015). This biosynthetic route enables microorganisms to synthesize PUFAs directly within an iterative chain elongation process, whereby specific double bonds are kept and rearranged. Which PUFA type is produced depends on the respective enzyme complex and the organism-specific PKS-like PUFA synthase (Gladyshev et al., 2013). The exact mechanism is not fully understood, but genetic shuffling, interchanging and multiplying certain enzyme domains created novel hybrid and cross-species PUFA synthases, thus the product spectrum could be rationally modulated (Gemperlein et al., 2019).

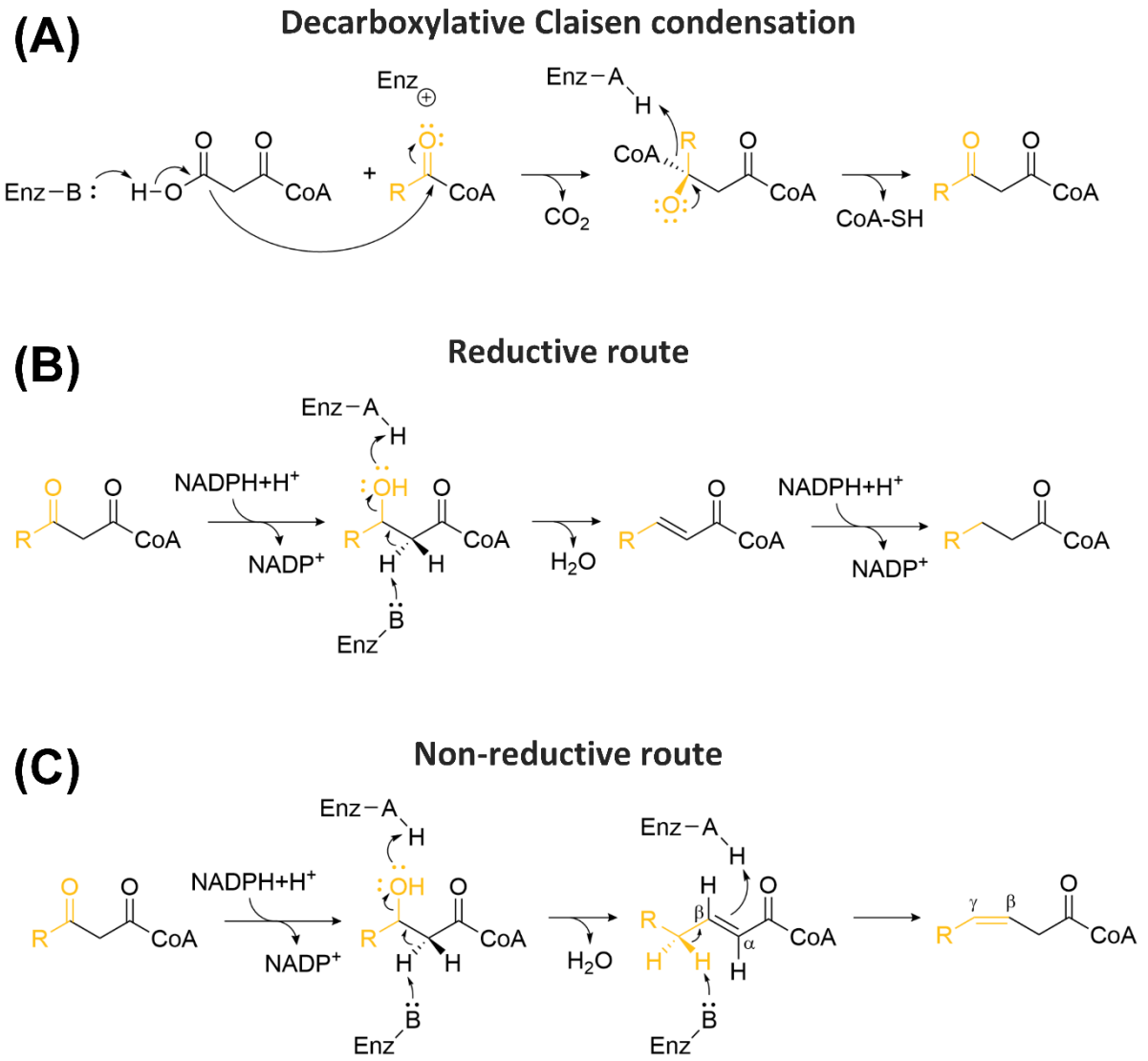

Figure 6: Enzymatic bio-catalysis of acyl-CoA in PKS-based PUFA synthases.

(A) Decarboxylative Claisen condensation. Due to a deprotonation, CO_2 is cleaved from malonyl-CoA following a nucleophilic attack at C_1 of the respective acyl-CoA (R=H or acyl chain). CoA is cleaved resulting in a β-keto-ester. Depending on the cycle and PKS synthase either (B) the β-keto-ester is reduced twice by NADPH or (C) reduced once and isomerized from a *trans*-α,β-double bond to a *cis*-β,γ-double bond. Enz = Enzyme; A = acid; B = base.

2.5 The origin of LC-PUFAs

Most organisms are unable to synthesize LC-PUFAs *de novo* due to the lack of desaturases that introduce a double bond after C9/10 in a fatty acid chain (Das, 2006). Thus, only a minority of organisms in the biosphere is able to produce EPA and DHA *de novo*. These organisms belong to the group of algae, fungi, mosses, and some bacteria (Sayanova & Napier, 2004; Uttaro, 2006), from which microalgae and species of the Thraustochytrids genus (e.g. *Schizochytrium* sp.) are known to be able to accumulate by far the highest amounts of LC-PUFAs (Gladyshev et al., 2013). Only a small percentage of the ~30,000 microalgae analyzed for fatty acid composition have been found to produce significant amounts of LC-PUFAs (Cohen et al., 1995). A list of organisms able to *de novo* synthesize LC-PUFAs is available in Gladyshev et al. (2013). Terrestrial LC-PUFA producers, like the myxobacteria *Aetherobacter* spp. (Garcia et al., 2016), are rare and contribute negligibly to global production (Kaštovská et al., 2007). Looking at the global production, algae produce more than half of the DHA and EPA existing world-wide (Guschina & Harwood, 2009b). Marine phytoplankton is producing 331.8 x 10^9 kg y^{-1}, marine macroalgae 1.2 x 10^9 kg y^{-1} and freshwater phytoplankton 28 x 10^9 kg y^{-1} (Gladyshev et al., 2013).

2.6 Shortage of LC-PUFA for human consumption

Despite the vast production of LC-PUFAs in marine organisms, only a small percentage of 0.2% is transferred into the terrestrial ecosystem. Water birds are the highest extractors with 432 x 10^6 kg y^{-1}, followed by human fishery with 180 x 10^6 kg y^{-1}. Other factors contributing to extraction include amphibiotic insects, riparian predators, drift of carrion or seaweeds (Gladyshev et al., 2009a). This indicates that there is no global scarcity of LC-PUFAs, yet humans still face a deficiency in these health-promoting molecules. The average human consumes about 16 kg fish (being their main source of EPA and DHA) per year, thus taking up 0.1 g LC-PUFAs per day (Gladyshev et al., 2009a), whereas for an general adult it is recommended to consume at least 0.5 g per day to maintain a healthy lifestyle (The French food safety agency with the lowest published recommendation of all food agencies; Li et al. (2021a)). Consuming fish to obtain sufficient LC-PUFA levels can increase the risk of harmful side-effects caused

by anthropogenic pollution. Heavy metals such as copper (Cu), cadmium (Cd), and particularly lead (Pb), accumulate in fish through the food chain, raising the need for benefit-risk ratios for fish consumption (Gladyshev et al., 2001; Gladyshev et al., 2009b). The same applies to pesticides, petroleum-based chemicals, or radionuclides (Barescut et al., 2011; Foran et al., 2005). Additionally, heavy metal pollution affects the efficiency of LC-PUFA transfer through the trophic chain, leading to even lower concentrations (Gladyshev et al., 2012). As industrialization progresses, maintaining a healthy diet becomes increasingly difficult due to factors such as intransparent supply chains, the addition of new food additives, and the pervasive impact of environmental pollution caused by human activities. In terms of LC-PUFAs, a good example for this challenge is the consumption of fish during pregnancy. While in 2004 the US Environmental Protection Agency recommended to limit the amount of fish consumed to 340 g per week due to heavy metal pollution (Lands, 2009), studies indicated that the intake of seafood of less than 340 g per week during pregnancy is associated with a risk for the infant to end up in the lowest quartile of the IQ distribution (Hibbeln et al., 2007).

Apart from the risk for the individual, it is in general not feasible for humanity to increase fish consumption since the oceans are already overfished (FAO, 2022), soon leading to a collapse of numerous fish populations (Brain & Prosser, 2022). Furthermore, fish as a resource is strongly dependent on season, location, and increasingly uncertain environmental conditions. Additionally, the LC-PUFA concentration declines with ongoing global warming as algae modulate their membrane fluidity by changing the membrane fatty acid saturation level. As water temperatures rise, the amount of unsaturated FAs decreases, consequently decreasing the levels in the whole trophic chain, including in the fish population (Colombo et al., 2020; Guschina & Harwood, 2009a). Ultimately, 96% of the human population may be at risk of not receiving sufficient supply of LC-PUFAs in the worst-case scenario (Colombo et al., 2020). Consequently, relying on fish as the primary source of LC-PUFAs for human consumption is no sustainable solution and there is an urgent need to find alternative PUFA sources.

2.7 Single-cell oils as possible future source for LC-PUFAs

Since the primary source of LC-PUFAs is microalgae, the supply of fish in aquaculture relies on external sources of harvested LC-PUFAs. The natural amount of microalgae present in aquaculture is often insufficient. As a result, the majority of produced fish oils (70%) from cheap fish feed, wild-caught fish and invertebrates are deployed as a PUFA source for fish feed (Sijtsma & de Swaaf, 2004). Therefore, aquaculture is not sustainable in its current form. For instance, in salmon aquaculture, the amount of fish biomass dissipated as feed exceeds the amount of fish harvested (Pauly et al., 2002).

A more sustainable and environment-friendly solution would be the decentralized production of high LC-PUFA containing microorganisms that serve as nutrient source in aquaculture or directly in human nutrition. The advantages over fish oils are numerous, as microbial production allows for targeted production of certain FAs from cheap and renewable resources at high yield without need for caught fish to obtain the LC-PUFAs. Microbial oil, normally referred as single-cell oils (SCO) as proposed by Colin Ratledge in 1976 (Ratledge, 1976) is defined as follows: "*single cell oil is the edible (triacylglycerol) oil that can be extracted from a microbial cell*" (Kyle & Ratledge, 1992). The idea of SCOs dates back to the late 19th century. Back then, the first organism being evaluated was *Claviceps purpurea* with a lipid content of 30% (w/w), followed by the analysis of *S. cerevisiae* in 1878. SCO research gained attention in Germany during the first World War when an alternative source for animal and plant oils was needed due to the disruption of trade relationships. The importance of SCOs further increased during World War II, when German researchers established a biotechnological process using *Geotrichum candidum* (milk mold) and other molds to produce SCOs. However, post-processing issues arose, leading to the direct use of biomass as feed for army horses. The German research remained dominant, leading to the Nobel prize for Professor F. Lynen in 1964 for the biosynthesis of fatty acids in yeast (Kyle & Ratledge, 1992). Over the years, the product spectrum increased from complex lipid mixtures for nutritional purposes to a wide variety of specific lipids and purified FAs.

Driven by the ongoing depletion and the negative impact of crude-oil usage on the environment, alternative bio-based sources for oleochemicals were intended to be established in the market. Oleochemicals are lipid-based molecules like

simple FAs, fatty alcohols (wax ester) or FA methyl esters (like Biodiesel) that find applications in various industries for the production of flavors, cosmetic additives, detergents, fuels or pheromones (Noweck & Grafahrend, 2006; Steen et al., 2010). The high demand of biodiesel cannot be accomplished by plant or animal-based lipids, since the require huge amounts of land and resources, consequently competing with the food production. Additionally, dependencies on climate, season and labor are further factors of uncertainties. Consequently, it is predicted that SCOs become the major producer of biodiesel in the future (Mathew et al., 2021). Nevertheless, as long as fossil-based products are cheaper and more demanded, SCO-based oleochemicals and fuels cannot compete since their cost-to-value ratio is not economically viable yet. The main cost driver here is product recovery, downstream processing, and purification. Since SCOs are stored intracellularly, the cell disruption and product extraction is the major obstacle to overcome to achieve a price-competitive bioproduct (Ochsenreither et al., 2016). However, high-value SCO enriched in LC-PUFAs could be already produced commercially (Madzak, 2021). Here, downstream processing costs are still high, but due to increasing demand, rarity in nature and high market price, profitable production is possible. As of today, several companies are producing LC-PUFAs which find application in DHA-supplemented infant formulas (Ochsenreither et al., 2016), human diet or fish feed (Tocher et al., 2019).

2.7.1 Natural producers of LC-PUFAs

Owing to their natural ability to produce LC-PUFAs (Gladyshev et al., 2013), autotrophic (photosynthetic) and heterotrophic, in particular decomposing microalgae are deployed to commercially produce SCO LC-PUFAs. Photosynthesis-based systems are cultivated in either open-pond systems or photobioreactors. However, open-pond systems are associated with challenges such as low cell densities, low growth rates, and issues with sterility, which often require the use of unfavorable high salinity media (Khozin-Goldberg et al., 2011). Photobioreactors on the other hand showed promising results in small-scale studies, but scale-up remains challenging. In a recent study by Gu et al. (2022), various microalgae species were tested in a small-scale screening, aiming to identify an process that has the potential to be scaled up to industrial production reliably. However, the researchers found no promising candidates, due to weak reproducibility and strain constraints, such as the inability to grow in suspension, fluctuations in light intensity, and hydrodynamic stress. These findings highlight the importance of developing more robust microalgae strains for industrial-scale production (Gu et al., 2022). Nevertheless, companies are interested in photosynthetic organisms for EPA production, like species from the genus *Nannochloropsis* (Khozin-Goldberg et al., 2011).

The above-mentioned limitations explain why light-independent heterotrophic microalgae are favored as LC-PUFA producers. The class of Thraustochytriaceae (e.g. *Schizochytrium* sp.) and the dinoflagellate *Crypthecodinium cohnii* (Mendes et al., 2009) are prominent LC-PUFA producing microalgae that have been commercialized by companies such as DSM for the production of DHA (Fedorova-Dahms et al., 2014). The first commercially available DHA-containing oil for infant formulas was DHASCO by Martek and OmegaTech made with *C. cohnii* (Ochsenreither et al., 2016). Currently, the lipid powder is manufactured using *Schizochytrium* sp and sold under the name DHASCO-B by DSM (Fedorova-Dahms et al., 2014). In these processes, microalgae are typically cultivated in artificial seawater and provided with glycerol or glucose as carbon source. However, raw sugar as substrate may become economically unfeasible in large-scale production (Du et al., 2021). Efforts were undertaken to substitute expensive raw materials by crude glycerol from biodiesel production (Lung et al., 2016; Pyle et al., 2008), wastewaters

(cheesemaking (Humhal et al., 2017); meat industry waste (Villarroel Hipp & Silva Rodríguez, 2018); spent media (Bagul & Annapure, 2020)), lignocellulosic hydrolysates (Patel et al., 2019), and many more to lower production costs. Increasing efforts and resources are spent to optimize all aspects of the process, including cultivation strategies, media optimization, bioreactor design, scale-up, downstream purification, and genetic engineering, with the aim to establish a cost-effective production process that is able to compete with fish oil-based processes (Du et al., 2021). Especially in microalgae, genetic engineering is a challenging task due to the complex nature of this novel biotechnological workhorse. Although there are some methods available for genetic modification, the efficiency of these methods remains poor today. In near future, newly developed techniques might improve the genetic engineering of microalgae (Du et al., 2021).

Besides, algae-based processes, the use of yeast and bacteria is an emerging option to produce LC-PUFAs, although exclusively in an academic context. Bacterial production was demonstrated in natural LC-PUFA producers like *Colwellia* species for DHA production (Kusube et al., 2017), albeit at very low growth rate and cell density (Wan et al., 2016). The same applies to the production of EPA by *Shewanella electrodiphila* (Zhang & Burgess, 2017) or recently discovered *Vibrio* strains (Estupiñán et al., 2020). It is noteworthy that all the stated bacteria were isolated in (deep) seawater, highlighting the unique role of LC-PUFAs in cold water as membrane structure modulators.

2.7.2 Heterologous producers of LC-PUFAs

Efforts have been undertaken to heterologously produce LC-PUFAs in established biotechnological organisms such as *Escherichia coli* (Amiri-Jami & Griffiths, 2010), lactic acid bacteria (Amiri-Jami et al., 2014) or *Pseudomonas putida (Gemperlein et al., 2016)*. In general, established workhorses have several advantages over natural producers. When it comes to large-scale production, natural producers may not always possess the necessary attributes required for biotechnological processes. In short, a producer strain needs to bring (1) robustness against the industrial conditions and contaminants (2) ease of genetic engineering (3) tolerance (pH, temperature, osmotic stress, toxic

compounds, reactive oxygen species (ROS), target product), (4) genetic stability, (5) high growth rate, (6) high possible cell densities, (7) a broad substrate spectrum, (8) use of biomass as byproduct, and a broad knowledge base (Nielsen, 2019). These abilities are either already given by the strains' nature or are achieved by genomic modifications or adaptive laboratory evolution (ALE, random mutagenesis). Every chassis strain once started as a wild-type organism with moderate basic features. In a proposed chart for the development of a chassis strain from scratch by Calero and Nikel (2019) the sequencing of the genome is the first step to become a potential cell factory chassis, followed by the establishment of robust genetic tools and metabolic models, which goes hand in hand with the physiological characterization by all forms of -omics technologies (genomics, transcriptomics, proteomics, metabolomics, lipidomics, fluxomics). Lastly, the strain could be streamlined by reducing the genome (deletion of undesired by-product formation and unnecessary cellular functions and structures etc.) and the development of a mutant collection for more specific applications. Understandably, no Swiss army knife was ever created; strain properties might be beneficial for one application but detrimental for another. Consequently, the selection of the right chassis strain is the base for a good process.

Potential organisms from the fungus kingdom have been tested for LC-PUFA production. *Ashbya gossypii* has been engineered to produce LC-PUFAs including EPA and DHA by inserting genes for elongases and desaturases. *S. cerevisiae* was engineered to produce the LC-PUFA eicosadienoic acid (EDA) but poor viability due to LC-PUFA-triggered increase in ROS (Guo et al., 2019; Johansson et al., 2016). Finally, oleaginous yeasts have proven suitable to produce and store high amounts of FAs in form of lipid bodies, such as *Rhodosporidium toruloides* (Arbter et al., 2019) and *Yarrowia lipolytica*, rendering them ideal candidates for heterologous PUFA production.

2.8 *Yarrowia lipolytica* as an oleaginous cell factory

In addition to the advantageous properties and applications already discussed, *Y. lipolytica* exhibits specific benefits and the necessary lipid machinery for the hyper-production of lipids. It is able to naturally accumulate lipids up to 30-50% of its cell dry mass (CDM) under certain starvation conditions. Meanwhile, genetically engineered strains are reaching lipid contents of up to 90%, known as obese strains (Beopoulos et al., 2009b; Blazeck et al., 2014; Dulermo & Nicaud, 2011; Qiao et al., 2015). *Y. lipolytica* naturally maintains high metabolic flux to the fatty acid precursors acetyl-CoA and malonyl-CoA. Lipid accumulation is triggered by nutrient limitation, whereas nitrogen starvation is convenient to realize thus the common choice (Beopoulos et al., 2009c). Additionally, excess concentrations of the carbon source combined with iron, phosphate, inositol, or zinc limitation stimulates *de novo* lipid biosynthesis (Beopoulos et al., 2009a). When *Y. lipolytica* detects a nutrient starvation, it switches from the biomass production to the lipogenesis, redirecting central carbon metabolism towards lipid storage until the excess carbon source is depleted. In need for energy, lipids are then catabolized on demand via β-oxidation. (Makri et al., 2010). As a result of the lipid accumulation, *Y. lipolytica* naturally maintains an elevated acetyl-CoA pool and a high pentose phosphate pathway (PPP) activity (Christen & Sauer, 2011). These properties render it an ideal chassis strain for all CoA thioester-based products (Lazar et al., 2018). *Y. lipolytica* has been the subject to produce SCOs, owing to its ability to produce the highest known concentrations of linoleic acid (LA; 50% of total fatty acids (TFA) (Beopoulos et al., 2009c; Liu et al., 2021). *Y. lipolytica* is able to intracellularly sustain up to 30% free FAs (Beopoulos et al., 2012; Tsigie et al., 2011). As demonstrated in studies with *S. cerevisiae*, exposure to high concentrations of unsaturated fatty acids result in elevated levels of reactive oxygen species (ROS) and radicals, ultimately leading to cell death (Johansson et al., 2016). Due to the high level of desaturation the risk for lipid peroxidation increases (Howlett & Avery, 1997), which propagates leading to a chain-reaction of radical generation. *Y. lipolytica* however exhibits high stress resistance towards oxidative stress in general. The yeast activates antioxidizing enzymes (foremost superoxide dismutase) and cell repair mechanisms upon oxidative stress (Lopes et al., 2009).

In the past, intense research aimed at producing various types of FAs and derivatives thereof. Wang et al. (2022) recently summarized the scientific efforts to establish *Y. lipolytica* as workhorse for FAs with tailored chain-lengths, opening the possibility to synthesize a broad lipid spectrum ranging from short-chain FAs (SCFA; C6), over medium-chain (MCFA, C12) to very long-chain FAs (VLCFA; C42) with variations in the degree of saturation (poly- or mono-unsaturated, to fully saturated), and even odd-chain FAs (Gemperlein et al., 2019; Park et al., 2020; Rutter et al., 2015; Wang et al., 2022).

Alternatively, PUFA-enriched biomass can be utilized directly e.g., as feed stock or SCOs. Extracted and purified FAs find application in pharmaceuticals or as food additives, thus belong to the group of nutraceuticals. A cornerstone of the last decade was the establishment of a genetically modified (GM) *Y. lipolytica* strain that has been engineered to produce EPA-enriched SCOs with a concentration of 56.6% of TFAs. Strain and bioprocess were patented by DuPont in 2009 (US2009/0093543A1), published in 2013 (Xue et al., 2013a) and since then commercialized as EPA-enriched biomass or SCO for feed and food applications: From 2010 to 2013, a SCO product for human consumption called New Harvest™ was advertised as a fish alternative for vegetarians but was eventually discontinued. Today, the EPA-rich biomass from DuPont is utilized for the production of the LC-PUFA rich salmon Verlasso™ by the company AquaChile (Madzak, 2021). The EPA process was the first commercialized bioprocess relying on a GM *Y. lipolytica*. The genetic modifications comprised the heterologous integration of elongases and desaturases with the aim to extend the aliphatic chain starting with the native LA molecule (C18:2). EPA yields were further improved by deleting competing pathways and adding multiple gene copies of crucial enzymes (Xie et al., 2015; Xue et al., 2013a). Using the same approach DuPont also patented a process for DHA production (US8685682B2, US20060115881A1), but here they only reached 5.6% DHA of TFAs (Wang et al., 2022).

2.8.1 LC-PUFA production in *Y. lipolytica* expressing heterologous myxobacterial polyketide synthase

Besides the above mentioned developments, recent efforts focused on the expression of myxobacterial PKS-like PUFA synthases in *Y. lipolytica* (Gemperlein et al., 2019). Strain Po1h served as chassis to express multiple myxobacterial PUFA synthases. Both native gene cluster variants and hybrid constructs were tested, resulting in LC-PUFA-producing strains with distinct LC-PUFA spectra depending on cluster design. Isolated soil bacteria *Aetherobacter fasciculatus* (SBSr002) and *Minicystis rosea* (SBNa008) served as donors for novel PUFA biosynthetic gene clusters (BGCs), along with a 4′ phosphopantetheinyl transferase (PPTase), resulting in strains producing either DHA or ω6 LC-PUFAs (arachidonic acid, docosatetraenoic acid, tetracosaenoic acid) as major FA, depending on the employed cluster. In order to vary and extend the product spectrum certain PUFA BGC domains were interchanged between the two cluster variants, resulting in strains with functional hybrid gene clusters that allowed for the synthesis of novel FAs in the range of C20:3 and C24:5. The combinatorial approach displays a promising tool to manufacture tailor-made FAs or FA mixtures, as LC-PUFA biosynthesis with the anaerobic PKS-based synthesis pathway demands significantly less redox power in the form of NADPH, compared to the elongase/desaturase-based approach. In particular for DHA, the PKS-based systems yielded DHA levels as high as 16.8% whereas the published results for DHA production by DuPont only reached 5.6% of TFAs. Consequently, the idea, i.e. strains and fermentation process need to be further optimized and tested, as it displays a potential candidate for an industrial application.

3 Materials and Methods

3.1 Chemicals and Enzymes

All chemicals and kits were purchased from Sigma-Aldrich if not stated otherwise. Restriction enzymes were FastDigest Enzymes from Thermo Scientific, if not stated otherwise. Plasmid preparations were done with QIAprep Spin Miniprep Kit (QIAGEN), PCR and Gel purifications of DNA were made with Wizard SV Gel and PCR Clean-Up System (Promega).

3.2 Plasmids and Strains

E. coli DH10B (Thermo Fisher Scientific, Waltham, MA, USA) was used for cloning purposes. The basic *Y. lipolytica* Po1h (CLIB 882) was taken from previous work (Gemperlein et al., 2019). Strains were maintained as glycerol stocks at -80°C. The plasmids pUC19 (NEB, Ipswich, MA, USA), as well as pACYC_assembly, pKG2-PIS and pSynPfaPptAf4, respectively (Gemperlein et al., 2019), were used for cluster assembly. All used strains and plasmids are listed in the supplement (Table S2 and S3).

3.3 Molecular design and genetic engineering

For the design of cloning strategies, the software SnapGene 6 (Insightful Science, San Diego, CA, USA) was used. The workflow for assembly of different PUFA cluster variants was as follows. In the first step, the gene sequence of interest and the sequence of the *Lip2t* terminator were amplified from the plasmid pSynPfaPptAf4. The corresponding promoter sequences were synthetized (GenScript, Piscataway Township, NJ, USA). The different elements (promoter, gene, and terminator) were then fused and integrated into the linearized vector pUC19 using restriction enzymes and Gibson assembly. Optionally, the respective number of UAS1B tandem repeats was integrated too (SmaI). PCR and sequencing were conducted to verify the correctness of each construct (Genewiz, Leipzig, Germany). The plasmids were transformed into *E. coli* DH10B by heat shock for amplification and isolation (Inoue et al., 1990).

Four single-gene constructs were then assembled and integrated into pACYC_assembly. The correct order of *pfa1, pfa2, pfa3*, and *ppt* was achieved using selective restriction (SdaI/ApaLI, AvrII/PacI, ApaLI/AclI, AclI/PacI, FastDigest Enzymes, Thermo Fisher) and ligation cycles (Fast-Link DNA Ligation Kit, Lucigen, Middleton, WI, USA). The plasmids were transformed into *E. coli* DH10B by heat shock for amplification and isolation (Inoue et al., 1990). The obtained four-gene clusters were validated by PCR and then integrated into the plasmid pKG2-PIS using restriction (SdaI/PacI, Thermo Fisher) and ligation (Lucigen). The plasmid was amplified and isolated as described above, and once again validated by PCR. Subsequently, the vector was linearized (SmiI/NotI, Thermo Fisher). The linearized DNA was integrated into *Yarrowia lipolytica* Po1h (YALI0_C05907g) using lithium acetate mediated heat shock transformation (Barth & Gaillardin, 1996). In short, competent cells were prepared by resuspending $5*10^7$ cells in 600 µL lithium-acetate (LiAc) solution (0.1 M, pH 6.0), followed by incubation for 1 h at 28°C. Afterwards, the cells were harvested (4000 x *g*, 1 min, RT), resuspended in 40 µL of LiAc solution, amended with 10 µL of Herring testes carrier DNA (10 mg mL^{-1} in TE buffer, denatured) and 500 ng of linearized target DNA, and incubated for 15 min at 28 °C. Afterwards, 350 µL of the LiAc-PEG solution (40% PEG 4000 in 0.1 M lithium acetate, pH 6.0) was added, followed by further incubation for 1 h at 28 °C. Finally, 40 µL DMSO was added, and the mixture was heat shocked at 39 °C for 10 min, resuspended in 600 µL LiAc solution, and plated on YNB-Glu_{10}-N_5. After 3-4 days of incubation at 28 °C, the grown colonies were checked for the correct integration by colony PCR. A positive clone was additionally checked for the presence of each of the four PUFA genes and qualitatively evaluated for DHA production using GC-MS analysis of its fatty acid composition after culturing in glycerol-based medium (see below), prior to cryo-conservation.

3.4 PUFA Cluster stability test

The presence of the four PUFA genes was tested in a shake flask experiment, cultivating the strains for seven days in YNB-Gly_{10}-N_5. Based on the cell count to OD_{600} correlation of $5.4*10^6$ cells at an OD_{600}=1 for Yarrowia lipolytica GB20, the corresponding volume for 100 cells was plated out on a YNB-Glu_{10}-N_5 agar plate.(Holkenbrink et al., 2018a) After 2-3 days incubation cells were checked by colony PCR with primers Pr33/Pr34, Pr35/Pr34, Pr36/Pr37 and Pr38/Pr34, probing the ORFs of *pfa*1/2/3 and *ppt*, respectively.

3.5 Media

Brain Heart Infusion Medium (BHI, Becton Dickinson, Heidelberg, Germany) in liquid or solid form was used to grow *E. coli* DH10B. For *Yarrowia lipolytica* Po1h YPD medium was used containing 10 g L^{-1} yeast extract, 20 g L^{-1} peptone and 22 g L^{-1} Glucose. All other *Yarrowia lipolytica* strains were grown in a chemically defined medium (YNB-Gly/Glu_{10}-N_5) with 1,7 g L^{-1} YNB (Sigma-Aldrich, Darmstadt, Germany), 10 g L^{-1} Glycerol or Glucose, 5 g L^{-1} $(NH_4)_2SO_4$ and 200 mM MES (2-(*N*-morpholino)ethanesulfonic acid; pH=6.7). For solidification of media 20 g L^{-1} agar (Becton Dickinson, Heidelberg, Germany) was used. For plasmid selection 100 µg mL^{-1} Ampicillin, 25 µg mL^{-1} Chloramphenicol or 50 µg mL^{-1} Kanamycin was used.

3.6 Shake flask cultivation.

Cultivation experiments were conducted in 500 mL baffled shake flasks, filled with 50 mL of medium and incubated on an orbital shaker (5 cm shaking diameter, 230 rpm, Multitron, Infors AG, Bottmingen, Switzerland) at 28 °C and 80% humidity. The preculture was inoculated with a single colony from a two-day pre-incubated plate culture, grown overnight, harvested (4000 x*g*, RT, 1 min), and used to inoculate the main culture to a starting OD_{600} of 0.1. All cultivations were conducted in biological triplicate.

3.7 Mini-bioreactor cultivation

Yarrowia lipolytica was cultivated in micro-bioreactors (BioLector 1, M2Plabs, Baesweiler, Germany) in 48-well flower plates (M2Plabs) with pH optodes for screening purposes in triplicates. Online measurement for growth (light scattering at 620 nm) and pH (optodes) in 10 min intervals. Temperature was set to 28 °C and humidity to 85%. Shaker speed was 1300 rpm, filling volume was 600 µL of YNB-Glu_{10}-N_5 medium. Wells were inoculated from an over-night preculture (YPD) to an OD_{600} = 0,1.

3.8 Determination of cell concentration

The cell concentration was inferred from photometric measurement at 600 nm. An experimentally obtained correlation for *Y. lipolytica* allowed to infer the concentration of the cell dry mass (CDM) from OD_{600} readings: CDM [g L^{-1}] = 0.424 × OD_{600} (Gläser et al., 2020).

3.9 Quantification of extracellular metabolites

3.9.1 Quantification of glycerol and citrate

Glycerol and citrate were quantified by HPLC (Agilent 1200 series, Agilent Technologies, Waldbronn, Germany) using an anion exchange column (300 x 7.8 mm, Aminex HPX-87H, Bio-Rad, Hercules, CA, USA) at 45 °C and 12 mM H_2SO_4 at a flow rate of 0.5 mL min^{-1}. The analytes were detected *via* refractive index measurement and quantified using external standards. The method allowed to assess also other organic acids and alcohols.

3.9.2 Quantification of phosphate.

Ion chromatography (Dionex Integrion, Thermo Scientific) was used to quantify phosphate in culture samples. The set-up included a carbonate-selective anion-exchange column (IonPac AG9-HC, IonPac AS9-HC, Dionex Integrion) at 35 °C as stationary phase and 12 mM Na_2CO_3 (0.25 mL min^{-1}) as mobile phase and was operated with eluent suppression (ERS 500 suppressor, 20 mA, Dionex

Integrion). Phosphate was detected using a conductivity analysis and quantified via external standards.

3.10 Extraction and transesterification of fatty acids

An amount of 5 mg of CDM was transferred into a glass vial, collected (12,000 x*g*, 4 °C, 5 min), and dried in a vacuum concentrator (Savant DNA 120 SpeedVac, Thermo Fisher) for 60 min at 65 °C and 9 mbar. Then, 300 µL of a mixture of methanol, toluene, and 95% sulfuric acid (50:50:2; v/v/v) was added for simultaneous extraction and transesterification into the corresponding fatty acid methyl esters (FAMEs). Hereby, *n*-3 heneicosapentaenoic acid methyl ester (HPA, 22:5, Cayman Chemical, Ann Arbor, MI, USA) was added as internal standard. The mixture was incubated at 80 °C for 24 h. After cooling down to room temperature, the reaction was neutralized with 250 µL of a stopping solution (0.5 M NH_4HCO_3 and 2 M KCl in H_2O). After phase separation (12,000 x*g*, RT, 5 min), the organic phase was taken further for analysis.

3.11 Analysis of FAMEs by GC-MS

The analysis was conducted on a GC-MS instrument (6890 GC, 5973 inert MSD, Agilent Technologies), whereby the FAMEs were separated on a fused silica high polarity column (HP-88, 30 m, 0.25 mm, 0.2 µm, Agilent Technologies). Samples (1 µL) were injected at a 5:1 split ratio using helium as carrier gas. The column was initially kept at 110 °C for 1 min and then heated until 240 °C at a heating rate of 4 °C min^{-1}. The injector, the MS transfer line, the ion source, and the quadrupole were kept at 250 °C, 280 °C, 230 °C, and 150 °C, respectively. After a 5 min solvent delay, the mass detector was operated in scan mode (*m/z* 25 - 500*)*. The analytes were identified based on retention time and fragmentation pattern using a mixed synthetic standard (Supelco 37 Component FAME Mix, Sigma-Aldrich) and pure DHA (Cayman Chemical). Quantification was based on HPA as internal standard.

3.12 Extraction and quantification of intracellular CoA thioesters

The analysis of CoA thioesters was performed as described previously (Glaser et al., 2020). In short, broth (containing 8 mg CDM) was transferred into the four-fold volume of an extraction and quenching buffer (95% acetonitrile, 25 mM formic acid, -20 °C), followed by the addition of an internal ^{13}C-enriched CoA thioester standard. After incubation for 10 min on ice, the solution was clarified from debris (15,000 x*g*, 4 °C, 10 min). The obtained supernatant was mixed with 10 mL of ice-cold deionized water. The residual pellet was washed twice with 8 mL ice-cold deionized water. All extracts were combined, frozen in liquid nitrogen, and freeze-dried. The obtained pellet was dissolved in 500 µL buffer (25 mM ammonium formate, pH 3.0, 2% methanol, 4 °C) and the obtained solution was filtered (Ultrafree-MC, GV 0.22 µm, Millipore, Germany). The CoA thioesters in the filtrate were analyzed by LC-ESI-MS/MS (Agilent Infinity 1290 System, QTRAP 6500+, AB Sciex, Darmstadt, Germany) (Glaser et al., 2020). Hereby, separation was based on a core–shell reversed phase column (Kinetex XB-C18, 100 × 2.1 mm, 2.6 µm, 100 Å, Phenomenex) at 40 °C as stationary phase and a gradient of formic acid (50 mM, adjusted to pH 8.1 with 25% ammonium hydroxide, eluent A) and methanol (eluent B) as mobile phase at 300 µL min^{-1}: 0–7 min, 0–10% B; 7–10 min, 10–100% B; 10–11 min,100% B; 11–12 min, 100–0% B; 12–15 min, 0% B. Multiple reaction monitoring (MRM) was used for detection. Samples were analyzed in biological triplicate.

3.13 Gene expression analysis using qRT-PCR

Cells were quickly collected by centrifugation (20,000 *xg*, 4 °C, 1 min). The obtained pellet was immediately frozen in liquid nitrogen. Total RNA was isolated using the RiboPure RNA Purification Kit (Invitrogen). RNA concentration and RNA quality was evaluated (NanoDrop 1000, Thermo Scientific, Agilent 2100 Bioanalyzer, RNA 6000 Nano kit, Agilent Technologies). Then, the RNA (250 mg) was converted into cDNA (Maxima First Strand Kit, with dsDNase, Thermo Scientific). The cDNA samples were diluted 1:100 in DEPC-treated water (Invitrogen, Waltham, MA, USA). The analysis was conducted in a real-time PCR system (QuantStudio 3 System, Thermo Scientific) using the PowerUp SYBR Green Master Mix (Applied Biosystems, Waltham, MA, USA) and Microamp Fast

Optical 96-Well plates (Applied Biosystems). Primers (Table S4) were designed using Primer3Plus, Primer-BLAST, and OligoCalc, respectively, and experimentally validated by PCR and a standard curve test (Kibbe, 2007; Untergasser et al., 2012; Ye et al., 2012). For normalization, the 25S rRNA gene (YalifMr30) was used (Jain et al., 2018; Kozera & Rapacz, 2013). Samples were analyzed in biological triplicate.

3.14 Flux balance analysis in *Yarrowia lipolytica*

Based on a genome-scale metabolic model (iYali4; MODEL1508190002) from Kerkhoven et al. (2016) a reduced model with 86 reactions of the central metabolism, including 86 metabolites and 6 compartments (cytoplasm, endoplasmic reticulum, mitochondria, peroxisome, lipid body, extracellular space) was created, including the heterologous reactions for DHA synthesis. The model includes relevant substrates (e.g. glucose, glycerol, acetate) and side-products. Metabolic demand for biomass formation (based on *S. cerevisiae*) was taken from Gruchattka et al. (2013). The software CellNetAnalyzer (MATLAB based) was used for the flux balance analysis (Klamt et al., 2007).

3.15 DHA production in a fed-batch process

The production performance of the DHA-producer *Y. lipolytica* Po1h::pSynPfaPptAf4 was evaluated in a fed-batch process. Fermentation was carried out in glucose and in glycerol-based medium using 1 L DASGIP bioreactors (Eppendorf, Jülich, Germany). The initial batch medium (300 mL), contained per liter: 25 g glucose or 25.6 g glycerol, 5 g $(NH_4)_2SO_4$ (C/N ratio 11), 1.7 g YNB w/o amino acids, 1 g KH_2PO_4, 200 mM MES (pH 5.5), and 1 mL antifoam (Antifoam 204, Sigma, Germany). The process was inoculated with exponentially growing cells from an overnight pre-culture. Feeding (600 g L^{-1} glucose or 600 g L^{-1} glycerol) was started at a rate of 1.5 mL h^{-1}, when the substrate was depleted. During the feed phase, the level of the carbon source was monitored online. The data were used to re-adjust the feed rate in order to avoid a limitation of the carbon source. Cultivation temperature was maintained constant at 28 °C. The pH and the pO_2 level were monitored online with a pH

electrode (Mettler Toledo, Gießen, Germany) and a pO_2 electrode (Hamilton, Höchst, Germany). The pH was kept constant at 5.5 ± 0.05 by automated addition of 6 M NaOH and 6 M HCl. The dissolved oxygen level was maintained above 30% of saturation during the batch phase and was reduced to 5% during the feed phase (Qiao et al., 2017) by variation of stirrer speed and aeration rate. Data acquisition and process operations were controlled by the DASGIP control software 4.0 (Eppendorf, Jülich, Germany).

4 Results and discussion

4.1 Medium design for the production of DHA in *Y. lipolytica*

Previous work has successfully expressed myxobacterial PKS-like PUFA synthases in *Y. lipolytica* aiming to produce various LC-PUFAs, however, only low quantities were reached in the unoptimized media (Gemperlein et al., 2019). To make biotechnological processes more attractive for industrial applications, high product titers must be achieved. Optimizing the medium is a crucial aspect of making the bioprocess economical. The choice of carbon, nitrogen and phosphate sources and their concentrations can have a significant impact on the metabolic pathways and consequently on the synthesis of the target product (Singh et al., 2017). This is particularly crucial for the lipid production in *Y. lipolytica*, as lipid accumulation is governed by complex and multifactorial regulatory mechanism (Bellou et al., 2016; Kolouchová et al., 2016). Accordingly, we conducted experiments to test the initial medium and establish stable initial conditions. Based on this, we further investigated the influence of various media components on DHA production to determine the most influential factors.

4.1.1 Basic DHA production in chemically defined minimal media at stable conditions.

YNB contains all vitamins, trace elements and salts needed for yeast growth (Wickerham, 1946). Commonly, a nitrogen source is contained in the commercial product, but also amino acids (AA) containing variants and versions for nutrient-based selection are available. For the conducted media development, the base variant without AA or nitrogen source was used. Optimal growth conditions, carbon and nitrogen sources, as well as concentrations and ratios thereof were tested.

As a reference, chassis strain Po1h was cultivated on the YNB-Glu_{10}-N_5 medium (pH=5.8) with 50 mM potassium phosphate buffer (Figure 7). The strain grew exponentially at a specific growth rate (μ_{max}) of 0.36 ± 0.01 to a biomass concentration of 5.29 ± 0.12 g L^{-1}, which corresponds to a biomass yield of 0.49 g_{CDM} g_{Glu}^{-1}. Biomass concentration slightly decreased in stationary phase. As the culture reached stationary phase after 13 h, pH has dropped from the initial 5.8 to 2.3, likely due to citrate secretion (Madzak, 2021). As a stabile pH is a crucial parameter in strain analysis, different buffer systems and their buffering capacity were further investigated.

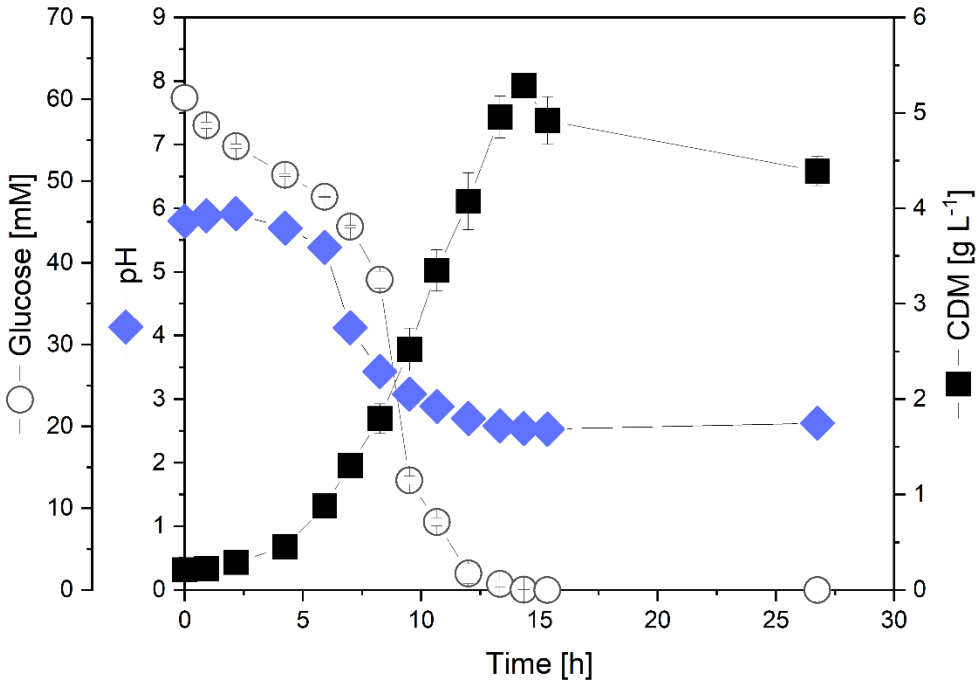

Figure 7: Cultivation profile of *Y. lipolytica* Po1h.
Cultivation was conducted in YNB-Glu_{10}-N_5 medium supplemented with 50mM potassium phosphate, measuring substrate concentration and pH. CDM: cell dry mass.

Biological hydrogen ion buffers keep pH changes within an acceptable range and thus assure reproducible and balanced growth of a microbe. Microorganisms depend on a certain pH range that allows their cell machinery, especially enzymes, energy generation and transport mechanisms, to function optimally. Simple buffering agents such as citric acid, acetic acid or phosphate offer a cheap solution for fermentation processes. However, these substances are potentially metabolized and may have undesired side effects or interfere with cellular processes, thus Norman Good and colleagues established a selection of

biological buffers called Good's buffers (Good et al., 1966). These currently twenty buffers vary in their applicable pH range and pK_a value and meet important chemical criteria such as good solubility, low toxicity, membrane impermeability and stability. As *Yarrowia* is known to secrete citrate and grows best at a pH around 6, the two buffering agents MES and ACES with one of the lowest pK_a values of all Good's buffers were chosen to be tested in *Yarrowia* cultivations. MES offers the lowest pK_a of all Good's buffers with a maximum buffer capacity at a pH of 6.1 (at 25 °C) and a usable pH range of 5.5 to 6.7. ACES buffers in a slightly higher pH range of 6.1-7.5 with a pK_a of 6.78. Together with the initially utilized phosphate buffer, MES and ACES were tested at varying concentrations and compared in the resulting growth rate and absolute pH drop (Figure 8).

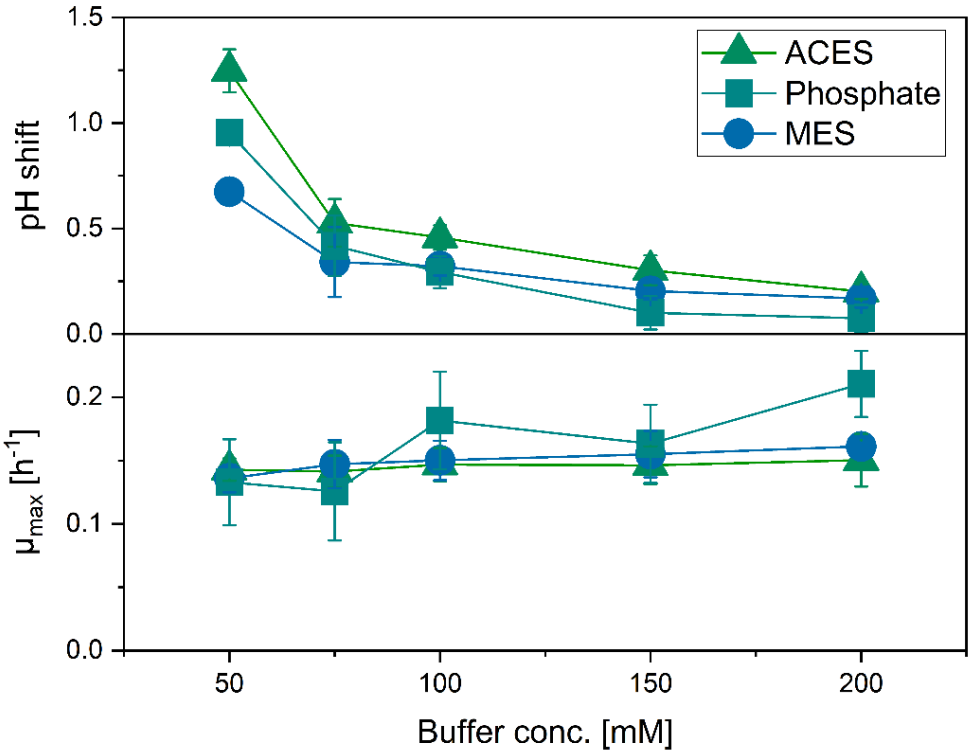

Figure 8: Biological pH buffer test for *Y. lipolytica* cultivations.

Test was conducted in a microbioreactor system in triplicates for every condition. pH shift was calculated in real time by on-plate reference wells for calibration. μ_{max} was calculated from the obtained growth data. ACES: N-(2-Acetamido)-2-aminoethanesulfonic acid, MES: 2-(N-morpholino)ethanesulfonic acid.

The comparison was carried out in a micro-bioreactor, parallelly testing 15 conditions in triplicates in a 48-well flower plate. After the cultures reached their maximal cell density, cultivation was stopped and analyzed for growth and pH. The maximal growth rate of all buffer systems remained between 0.14 and 0.15 h^{-1}, whereas ACES and MES resulted in a stable and similar μ_{max} for all buffer concentrations, confirming the properties of Good's buffer having no influence on growth. Phosphate buffer seems to affect growth rate leading to slight fluctuation in growth. As for the shift in pH throughout the cultivation, all buffer systems improved by increasing the buffer concentration. An increase to 200 mM of each buffer led to moderate pH shift of 0.2, 0.16 and 0.07 for ACES, MES, and phosphate buffer, respectively. Phosphate as a simple and cheap buffer resulted in the best buffering performance and potential growth benefits, whereas MES with its properties as a Good's buffer exhibits sufficient buffering capacity and has the most acidic buffering range. For further investigation MES and phosphate buffer were selected to be tested in a standardized cultivation setup (Table 1). Since the buffers have different pK_a values, the initial pH was set to 6.7 for phosphate and 5.8 for MES. *Y. lipolytica* is able to grow in a broad range of pH from 3.5 to 8 (Sutherland et al., 2014), however within that range cell morphology and growth rate differ. *Y. lipolytica* is more likely to grow in a yeast-like morphology with decreasing pH (Ruiz-Herrera & Sentandreu, 2002). Optimal growth was observed at pH 5.6 (Timoumi et al., 2017)

Table 1: pH buffer performance of MES and phosphate buffer.

Shake flask cultivations were conducted in YNB-Glu_{10}-N_5 (n=3). pH shift was measured from the difference from inoculation to the lowest point during cultivation. Initial pH in the media: phosphate - 6.5 and MES - 5.8, respectively.

Buffering agent	100 mM		200 mM	
	μ_{max} [h^{-1}]	pH shift	μ_{max} [h^{-1}]	pH shift
MES	0.26 ± 0.02	2.20 ± 0.08	0.26 ± 0.02	0.55 ± 0.01
Phosphate	0.27 ± 0.01	0.56 ± 0.01	0.25 ± 0.01	0.25 ± 0.01

Both buffering enabled maximal growth rates independent from the chosen concentration. pH dropped in 100 mM MES. Here, the buffer capacity was insufficient to buffer at the lower acidic end of its pH range of 5.5 to 6.7. For all other conditions moderate pH shifts of 0.55 and 0.25 for MES and phosphate,

respectively, were measured. Consequently, both buffers were considered suitable for a production medium and were further tested on DHA-producing *Yarrowia* strains, since pH range and phosphate availability may influence DHA biosynthesis.

DHA production tests were conducted with strain *Y. lipolytica* Po1h::Af4, in standard YNB-Glu_{10}-N_5 medium in combination with the preselected buffer systems (Figure 9). As a reference, the base condition with 50 mM phosphate buffer was set to pH = 6.5, as phosphate buffers best at neutral pH (Figure 9A). The culture grew exponentially with a μ_{max} of 0.23 ± 0.01 h^{-1} reaching a maximal cell concentration of 5.9 ± 0.1 g L^{-1}. As for the wild type *Y. lipolytica* Po1h, OD decreased slightly in stationary phase and pH dropped by 3 from 6.65 to 3.5 and increased again to 6 in stationary phase, likely upon citrate re-uptake, which later analysis of extracellular citrate concentrations in *Yarrowia* cultivations revealed. DHA concentration reached a maximal CDM of 5.7 mg g_{CDM}^{-1} after approximately 20 h. When increasing the buffer capacity to 200 mM phosphate, pH was stable at around 6.5 whereas the DHA end concentration of 4.85 mg g_{cdw}^{-1} was about 15% lower compared to 50 mM (Figure 9B). The maximal specific growth rate was higher (0.32 ± 0.01 h^{-1}) although maximal cell concentration was lower (4.85 g L^{-1}). First DHA accumulation could be detected 70 hours after glucose depletion, about 30 h later than in the lower buffered condition.

MES buffered cultivations at 5.6 and 6.5 maintained their pH and reached DHA end concentrations of 5.25 and 7.64 mg g_{cdw}^{-1} after 210 h, respectively (Figure 9C and D). Both MES-based conditions reached similar maximum cell concentrations (5.6 g L^{-1}) but differed in growth rate. At higher pH, cells grew faster than at lower pH (0.34 h^{-1} vs. 0.28 h^{-1}). Due to the substitution of phosphate buffer with MES, the phosphate level was decreased from 207.35 mM (200 mM of phosphate buffer and 7.35 mM from YNB) to 7.35 mM (from YNB only). This positively influenced DHA production regarding DHA content and yield, which will be investigated in the later stages of media optimization in detail. As the utilization of MES at a pH of 6.5 offers unaffected growth, stable pH and improved DHA production performance, buffer system and pH were applied further media development.

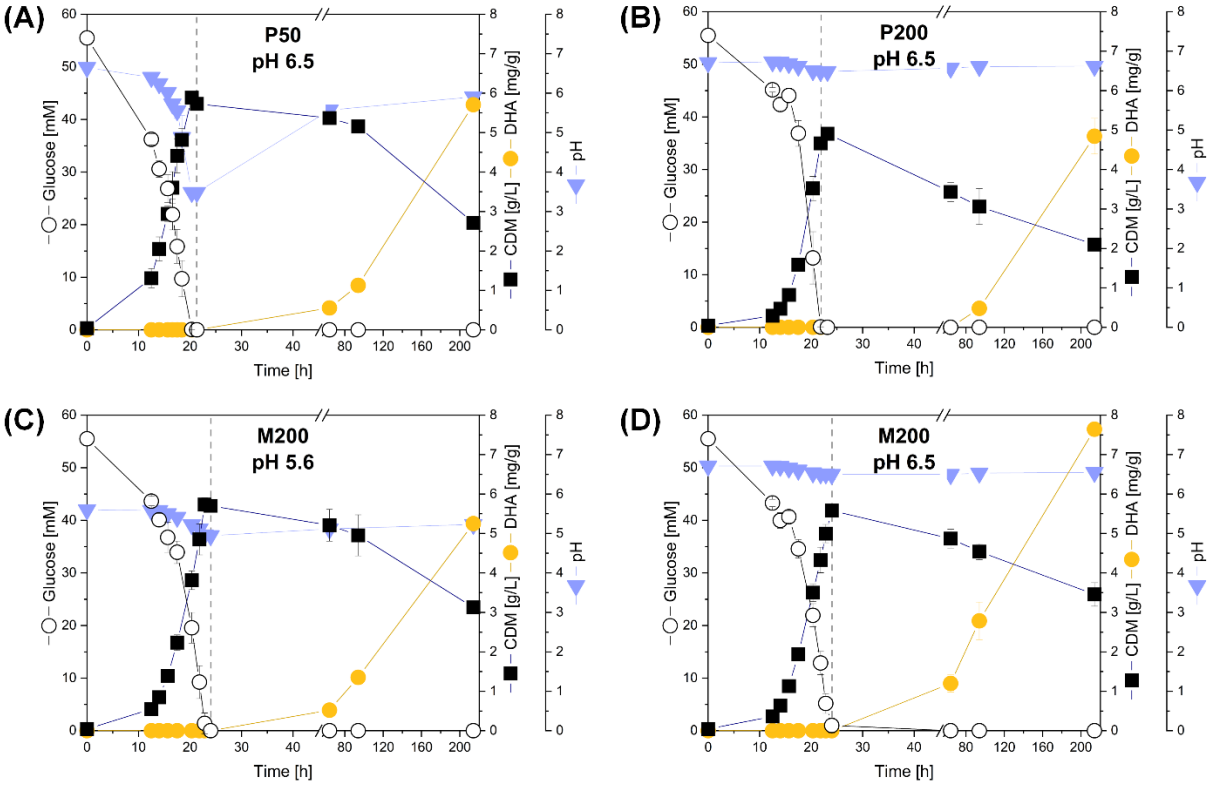

Figure 9: Influence of buffer and pH on cell growth and DHA production in *Y. lipolytica*.

Cultivations were conducted in YNB-Glu_{10}-N_5 medium with four different buffer/pH setups. (A) 50 mM phosphate buffer; pH 6.5. (B) 200 mM phosphate buffer; pH 6.5. (C) 200 mM MES buffer; pH 5.6. (D) 200 mM MES buffer; pH 6.5. Dotted line indicates carbon source depletion.

4.1.2 Advanced DHA production by media design

For further media optimization, a combinatorial component test was set up to improve DHA production. Thereby, three carbon and two nitrogen sources, namely acetate, glucose, and glycerol, as well as ammonium chloride and ammonium sulfate were tested. Additionally, the influence of YNB was included in the study. Concentrations of the components were altered in such a way that different C/N and C/P ratios were achieved. *Yarrowia lipolytica* as an oleaginous yeast triggers the *de novo* lipid accumulation when sensing a nutrient limitation in combination with an excess of the carbon substrate. Commonly, nitrogen limitation is employed as a means of controlling metabolic shift, but other constraints have been utilized in order to achieve this goal (Beopoulos et al., 2009b). As indicated in the previous pH experiment, limitation in phosphate as a substantial ingredient in YNB might positively influences DHA productivity. To this end, YNB was once supplemented at recommended concentrations (1.7 g L^{-1}) and once at limited levels (0.85 g L^{-1}) and growth and production was compared.

DHA-producer strain Po1h::Af4 was cultivated in shake flask at various growth conditions and rated by relevant performance parameters, i.e., final DHA titer, product and biomass yield (Table 2). The cultivations were conducted in shake flasks experiments with a duration of around seven days (~180 h) and analyzed for substrate, ammonium, citrate as a side product, DHA, total lipid, and biomass. From these values the performance of the condition was evaluated. The media composition of each condition is stated in Table 2. As a reference, initial DHA production setup, as well as two previous setups were analyzed (Table 2; Conditions 0-3).

Table 2: DHA production performance of *Y. lipolytica* grown in various media formulas.

Shake flask cultivations were carried out in triplicates (n = 3). Performance parameters were determined after 200 h of cultivation.

#	Condition description	C/N ratio C/P ratio	Titer [mg_{DHA} L^{-1}]	DHA [% of TFAs]	$Y_{X/S}$ [g_{CDM} C-$mole^{-1}$]	$Y_{P/X}$ [mg_{DHA} g_{CDM}^{-1}]
0	Glucose (0.666 C-mole L^{-1}, 0.076 N-mole L^{-1}, 1.7 g L^{-1} YNB, 50 mM P buffer)	9 12	86.10 ±3.22	10.54 ±0.98	10.12 ±0.46	12.78 ±0.32
1	Glucose (0.333 C-mole L^{-1}, 0.076 N-mole L^{-1}, 1.7 g L^{-1} YNB, 200 mM P buffer)	4 2	19.76 ±0.79	7.11 ±0.36	9.89 ±0.35	6.67 ±1.51
2	Glucose (0.333 C-mole L^{-1}, 0.076 N-mole L^{-1}, 1.7 g L^{-1} YNB, 200 mM MES buffer)	4 45	38.69 ±1.42	13.54 ±0.29	13.06 ±0.34	10.50 ±0.57
3	Glucose (0.99 C-mole L^{-1}, 0.028 N-mole L^{-1}, 1.7 g L^{-1} YNB, 200 mM P buffer)	35 5	5.15 ±0.52	2.33 ±0.13	10.21 ±0.07	0.60 ±0.07
4	Glucose (0.99 C-mole L^{-1},0.028 N-mole L^{-1}, 0.85 g L^{-1} YNB,200 mM P buffer)	35 5	14.30 ±1.81	4.62 ±0.16	10.36 ±0.02	1.89 ±0.24
5	Glucose (0.99 C-mole L^{-1}, 0.028 N-mole L^{-1}, 0.85 g L^{-1} YNB, 200 mM MES buffer)	35 269	79.73 ±2.67	15.15 ±0.52	8.81 ±0.17	10.20 ±0.19
6	**Glucose (0.99 C-mole L^{-1}, 0.076 N-mole L^{-1}, 0.85 g L^{-1} YNB, 200 mM MES buffer)**	13 269	**104.79 ±11.23**	**16.56 ±1.69**	8.69 ±0.15	11.21 ±1.44
7	Glycerol (0.333 C-mole L^{-1}, 0.076 N-mole L^{-1}, 1.7 g L^{-1} YNB, 200 mM P buffer)	4 2	47.89 ±4.91	11.77 ±2.33	13.25 ±1.09	12.80 ±2.75
8	Glycerol (0.333 C-mole L^{-1}, 0.076 N-mole L^{-1}, 1.7 g L^{-1} YNB, 200 mM MES buffer)	4 45	77.48 ±5.90	12.11 ±0.24	15.65 ±0.04	14.55 ±0.91
9	Glycerol (0.333 C-mole L^{-1}, 0.076 N-mole L^{-1} (NH_4Cl), 1.7 g L^{-1} YNB, 200 mM MES buffer)	4 45	75.74 ±1.21	13.35 ±0.35	14.48 ±0.19	**14.53 ±0.63**
10	Glu+Gly (0.333 C-mole L^{-1}, 0.076 N-mole L^{-1}, 1.7 g L^{-1} YNB, 200 mM MES buffer)	4 45	58.85 ±1.49	14.43 ±2.76	14.45 ±0.41	13.26 ±0.20
11	**Acetate (0.6 C-mole L^{-1}, 0.076 N-mole L^{-1}, 1.7 g L^{-1} YNB, 200 mM P buffer)**	8 3	42.10 ±0.71	**16.78 ±0.72**	6.02 ±0.16	**16.39 ±0.71**

Initially, different nutrient limitations were tested (Figure 10). To achieve the desired restriction, the carbon source concentration was increased to ~1 C-mole concomitant with an excess in carbon. A common approach to trigger lipid accumulation is the application of high ratios of C-to-N (Table 2, Condition 3; Figure 10A). At C/N of 35, ammonium and glucose depleted after 20 and 40 h, respectively and a maximal cell concentration of 13.4 g L^{-1} could be achieved. DHA production started during stationary phase at around 90 h reaching 0.6 mg g_{CDW}^{-1}. Citrate accumulated extracellularly in the late exponential phase peaking at 3.4 g L^{-1} and was subsequently reconsumed. When halving the YNB concentration to 0.85 g L^{-1}, DHA production performance improved and a final titer of 1.9 mg g_{CDW}^{-1} was reached (Table 2, Condition 4; Figure 10B). The reduction of YNB led to a constraint supply of essential vitamins, and trace elements, of which several have been reported to modulate *de novo* lipid biosynthesis (Beopoulos et al., 2009a). Additionally, a reduction in phosphate and magnesium supply has been suggested as potential cues to initiate lipid accumulation (Bellou et al., 2016; Wierzchowska et al., 2021). As each YNB component may potentially have beneficial or detrimental effects on fatty acid and lipid biosynthesis investigation of each component will likely allow for further modulation of DHA production.

In the next scenario, both nitrogen and phosphate were lowered compared to the carbon source glucose (C/N ratio 35, C/P ratio 269) to provoke lipid accumulation (Kolouchová et al., 2016). The substitution of phosphate buffer by MES buffer, resulted in a 5-fold increased DHA production (Figure 10C, Figure 11B). Compared to phosphate buffer-based growth, maximal cell concentration was reached significantly later at ~80 h, specific growth rate was 11% lower and maximal cell density was 25% lower.

The lowered initial phosphate concentration of 3.6 mM potentially results in an early restriction of phosphate, which triggers the transition from exponential growth phase to lipid accumulation phase, in which growth slows down (Papanikolaou & Aggelis, 2011). In this phase, total lipid content increases until the carbon source is depleted. The excess carbon in form of citrate is channeled from the mitochondria into the cytosol via the citrate-malate shuttle where it is cleaved by ATP-citrate lyase (ACL) into acetyl-CoA and oxaloacetate:

$$\text{Citrate + HS-CoA + ATP} \rightarrow \text{Acetyl-CoA + oxaloacetate + ADP + } P_i$$

Excess citrate which cannot be converted is exported into the medium. Consequently, elevated citrate level of up to 12 g L^{-1} were detected in the culture supernatant, which was slowly re-consumed by the cells (Figure 10C). This setup resulted in 10 mg g_{CDW}^{-1} DHA with a final titer of 79 mg_{DHA} L^{-1}. An unrestricted supply of ammonium (C/N 13) in combination with MES buffer led to minor improvement DHA production performance underlining the importance of phosphate limitation over that of nitrogen (Figure 10D). In this setup 11.4 mg g_{CDW}^{-1} was reached with a titer of 105 mg_{DHA} L^{-1} (Table 2, Condition 6; Figure 10D).

Final performance indicators are summarized in Figure 11 A and B. Intracellular DHA concentration could be increased 18-fold, the DHA fraction in total fatty acids about 7-fold (Figure 11A), achieved by restriction of YNB and phosphate supply. Less pronounced, the unlimited supply of nitrogen allowed for even higher DHA titers exceeding 100 mg_{DHA} L^{-1} within 190 h, which corresponds to a space-time yield (STY) of 0.55 mg_{DHA} L^{-1} h^{-1} (Figure 11B). An improved cell viability and consequently a higher cell density though positively affected DHA accumulation.

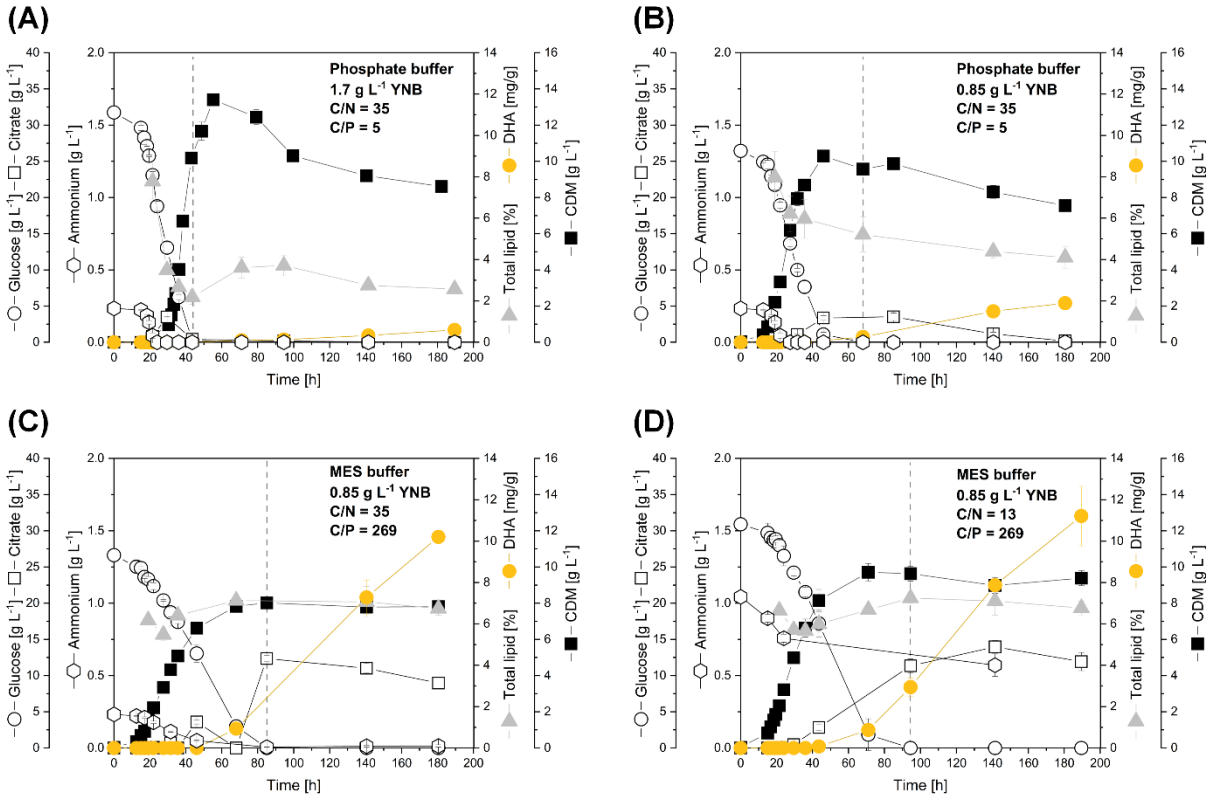

Figure 10: Investigation of the influence of buffer system, C/N and C/P ratio, as well as YNB supplementation on DHA production in *Y. lipolytica* Po1h::Af4

Cultivations were conducted in shake flasks for 190 h with various media setups. Puffer concentration was 200 mM. (A) N limitation: C/N = 35, phosphate buffer, 1.7 g L^{-1} YNB. (B) N limitation: C/N = 35, phosphate buffer, 0.85 g L^{-1} YNB level. (C) N+P limitation: C/N = 35 and C/P = 269, MES buffer, 0.85 g L^{-1} YNB. (D) P limitation: C/N = 13, C/P = 269, MES buffer. Dotted lines indicate carbon source depletion and entry into stationary phase.

A comparable picture emerged when glucose was replaced by glycerol. Again, the substitution of phosphate buffer with MES resulted in an overall superior production performance (cultivation profiles not shown, Figure 11C & D). Glycerol has been described as the preferred substrate for *Y. lipolytica*, particularly offering fast growth rates and high substrate uptake rates regardless of various concentrations (Rywińska et al., 2013; Workman et al., 2013). Crude glycerol from biodiesel production displays a cheap substrate (Gao et al., 2016) and *Y. lipolytica* exhibits a high tolerance against toxic compounds and hydrophobic substances. As glycerol forms the C3 backbone of triacylglycerides (TAGs) it displays a metabolically cheap precursor in this regard (Dulermo & Nicaud, 2011). Upon examining the stoichiometry of glycerol assimilation and generation of the precursor acetyl-CoA in the cytosol, it is found that an extra NADH and ATP is generated in comparison to an equimolar (C-mole) amount of glucose:

1 Glycerol +1 ADP +3 NAD^+ +1 CoA → 1 Acetyl-CoA +1 ATP +3 NADH

0.5 Glucose +2 NAD^+ +1 CoA → 1 Acetyl-CoA +2 NADH

In *Y. lipolytica,* glycerol can entry central carbon metabolism by (1) oxidation to dihydroxyacetone and subsequent phosphorylation to dihydroxyacetone-phosphate (DHAP) or (2) phosphorylation to glycerol-3-phosphate (G3P) and oxidation to DHAP. Both cases result in the generation of one reduction equivalent ($NADH/FADH_2$) and consumption of one ATP.

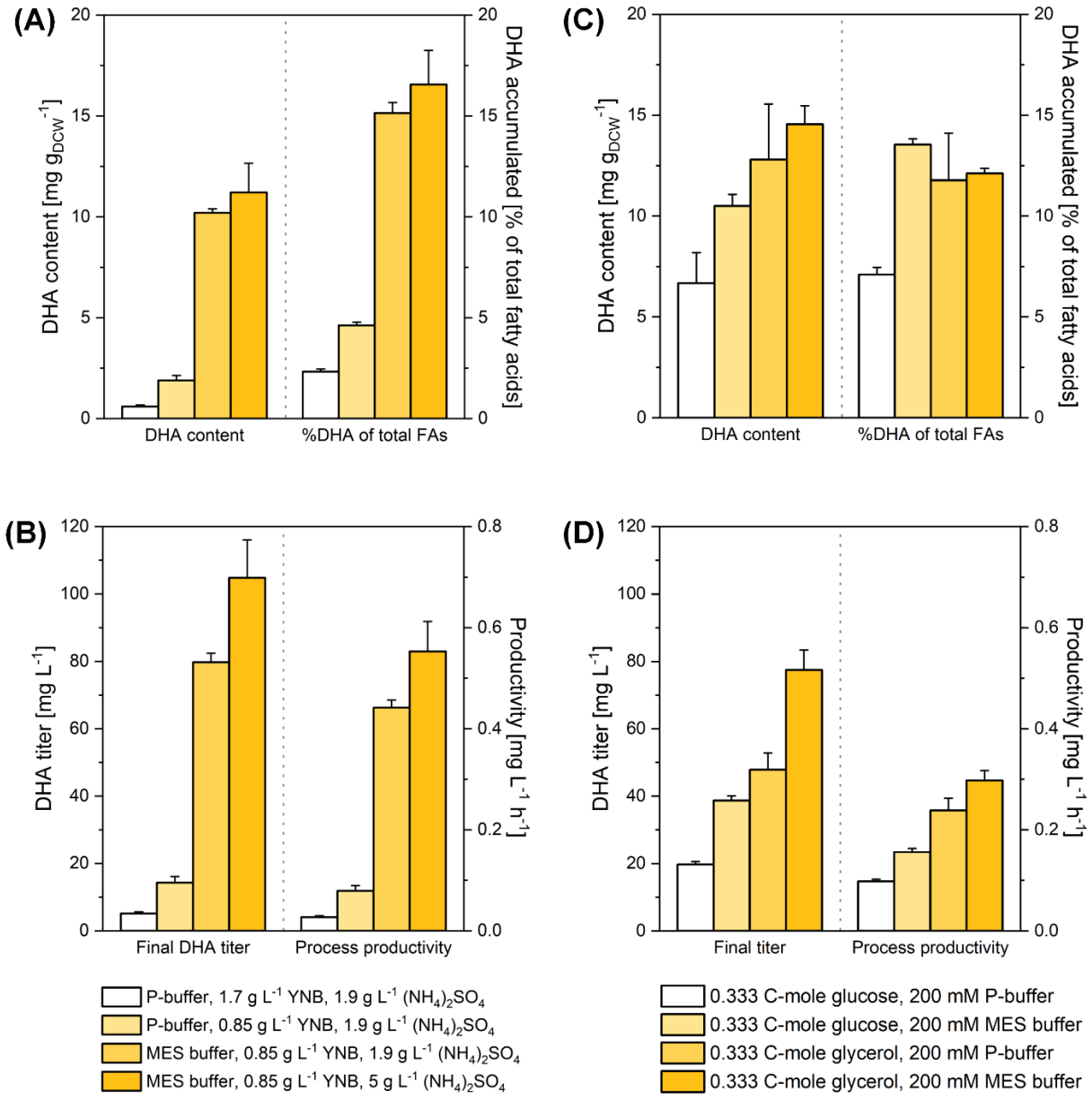

Figure 11: DHA production improvement by optimization of media composition.

Shake flask cultivations of *Y. lipolytica* Po1h::Af4 were carried out in triplicates. Performance parameters were determined after 200 h of cultivation. YNB-based medium varying carbon source, nitrogen source, YNB concentration and buffer system was used.

Overall, the substitution of glucose with glycerol doubled the final titer in both phosphate and MES-based media improving from 20 mg_{DHA} L^{-1} to 48 mg_{DHA} L^{-1} and 39 mg_{DHA} L^{-1} to 78 mg_{DHA} L^{-1}, respectively (Figure 11D). When equimolar mixtures of glucose and glycerol were supplied, both substrates are co-consumed from the start of the cultivation, however glycerol is consumed with a higher rate, thus depleting first while glucose consumption is suppressed (Yuzbasheva et al., 2018). *Y. lipolytica* generally prefers glycerol over glucose (Workman et al., 2013), which is converse to most organisms preferring glucose as the most abundant monosaccharide in nature (Erian et al., 2022). Interestingly, the overall performance of the 1:1 mixture corresponds to the averaged performance when using each substrate individually (see Table 2), thus was not significantly beneficial.

Acetate is assimilated into the metabolism by the Acetate—CoA synthetase (ACS) forming acetyl-CoA.

$$1\ \text{Acetate} + 1\ \text{CoA} + 1\ \text{ATP} \rightarrow \text{Acetyl-CoA} + 1\ \text{AMP} + PP_i$$

Since this is the starter unit for DHA and precursor for malonyl-CoA as an elongation unit, an acetate-based cultivation displays an interesting carbon source for fatty acid synthesis (Liu et al., 2016). When grown on 300 mM acetate (0.6 C-mole), an intracellular DHA concentration of 16.4 mg_{DHA} g_{CDM}^{-1} with 16.8% DHA of TFA could be achieved (Table 2, Condition 11). Nevertheless, the use of acetate resulted in low biomass concentrations and low biomass yields, which eventually leads to low overall titers. Additionally, acetate uptake involves a protonation, resulting in basification of the media, which had to be neutralized by acid titration. Consequently, to exploit the full potential of acetate, further investigations are needed. Applying a mixed carbon source potentially renders a possibility to overcome the low biomass yield, either as a batch or two-phase fed-batch, where acetate feeds in the *de novo* lipid synthesis, whereas glycerol would be metabolized for biomass generation.

To support the findings, flux balance analysis (FBA) was conducted for the carbon sources acetate, citrate, glucose, and glycerol (see Figure S 1 to S5), to estimate maximal theoretical DHA yields thereof (Figure 12). The calculated

values represent maximal product yields based on the optimal stoichiometric flux distribution through central carbon metabolism. As DHA requires a certain ratio of precursors, an optimal carbon source would facilitate an efficient metabolic flux resulting in the respective ratio of precursors and cofactors:

$$11\ \text{Acetyl-CoA} + 10\ \text{ATP} + 10\ CO_2 + 14\ \text{NADPH} \rightarrow 1\ \text{DHA} + 10\ (\text{ADP} + P_i) + 14\ \text{NADP}$$

Apart from the precursor acetyl-CoA, metabolic pathways for ATP and NADPH generation need to be active. For acetate and citrate sufficient ATP is generated in the tricarboxylic acid (TCA) cycle and oxidative phosphorylation (Figure S 5 and Figure S 4). For NADPH generation the pentose phosphate pathway (PPP) is used, whereas malic enzyme (MAE) is not active under simulated optimal DHA-producing conditions. The preference of PPP over MAE has been reported *in vivo*, where the ratio has been found to be 2:1 (Wasylenko et al., 2015). As acetyl-CoA is directly generated from acetate and citrate no other pathway needs to be active in this regard and resulted in a theoretical yield of 0.18 g g^{-1} and 0.19 g g^{-1}, respectively (Figure 12).

Glucose on the other hand is metabolized through glycolysis and PPP, thus generating sufficient amounts of ATP and NADPH without the need activate the TCA cycle (Figure S 3). ATP is additionally generated by oxidative phosphorylation from NADH and other reducing equivalents. Pyruvate is converted into citrate in the mitochondria and then exported via the citrate-malate shuttle. In the cytoplasm, ATP citrate lyase (ACL) generates acetyl-CoA for DHA synthesis. The residual cytoplasmic oxaloacetate is converted into malate which is again needed to drive the citrate-malate shuttle. The same distribution was found when feeding glycerol, whereas PPP was less active since an annotated glycerol dehydrogenase (GCY1) could potentially generate additional NADPH (Figure S 1). As for the obtained results from the direct comparison of glucose and glycerol, the theoretical yield for glucose was found to be lower than the yield for glycerol-based metabolism with 0.27 and 0.3 g g^{-1}, respectively (Figure 12). Interestingly, an equimolar (C-mole) amount of glycerol and glucose, results in yields and flow distributions representing the means of the single substrates (0.285 g g^{-1}), which was found in the *in vivo* experiments as well.

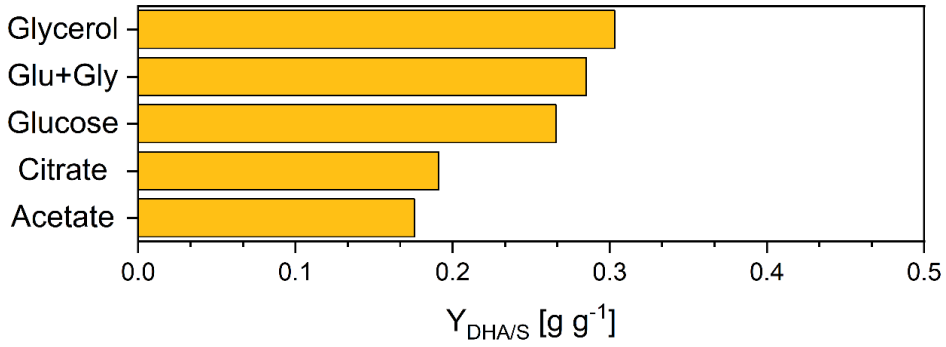

Figure 12: Flux balance analysis for DHA production on different carbon sources.
Theoretical product yield per gram of substrate was calculated by FBA in CellNetAnalyzer from the relative flux values. For the mixture of glucose and equimolar (C-mole) ratio was assumed.

Next to carbon sources, two nitrogen sources, namely ammonium sulfate and ammonium chloride were compared to investigate their influence on growth and production (Table 2; Condition 8 and 9). However, only minor improvement was achieved when $(NH_4)_2SO_4$ was used. It was therefore selected for further use.

Concluding the media development, phosphate restriction and the use of glycerol a carbon source showed the biggest improvements (Figure 11). Additionally, a lower level of YNB and excess nitrogen in form of ammoniumsulfate are advantageous for DHA production. As acetate shows promising results, further investigations are needed to fully elucidate its potential as carbon substrate. In a later step, the most promising settings were tested in small-scale bioreactor fermentations to test production performance in an industry-like production setup.

4.1.3 Comparison between shake flask and bioreactor production

Since biotechnological production processes are usually realized in large fermenters, the transfer from shake flask to bioreactors is critical first step in scale-up and commercialization of a new bioprocess. Due to the automatic monitoring and control of process parameters like temperature, pH, dissolved oxygen or foam formation, production performance might strongly differ from that in shake flask experiments. One key factor is the supply of dissolved oxygen, which is often inadequate in shake flasks due to limited measurement and control capabilities. In contrast, bioreactors allow for precise regulation of dissolved oxygen levels. Another advantage of bioreactor setups is the ability to maintain a stable pH with minimal fluctuations, whereas pH control in shake flasks heavily relies on buffer capacity. Temperature control, on the other hand, is generally expected to be well-maintained at both systems and is less likely to pose challenges during the transfer process.

The influence was assessed by conducting parallel cultivations of *Y. lipolytica* Po1h::Af4 in both shake flasks and a bioreactor under identical conditions (Figure 13A and B; Table 3, Condition 1 and 2). The experimental conditions were determined based on the findings from the previous media evaluation, resulting in the use of higher concentration of glycerol (30 g L^{-1}; C/N=13), and MES buffer. In addition to these conditions, the bioreactor cultivation was carried out without the use of a buffer and with a lower pH (Figure 13C and D; Table 3, Condition 3 and 4). Each experiment was inoculated from the same preculture and the same medium was supplied (except buffer system).

The shake flask culture showed normal growth and glycerol consumption. CDM reached maximum levels of 16.5 g L^{-1} and decreased to 13 g L^{-1} by the end of the cultivation. The pH decreased from 6.5 to as low as 5.6 as a result of citrate secretion (max. 4.5 g L^{-1}). However, towards the end of the cultivation, the pH increased to 6.2 due to the partial reuptake of citrate. DHA production started after ~50 h and reached intracellular levels of 17.5 mg_{DHA} g_{CDM}^{-1} and a titer of 230 mg_{DHA} L^{-1} (Figure 13A; Table 3, Condition 1). In contrast, the corresponding condition in the bioreactor exhibited significantly poorer performance, with only 63.5 mg_{DHA} L^{-1} and 5.8 mg_{DHA} g_{CDM}^{-1} achieved (Figure 13B; Table 3; Condition 2). Although the cell concentration reached similar levels (15.8 g L^{-1}), it decreased to 10 g L^{-1} over time. Citrate levels were lower (max. 0.2 g L^{-1}) and

was fully consumed after 160 h. The bioreactor without buffer and with the lower pH (Figure 13C and D) showed similar behavior in all tested parameters. DHA levels were slightly lower compared to the reference bioreactor condition, with concentrations of 50.4 and 53.2 mg_{DHA} L^{-1} (Table 3, Condition 3 and 4).

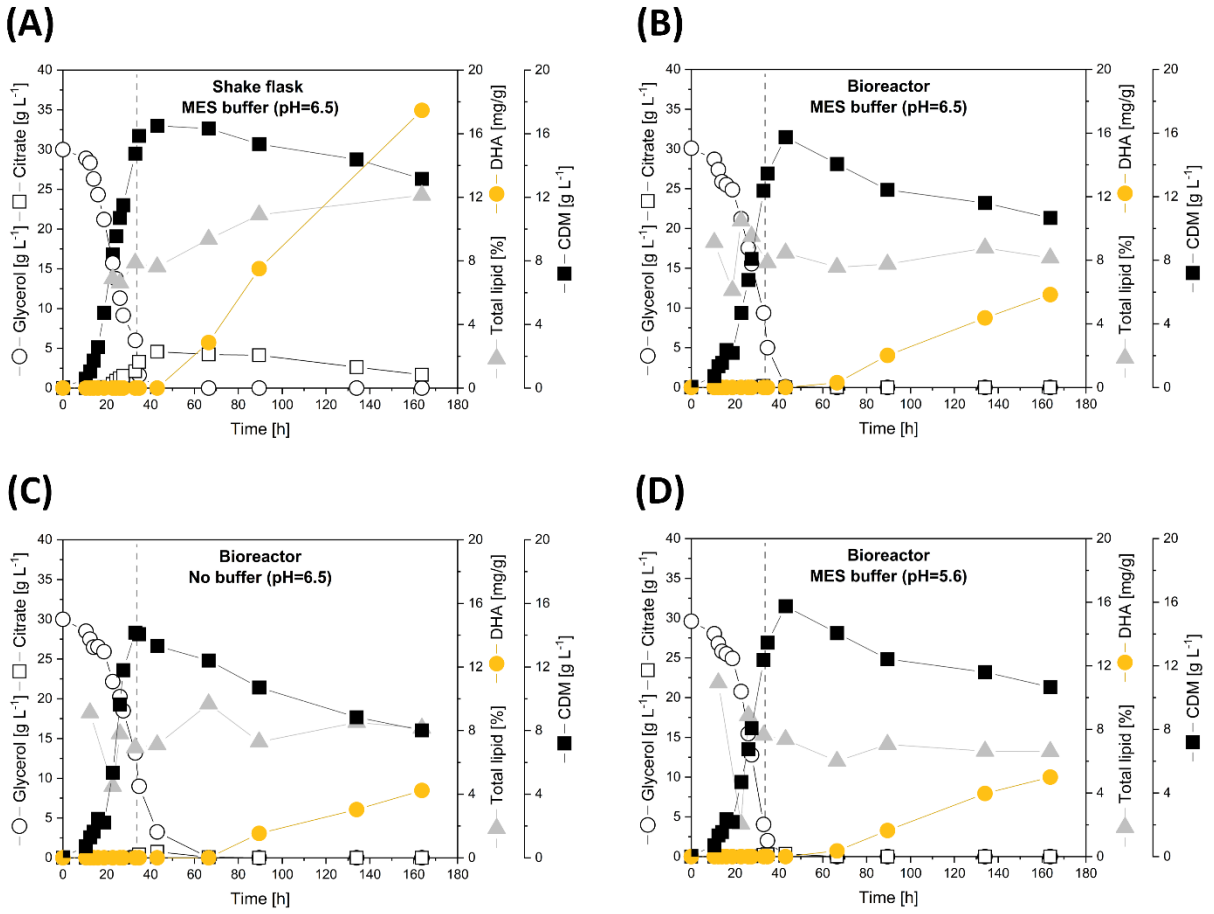

Figure 13: Cultivation profiles of *Y. lipolytica* Po1h::Af4 in bioreactor and shake flask.

Cultivation was conducted in YNB-Gly_{30}-N_5 (n=1), T = 28 °C (A) Shake flask cultivation with MES buffer at pH=6.5, No pH or DO control (B) Bioreactor cultivation with MES buffer at pH=6.5; (C) Bioreactor cultivation without buffer at pH=6.5; (D) Bioreactor cultivation with MES buffer at pH=5.6; pH for Bioreactor cultivations were maintained using 5 M HCl and 6 M NaOH. Dissolved oxygen was kept at 5% adjusting the stirrer rate. Coefficients of variation (CVs) across biological replicates were below 5% for biomass, substrate, and below 10% for PUFA and native fatty acid content.

Table 3: Comparative analysis of DHA production in shake flask and bioreactor.

Cultivation was conducted in YNB-Gly_{30}-N_5 (n=1), MES buffer, T = 28 °C. For the bioreactor cultivation pH was maintained at 6.5 using 5 M HCl and 6 M NaOH. Dissolved oxygen was kept at 5% adjusting the stirrer rate. Shake flask cultivation: No pH or DO control.; Coefficients of variation (CVs) across biological replicates were below 5% for biomass, substrate, and below 10% for PUFA and native fatty acid content.

#	Condition description	pH	Titer [$mg_{DHA}\ L^{-1}$]	DHA [% of TFAs]	$Y_{P/X}$ [$mg_{DHA}\ g_{CDM}^{-1}$]	$Y_{P/S}$ [$mg_{DHA}\ g_{Gly}^{-1}$]
1	Shake flask MES buffer	6.5	**229.8**	**14.4**	**17.5**	**7.66**
2	Bioreactor MES buffer	6.5	63.5	6.7	5.8	2.11
3	Bioreactor no buffer	6.5	50.4	5.2	4.2	1.68
4	Bioreactor MES buffer	5.6	53.2	7.6	5.0	1.80

The observed differences in DHA production performance between cells grown in uncontrolled shake flasks and controlled bioreactors suggest variations in the metabolic mode between these two growth environments. While medium composition and temperature are consistent, the controlled pH and dissolved oxygen (DO) levels in the bioreactor may have a negative impact on DHA production.

In the shake flask setup, the pH dropped to 5.6, while in the bioreactor, the pH was strictly maintained at 6.5. Interestingly, when the pH in the bioreactor was lowered to 5.6, the production levels were nearly the same as those observed at pH 6.5, indicating that a less restricted pH control, allowing for a pH range, might be beneficial for DHA production. *Y. lipolytica* is known to be sensitive to the availability of dissolved oxygen (Bati et al., 1984; Kavšček et al., 2015), favoring citrate and lipid accumulation under uncontrolled oxygen-limited conditions by down-regulating the TCA flux (Sabra et al., 2017). The strict oxygen supply of 5% may have an detrimental effect on DHA production. In contrast, in the shake flask setup where oxygen is not controlled and potentially becomes insufficient at a later stage, a metabolic shift may occur, which could explain the higher DHA production observed. Other factors such as stirring and aeration may also influence cell viability, morphology or metabolism. The transition from shake flask to bioreactor-based DHA production appears to be a challenging task when using *Y. lipolytica*, as multiple factors and their interaction may perturb biomass

growth, by-product secretion (i.e. citrate) and DHA biosynthesis. The influence of oxygen, in particular, should be further investigated as it plays a critical role in growth and lipid accumulation in *Yarrowia*. These preliminary observations provide interesting insights for future experiments in optimizing the bioprocess for DHA production.

4.2 Adapted PUFA cluster architecture

In the previous work the myxobacterial PUFA cluster was adapted by exchanging parts of the PUFA genes yielding hybrid PUFA clusters from different species, in order to alter the product spectrum (Gemperlein et al., 2019). The peripheral design, in particular the promoter architecture was never changed. It is, however, well known that the expression of genes in *Y. lipolytica* is based on a complex genetic architecture, that involves various elements of control such as distal and proximal upstream activating enhancers, promoters, terminators, and intron sequences. The combinatorial use of such elements offered space for additional improvement of DHA production (Le Hir et al., 2003b; Portela et al., 2017; Shabbir Hussain et al., 2016), given the fact that our present knowledge on how to express myxobacterial genes in the yeast is low.

Here, we explored different designs to overexpress the four-gene Af4 cluster for DHA overproduction in *Y. lipolytica*. In an initial test round, different core promoters, UAS tandem repeats, terminators, and introns were systematically combined which yielded a set of different PUFA clusters to be genomically integrated into the yeast. The obtained mutants were evaluated for performance. In addition, multi-omics analysis unraveled several features of the strains, including (i) genetic stability, (ii) individual expression levels of the PUFA genes, and (iii) intracellular availability of the DHA precursors acetyl-CoA and malonyl-CoA. Based on the gained understanding, further optimization cycles iteratively balanced and optimized the expression of the individual genes in the cluster.

4.2.1 Constitutive *TEF* promoter based PUFA cluster expression.

Towards recombinant DHA overproduction in *Y. lipolytica*, we aimed to optimize the expression of a myxobacterial four-gene cluster, encoding a polyketide-like PUFA synthase (Gemperlein et al., 2014). To streamline the experimental workflow for the construction of different cluster variants, we set up a modular cloning approach. Inspired by the recently developed YaliBrick concept for smart genetic engineering of the yeast (Wong et al., 2017b), we used a set of highly specific restriction enzymes to create unique cleavage sites during cloning (SmaI, SdaI, ApaLI, AclI, AvrII, PacI, AjuI, NotI, SmiI) which enabled a straightforward combinatorial assembly of the cluster genes with different genetic control elements of interest in the correct order (Figure 14**,** Figure 15A). This approach also allowed for an easy replacement of individual sequence elements during later optimization. At the start, we designed a basic cluster that expressed each of the four genes (*pfa1, pfa2, pfa3, ppt*) under control of the constitutive *TEF* promoter (P_{TEF}), a common promotor used by various labs for overexpression in *Y. lipolytica* (Müller et al., 1998). In the first step of construction, individual gene-terminator fusion constructs were integrated into plasmids that carried the well-characterized P_{TEF} promoter upstream of the integration site. The plasmids were amplified in *E. coli* and used to obtain the corresponding promoter-gene-terminator cassettes (Figure 14A). The four single-gene cassettes were then cloned stepwise into an assembly vector using restriction digest which provided the entire synthetic 19.1 kb PUFA cluster in the vector (Figure 14 B and C)

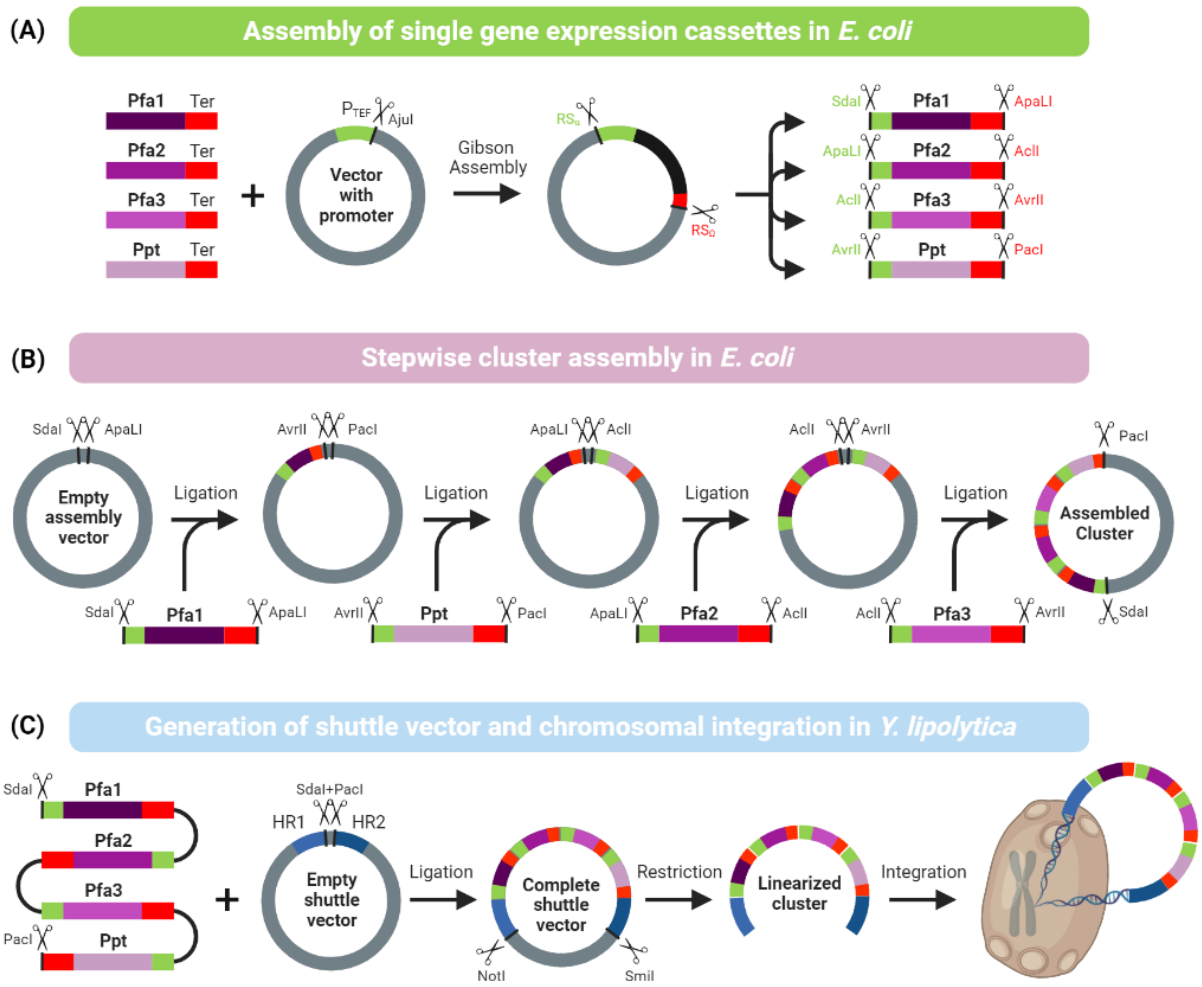

Figure 14: Genetic workflow for engineering the genome of *Yarrowia lipolytica* using highly specific restriction enzymes to enable correct modular assembly of synthetic four-gene clusters.

The workflow involves amplifying the single PUFA cluster genes (*pfa1-3* and *ppt*) and fusing them with the *Lipt2t* terminator. The resulting gene fragments are then integrated into a pre-configured promoter vector using Gibson assembly, and the vector is linearized using the restriction enzyme *AjuI* (A). The single gene cassettes are subsequently integrated in a defined order (*pfa1, ppt, pfa2, and pfa3*) using unique restriction sites (B) to create the complete four-gene cluster. The final step involves integrating the cluster, flanked by two homologous regions, into a shuttle vector using restriction and ligation. The cluster is then linearized for chromosomal integration into *Y. lipolytica* (C).

Genomic integration of the cluster into the non-producing host *Y. lipolytica* Po1h yielded strain *Y. lipolytica* TEF Af4. When grown on a glycerol-based minimal medium the mutant formed 0.8 mg g^{-1} of DHA within 185 h, displaying 1.3% of total fatty acids (Figure 15B). Hereby, the strain exhibited consumed all glycerol during an initial phase of exponential growth (μ = 0.34 h^{-1}) and reached a maximum concentration of cell dry mass of 6.3 g L^{-1} (Figure 16A). Citrate, an often-observed overflow metabolite of the yeast, was formed only in traces (< 1 mM). DHA was only detectable after 85 h. The parent non-producing host *Y. lipolytica* Po1h did not form DHA (as expected) but otherwise revealed similar growth behavior (data not shown). Taken together, a simple Af4 cluster design was sufficient to enable DHA formation in *Y. lipolytica*. However, DHA was formed only at low level, and it was surprising to see that the product accumulated only during the late stationary phase, given the presumably constitutive nature of the used promotor (Wong et al., 2017a).

Towards improved production, we created four P_{TEF}-based variants. In comparison to the basic strain TEF Af4, the second-generation mutants comprised different sets of additional genetic control elements, upstream and downstream of the *TEF* promoter. Hereby, the established workflow proved very efficient, as the new design could be quickly, easily, and precisely realized. The incorporation of the 5' *TEF* intron between the promotor and the corresponding gene resulted in strain *Y. lipolytica* TEF INT Af4 which, favorably, revealed four-fold increased DHA production (Figure 15B). The implementation of blocks of four upstream activating elements, upstream of each of promotor, resulted in the production of nine-fold more DHA in *Y. lipolytica* UAS1B4 TEF Af4, as compared to the parent strain (Figure 15B). *Y. lipolytica* UAS1B4 TEF INT Af4, comprising both modifications, achieved an even higher DHA content of 7.3 mg g_{CDM}^{-1} (Figure 15B). Favorably, the two modifications acted synergistically. It was interesting to note that strain UAS1B4 TEF INT Af4 visibly formed DHA already after 40 h, and that the cells maintained high productivity until the end of the process, while the overall growth behavior remained rather unaffected.

Previously, it had been shown that more than four UAS1B copies can result in even stronger gene expression in *Y. lipolytica* (Blazeck et al., 2011b). This option appeared promising to be tested, because the UAS1B elements were obviously

beneficial for DHA overproduction (Figure 15B). Therefore, we constructed an extended 26.3 kb cluster variant that additionally comprised a block of sixteen UAS1B elements in front of each P_{TEF}. The synthetized and assembled cluster was genomically integrated into the wild type, yielding strain UAS1B16 TEF INT Af4. Different to the expectation, this version, however, did not produce any DHA (Figure 15B) but was otherwise unaffected in substrate use, growth, and biomass formation (Figure S 6).

Taken together, all P_{TEF}-based strains (except the one with sixteen UAS1B repeats) enabled DHA production. As shown, the genetic architecture of the heterologous PUFA cluster influenced the achieved DHA level, indicating that the production performance was transcriptionally limited. All P_{TEF}-based strains exhibited similar characteristics regarding the use of glycerol and phosphate as well as growth. Therefore, neither the expression of the PUFA cluster nor the accumulation of DHA production seemed to have an impact on the gross metabolic strain characteristics.

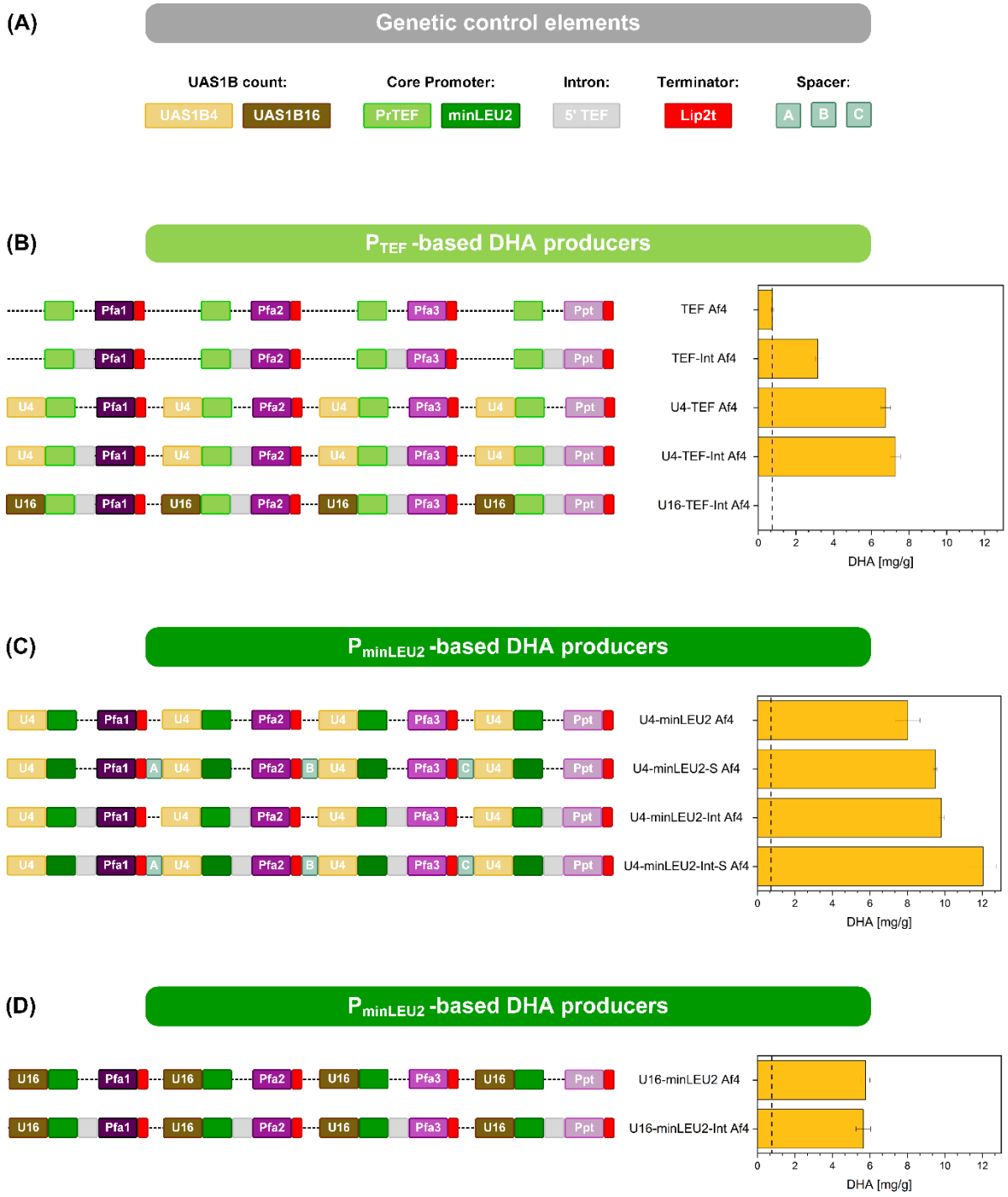

Figure 15: Metabolic engineering of *Yarrowia lipolytica* for the overproduction of docosahexaenoic acid (DHA) using synthetic heterologous gene clusters with different genetic architecture.

The study explored different genetic control elements in a combinatorial manner, including UAS1B elements of different length, the two core promoters P_{TEF} and $P_{minLEU2}$, the 5' *TEF* intron, 200 bp spacers, and the *Lip2t* terminator (A). The first-generation strains based on the TEF promoter are shown in panel B, along with their corresponding genomic layouts and DHA production performance. The third-generation strains based on the *minLEU2* promoter are shown in panel C and D. Intracellular DHA levels were measured in glycerol-grown cultures after 185 hours. The data represent the mean value and the standard error (n=3).

4.2.2 Stationary-phase minimal LEU2 promoter based PUFA cluster expression.

As shown above, the recombinant strains formed DHA mainly during the stationary phase (Figure 16). We therefore included the minimal *LEU2* promotor ($P_{minLEU2}$) for further development. This promotor was supposed to act as a quasi-constitutive promoter (Madzak et al., 2000) with high activity during the early stationary phase (Nicaud et al., 2002). We constructed a set of third-generation strains, following the established modular workflow. For comparison, we included different numbers (4 and 16) of UAS1B tandem repeats. Two genomic mutants were generated, namely *Y. lipolytica* UAS1B4 LEU2 Af4, and UAS1B16 LEU2 Af4, respectively (Figure 15C). After validation by PCR and sequencing, the two strains were evaluated.

The variant with four UAS1B tandem copies accumulated 8 mg g_{CDM}^{-1} DHA (Figure 16C), significantly more than the corresponding P_{TEF} counterpart. The strain UAS1B16 LEU2 Af4 was found less efficient (Figure S 6). We focused on the UAS1B4 strain for a fourth optimization round. The additional insertion of *TEF* introns at the 5' end of each gene increased DHA production to 10 mg g_{CDM}^{-1} in the mutant *Y. lipolytica* UAS1B4 LEU2 INT Af4, almost 25% more than in the strain without the intron (Figure 16D). Alternatively, we placed 200 bp spacer sequences between each terminator and promoter sequence, to reduce the competition for protein binding (Song et al., 2016). Likewise, this yielded improved DHA production. Finally, we used introns and spacers in combination and constructed the fifth-generation strain *Y. lipolytica* UAS1B4 LEU2 INT S Af4 (Figure 15C). When evaluated in the production set-up, it achieved 12 mg DHA g_{CDM}^{-1}, the highest value among all constructed producers. In this regard, the best setup enabled 16-fold better production than the P_{TEF}-based design used initially.

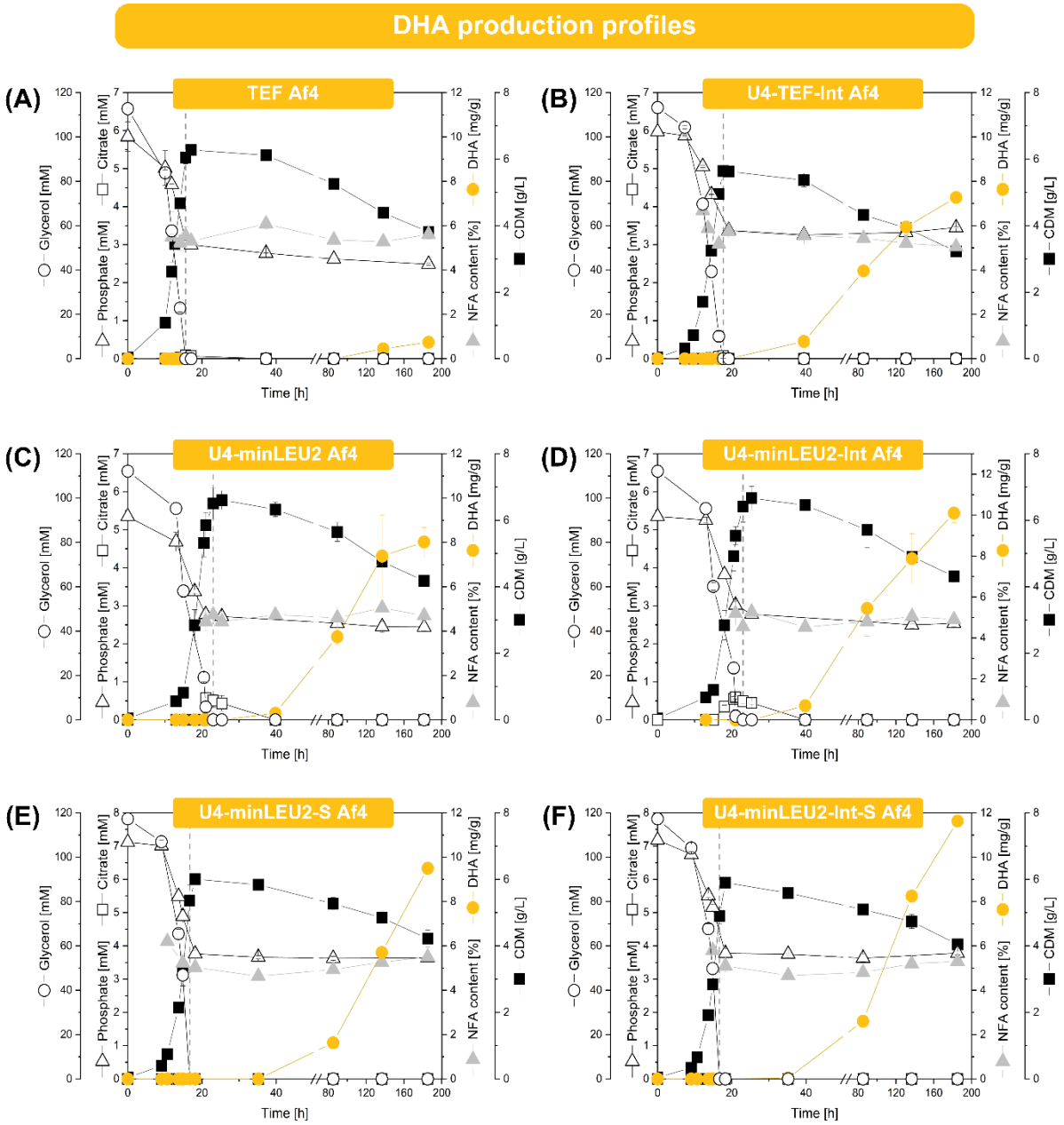

Figure 16: Enhanced DHA production in recombinant *Y. lipolytica* mediated through synthetic PUFA clusters with a streamlined genetic architecture.

The strains were cultivated in a glycerol-based minimal medium over 185 hours. The time point of glycerol depletion is indicated by a dotted line. The data display mean values and standard errors from three biological replicates. NFA = native fatty acids.

As shown, we created a spectrum of novel DHA-producers by combinatorically exploring a set of regulatory control elements, including the promoters P_{TEF} (Dulermo et al., 2017a) and $P_{minLEU2}$ (Gemperlein et al., 2019), upstream activating sequence blocks (UAS1B) of different lengths (Blazeck et al., 2011b), introns (Tai & Stephanopoulos, 2013), and intergenic spacers (Song et al., 2016). We generally designed the different cluster variants in monocistronic form. Each gene was expressed from its own promotor and separated from upstream transcription by a terminator. This architecture was chosen to avoid transcriptional inhibition effects that may have resulted in the case of multi-gene expression from one promoter (Shearwin et al., 2005) and non-functional mRNA maturation, observed for pseudo-operon configurations in the yeast (Wong et al., 2017b).

The different synthetic cluster mutants strongly varied in DHA accumulation (Figure 15**,** Figure 16). The configuration with blocks of four UAS1B elements upstream of the $P_{minLEU2}$ and an intergenic spacer, upstream of the promoter, respectively, worked best. The corresponding mutant accumulated 20% more DHA than the second-best strain and sixteen-fold more than the basic strain that expressed a minimal cluster. This finding demonstrated that (i) DHA production efficiency was transcriptionally limited. Furthermore, it revealed the potential of streamlining the promoter architecture of bacterial multi-gene clusters for optimized performance in *Y. lipolytica*.

As shown, strains that expressed the DHA-cluster under control of P_{TEF} yielded less product (Figure 15). This finding was a bit surprising, given the fact that P_{TEF} mediates strong constitutive expression and is often preferred for metabolic engineering of *Y. lipolytica* (Blazeck et al., 2011a; Dulermo et al., 2017b; Sun et al., 2022). Here, it was indeed active in all culture phases, but P_{TEF}-driven expression fluctuated over time (Figure 18). A previous study of the related promoter of the gene *TEF1* in *Pichia pastoris* encoding the translation elongation factor alpha-1 revealed growth-associated expression (Ahn et al., 2007). In this regard, the expression of the cluster under control of P_{TEF} might not have optimally matched with DHA biosynthesis, occurring only during the stationary phase (Figure 16). On the other hand, the intuitive use of $P_{minLEU2}$ in the initial DHA producer (Gemperlein et al., 2019) in retrospect proved to be a good choice.

4.2.3 PCR-based cluster stability test.

As shown, strains with 16 UAS1B elements upstream of each of the four cluster genes failed to efficiently produce DHA, independent whether the P_{TEF} or the $P_{minLEU2}$ promoter was used (Figure 15**,** Figure S 6). Interestingly, two of these strains showed a superior production performance during early stages of the process bevor fading out (Figure 17B, Figure S 6). Genetic instability was one of the possible reasons for this behavior. We therefore screened for the stability of the genomic PUFA cluster during production. Because sequencing of the cluster appeared challenging due to the highly repetitive sequence, we used PCR to determine the presence of each heterologous gene (Figure 17A). The PCR-based approach had been established for the synthetic biology work to verify the presence of the intact cluster in newly generated mutants, prior to inoculating them for cryo preservation. Here, we applied it to screen for cluster stability during the DHA production process, i. e. during the exponential phase (12 h) and during the late stationary phase (185 h) of the main culture, inoculated from a two-day pre-incubated culture. Altogether, cells were grown for about two weeks in each set-up. For each strain, 40 clones were analyzed (Figure 17A, Table 4).

The analysis revealed that higher UAS1B copy numbers caused genetic instability, partially leading to significant loss of production performance. Strains without UAS1B tandem repeats were found completely stable over the entire cultivation period (Figure 17B and C). Mutants with four UAS1B tandem repeats in front of each gene remained largely intact (Figure 17B and C). However, selected clones exhibited the loss of one of the genes during the production process, namely *pfa1* or *pfa3*. These mutation events were rare, and this picture did not change in related strains that were based on another promoter and an additional intron. Approximately, 98% of the tested clones were still intact at the end of the process. However, the findings revealed the occurrence of undesired recombination events within UAS1B4-based clusters.

Table 4: Mutation frequency of PUFA cluster genes.

Investigation of genetic stability of the heterologous four-gene cluster *pfa1, pfa2, pfa3 and ppt* expressed in the genome of recombinant *Y. lipolytica* for the production of the omega-3 fatty acid DHA. After culturing for two weeks, the cell populations were analyzed for the presence of the intact cluster. For each strain, 40 clones were analyzed for the presence of the individual cluster genes using PCR. The obtained patterns provided the genetic layout of each clone, providing an overview on the frequency of different mutation events, given as relative fractions in percent.

Mutation frequency

Relative fraction [%]				UAS1B4			UAS1B16		
				TEF Af4	TEF Int Af4	minLEU2 Af4	TEF -Int Af4	minLEU2 Af4	minLEU2 Int Af4
pfa1	pfa2	pfa3	ppt	97	97	97	0	42	13
pfa1	pfa2	X	ppt	0	0	3	5	5	11
pfa1	X	pfa3	ppt	0	0	0	0	11	0
X	pfa2	pfa3	ppt	3	3	0	0	8	2
pfa1	X	X	ppt	0	0	0	90	24	37
X	X	X	ppt	0	0	0	5	11	37

UAS1B16-based gene clusters were found structurally unstable (Figure 17B and C**)**. The two mutants *Y. lipolytica* U16-minLEU2 Af4 and U16-minLEU2-Int Af4 gradually lost parts of the cluster during cultivation. After 12 h, up to 90% of the tested clones still contained all cluster genes. At the process end, however, only 60% of the U16-minLEU2 Af4 clones were found intact. The population of U16-minLEU2-Int Af4 comprised even only 20% of genetically correct cells, indicating that the additional intron sequence further decreased stability. The population of strain UAS1B16-TEF-Int Af4 had largely lost the genes *pfa2* and *pfa3* already at the beginning of the production process. Obviously, this was the reason for the lack in DHA production, observed for this mutant. It furthermore appeared that the strain had already decomposed during pre-culturing. Taken together, strains with four UAS1B elements appeared optimal, as they offered high stability together with high production efficiency. It was interesting to note that the last cluster gene *ppt* was not affected in stability in any of the mutants.

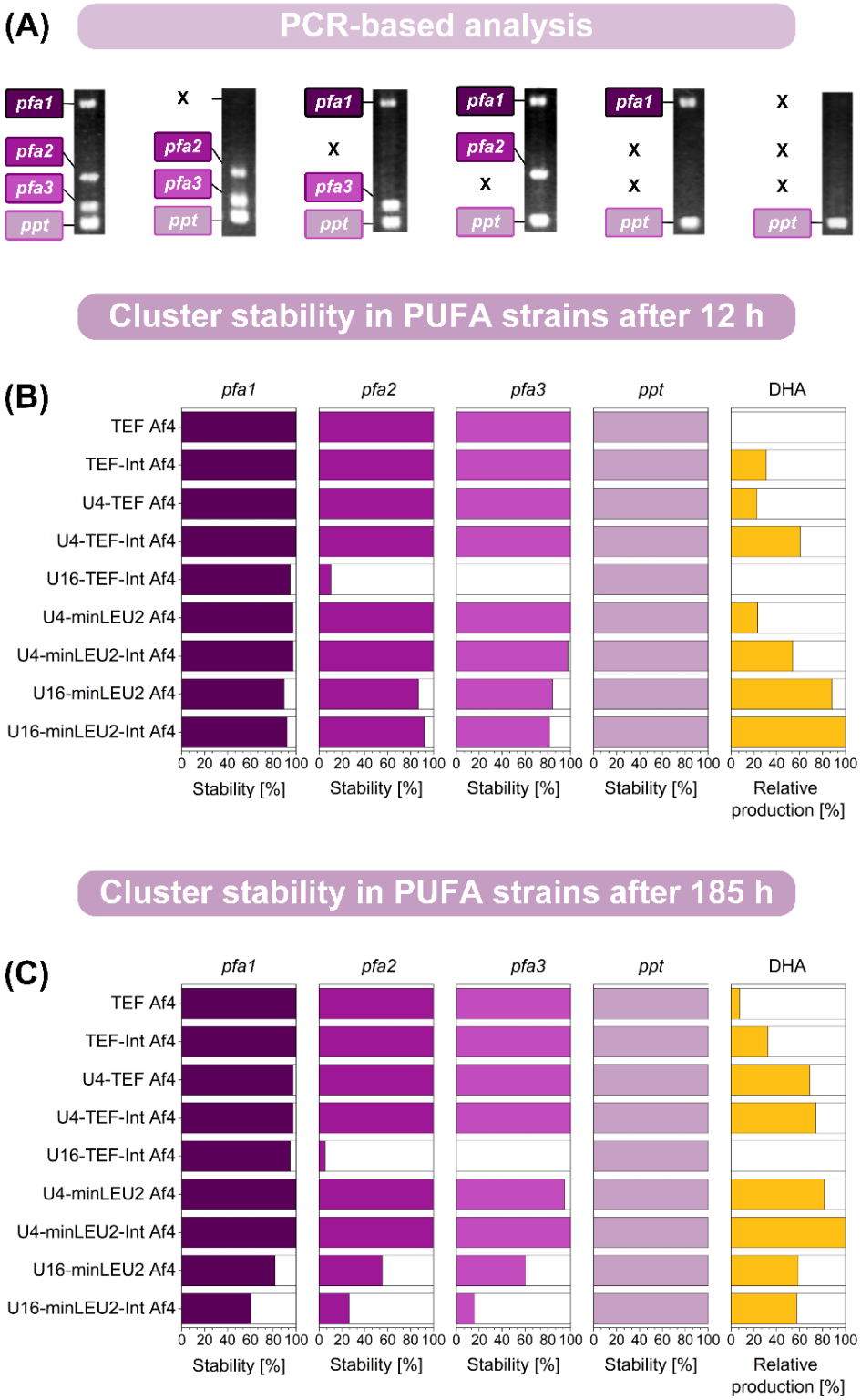

Figure 17: Evaluation of genetic stability in recombinant *Y. lipolytica* strains expressing synthetic four-gene clusters for heterologous DHA production.

The strains were sampled from the DHA production process after 12 hours and 185 hours. From each culture, 40 clones were simultaneously analyzed by colony PCR for the presence of each of the four cluster genes, *pfa1, pfa2, pfa3, and ppt*, respectively, using gene-specific primers. The primer pairs resulted in PCR products with different lengths, 1.72 kb (*pfa1*), 0.91 kb (*pfa2*), 0.73 kb (*pfa3*), and 0.61 kb (*ppt*), allowing for clear discrimination (A). The genetic stability of the PUFA clusters was evaluated after 12 h (B) and 185 h (C). The relative DHA production was inferred from the cultures during the early production phase (40 h). For every strain and sampling time point, 40 clones were evaluated for their stability.

As shown, the use of UAS1B elements strongly enhanced the expression of all cluster genes (Figure S 7), matching the previous observation that *Yarrowia* promoters are enhancer limited (Blazeck et al., 2011a). Functional clusters with blocks of sixteen elements in front of each cluster gene enabled the highest DHA production, as observed during the early phase of production (Figure 16). However, these cluster configurations were found unstable over time. Recombination events resulted in the loss of genes, preferentially the genes in the middle of the cluster. In rare cases, the first gene *pfa1* was lost too, whereas *ppt*, located outside of the potentially recombining homology domains, was found stable. As shown, only a subpopulation of cells was still capable to form the product during later stages of the process (Figure S 6). The additional repetitive use of the *TEF* intron destabilized the cluster further (Figure 17). Strain U16-TEF-Int Af4 unfavorably even failed to produce DHA in the main culture (Figure S 6). Almost all cells exhibited a damaged PUFA cluster already during early stages of the production process. At a low frequency, also mutants with four tandem repeats lost parts of the cluster (Figure 17). Without doubt, genetic stability is a crucial factor of microbial cell factories to ensure reproducible performance and constant product quality (Moore et al., 2022) but little has been reported on *Y. lipolytica* in this regard. Notably, cloning of the five-step violacein pathway yielded *Y. lipolytica* phenotypically different clones (Wong et al., 2017b). This observation indicated the possibility of genetic instability of the cluster among other effects, but the phenomenon was not further explored. The violacein cluster, however, was monocistronic and comprised several *TEF* promoters with introns, having the same configuration as the clusters designed in this work. In light of our findings, genetic instability of the cluster was the likely reason for the observed heterogeneity in the previous study (Wong et al., 2017b).

The major reason for genetic instability were the four UAS1B16 blocks, present in the cluster in a distance between 2.1 and 8.4 kb. Previously, UAS1B tandem repeats have been identified as powerful elements to enhance gene expression in *Y. lipolytica* (Blazeck et al., 2011b). Single UAS1B12 and UAS1B16 copies, respectively, were analyzed for genetic stability given their highly repetitive nature (Blazeck et al., 2011b). After 192 h of non-selective culturing (36 doublings), 17 out of 20 UAS1B12-based plasmids were found intact, while, in 3 cases, the tandem repeats were truncated down to UAS1B3. Overall, this

suggested rather good stability of the elements themselves. Different to that, our findings show that repetitive UAS1B16 blocks in certain proximity, meant to drive individual promoters in synthetic multi-gene clusters, should be avoided in *Y. lipolytica*.

Naturally, *Y. lipolytica* carries only a single copy of UAS1B as proximal enhancer, together UAS2B as distal enhancer, to drive expression of the *xpr*2 gene (Blanchin-Roland et al., 1994). In this regard, the introduced UAS1B16 blocks in close proximity displayed a rather unnatural layout which might explain the degeneration over time. Beneficially, UAS1B4 tandem repeats worked quite well and enabled a significant upregulation of expression together with stable production over up to two weeks, and these motifs appear recommendable. In any case, genetic stability monitoring of genome-based *Y. lipolytica* strains, cultured under non-selective conditions, seems important when evaluating recombinant producers to avoid being misguided in the interpretation of metabolic engineering efforts (Jones, 2014). Notably, the degenerated strains did not reveal any visible phenotypic difference (except lower DHA titers). The discovery of genetic instability was therefore essential to understand why the apparently “strongest” clusters performed that weak.

For future studies, several options appear promising to improve the employed PUFA cluster architecture and enable stable high-level expression, even beyond the well-working monocistronic UAS1B4-based design, developed here. The individual cluster genes could be distributed to different loci (including different chromosomes) in the genome to minimize recombination events. Such a layout should be stable, even when used with blocks of sixteen or more UAS1B tandem repeats (Blazeck et al., 2011b). Such a strategy would be linked to increased effort in finding suitable expression loci and constructing the producers stepwise but appears promising given the meanwhile fast and powerful genomic engineering technologies for *Y. lipolytica* (Markham & Alper, 2018; Sun et al., 2022; Tsirigka et al., 2023; Wong et al., 2017b). One might also think about expressing the cluster from two sequence blocks with two convergently (tail-to-tail) oriented genes each to maximize the distance between the repetitive elements and further enhance expression (Yeung et al., 2017). In addition, strains based on UAS1B6, UAS1B8 or UAS1B10 blocks, respectively, could

provide a useful compromise between expression strength and stability. Finally, one could also try to express the cluster as bacterial-type polycistronic operon using a single promoter that is driven by only one large UAS1B element, although this architecture seems inferior to the monocistronic design in the yeast (Wong et al., 2017b).

4.2.4 Influence of the genetic control elements onto the PUFA cluster gene expression

The control of gene expression in *Y. lipolytica* is complex and not fully understood (Dulermo et al., 2017b). In this regard, we studied the obtained mutants for expression of the PUFA cluster genes during the exponential growth phase, the early production phase, and the late production phase, using qRT-PCR. Although the observed patterns were generally complex, several significant findings could be extracted. As exemplified for strains TEF Af4 and U4-TEF Af4, the use of the UAS1B elements strongly increased the expression of all cluster genes, independent of the time point during the fermentation (Figure 18A). The expression increase was strongest during the early and the late stationary phase, respectively, and resulted in up to ten-fold higher expression levels for the genes *pfa1* and *pfa2*. In this regard, the use of the activating sequence motifs shifted expression of the clusters towards the stationary phase, when most of the DHA was produced. Similar enhancing effects were also observed for other mutants (Figure S 8).

On the other hand, interesting findings resulted for the incorporation of the *TEF* intron between promoter and cluster gene. First, when used in combination with P_{TEF}, the presence of the intron caused time and gene dependent alterations of the expression level (Figure 18C and D). It seemed to preferentially increase the expression of *pfa2* and *pfa3*, the two inner cluster genes, while it rather caused a decrease in expression of the two flanking genes *pfa1* and *ppt*. For *pfa3* and *ppt*, the stimulating and attenuating effect, respectively, was observed in all culture phases. For *pfa1* and *pfa2*, however, an effect was only observed for the exponential phase (when DHA was not produced). On average, normalized to the expression level of *pfa1* (set to 1), the use of the intron resulted in a pronounced re-balancing of gene expression (Figure 18C). The two inner genes,

which were expressed about two-fold less than the two outer genes in strain TEF Af4, were strongly upregulated by the intron. This resulted in an almost four-fold higher expression ratio between inner and outer genes. Interestingly, the use of the *TEF* intron did not cause similarly significant changes in strains that were based on $P_{minLEU2}$, eventually due to an incompatibility of the naturally non-cooperating genetic elements (Figure S 7).

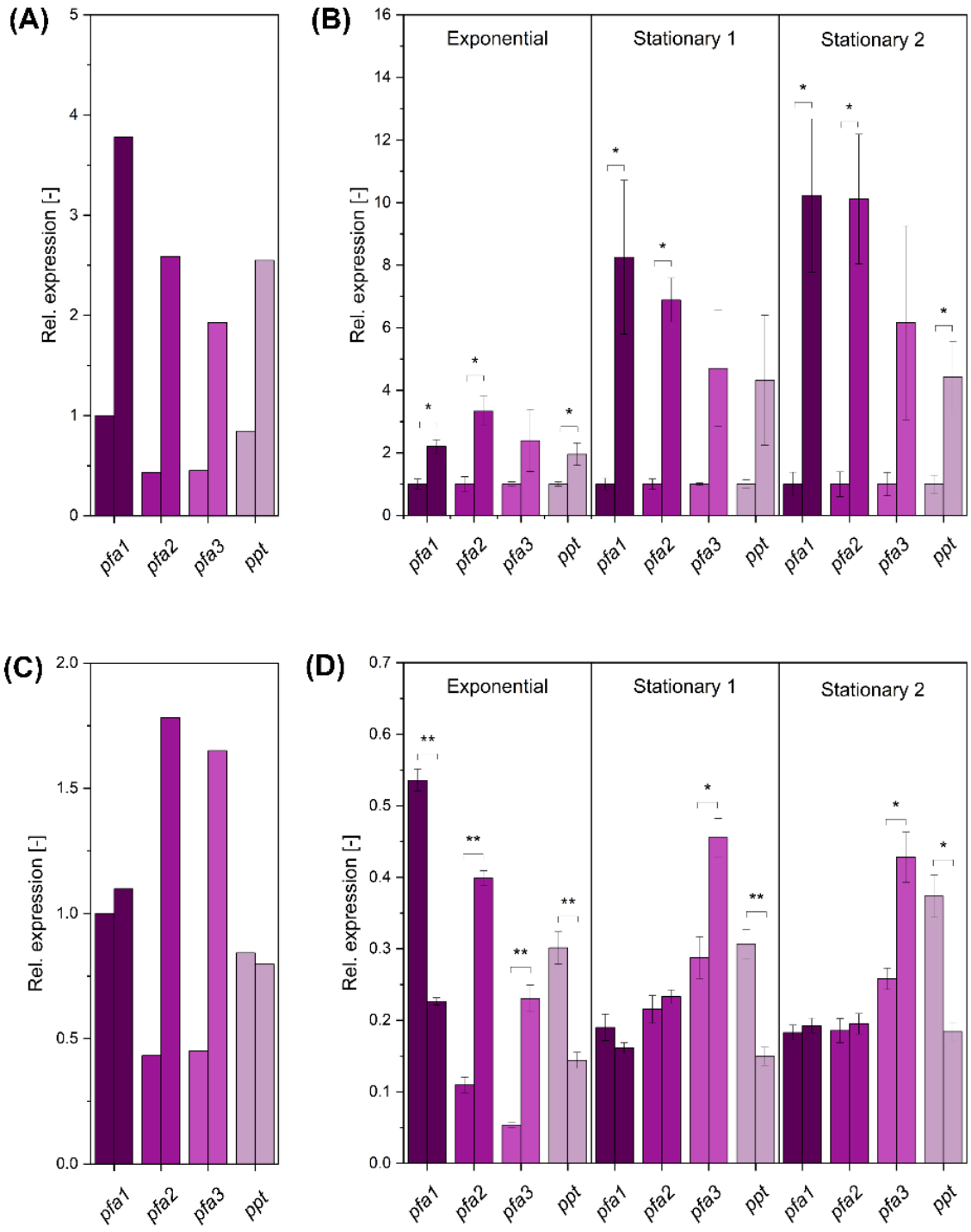

Figure 18: Impact of genetic control elements on the expression of the myxobacterial cluster genes in *Y. lipolytica*.

Average expression during glycerol-based production in strains TEF Af4 (left bars) and U4-TEF Af4 (right bars) (A). Time resolved expression during the exponential phase, the early production (stationary 1), and the late production phase (stationary 2) in strains TEF Af4 (left bars) and U4-TEF Af4 (right bars). The expression levels are normalized to expression in TEF Af4 (B). Average expression during glycerol-based production in strains TEF Af4 (left bars) and TEF-Int Af4 (right bars) (C). Time resolved expression during the exponential phase, the early production (stationary 1), and the late production phase (stationary 2) in strains TEF Af4 (left bars) and TEF-Int Af4 (right bars). The expression levels are normalized to expression in TEF Af4 (D). For each time point, the relative expression was calculated as ratio of expression of a single gene, compared to all four PUFA genes. Gene expression was measured using qRT-PCR, and the data provide mean value and standard errors from three biological replicates. Statistical significance was assessed by a Students T-test. *: p=0.05; **: p=0,01.

The promoter architecture has a huge potential to balance transcription in the oleaginous yeast *Y. lipolytica* (Portela et al., 2017). As example, the expression of a two gene-pathway as one operon, a pseudo-operon, and in monocistronic resulted in significantly different expression levels (Wong et al., 2017b). The resulting transcriptional responses are, however, difficult to predict, suggesting systematic testing and fine-tuning of different genetic layouts for a given problem (Wong et al., 2017b). Efficient refactoring of biosynthetic gene clusters (BGCs) in heterologous hosts can be important to achieve high production efficiency (Li et al., 2021b), supported by a range of prominent examples (Birchler & Veitia, 2010; Gießelmann et al., 2019; Montiel et al., 2015; Pauli et al., 2023; Rohles et al., 2022; Rohles et al., 2018; Shao et al., 2013). About 15% of the genes of *Y. lipolytica* contain introns (Mekouar et al., 2010), rendering this element important for expression control in the yeast (Le Hir et al., 2003a). Here, the introduction of the *TEF* intron resulted a mixed outcome (Figure 18**,** Figure S 7). Similarly, previous studies revealed a complex picture. As example, the *TEF* intron had a positive influence on GFP expression for multiple promoters, including P_{TEF} but caused no effect when using the *GPD* promoter (Cui et al., 2021b). In another study that aimed at fatty ester production, the *TEF* intron revealed strongly reduced gene expression under control of UAS1B4 P_{TEF}, whereas the combination with the core P_{TEF} had no influence (Gao et al., 2018). Moreover, introns revealed positional effects when integrated in two-gene configurations (Wong et al., 2017b). Here, we observed significant promoter- and gene-specific effects of the *TEF* intron (Figure 18**,** Figure S 7). It modulated expression of the cluster genes, when combined with the *TEF* promoter but caused only marginal effects in $P_{minLEU2}$-based mutants (Figure 18**,** Figure S 7). With regard to the cluster genes, the *TEF* intron reduced the expression of the first and the last gene, *pfa1* and *ppt*, while amplifying the expression of the two middle genes *pfa2* and *pfa3* in different phases of the cultivation, respectively (Figure 18). Obviously, the functionality of the intron depended on the genetic environment within the PUFA cluster, differing from the UAS1B elements, which enabled a generally increased gene expression. Both elements were found useful, and, beneficially, yielded synergistic effects (Figure 15). As shown, a strong total expression of the PUFA cluster genes (up to a certain level; Figure 19D) as well as a high expression ratio of (*pfa2*+*pfa3*) versus (*pfa1* + *ppt*) (Figure

19E) emerged as important features of high-level producers. In addition, we found positive effects, when introducing a spacer between to genes (Figure 15). In this regard, the three control elements offer promising complementary properties to streamline expression further.

4.2.5 Enhanced DHA biosynthesis results in the depletion of intracellular acetyl-CoA and malonyl-CoA.

The assembly of one molecule of DHA required the supply of one acetyl-CoA and ten malonyl-CoA units. As efficient precursor supply was known to be crucial for metabolite overproduction, it was interesting to see, if the different levels of production among the created strain genealogy affected the availability of the two CoA-thioester pools. Using careful quenching and extraction for sampling and LC-MS/MS for analysis, based on internal ^{13}C-labeled standards, we quantified the absolute levels of several CoA-thioesters during the phase of DHA production (Figure 19). Acetyl-CoA was the most abundant one, followed by succinyl-CoA, whereas malonyl-CoA, propionyl-CoA, and butyryl-CoA were present at 10-50-fold lower level. The different producers revealed strong variations in CoA-thioester abundance (Figure 19A). Interestingly, the intracellular levels decreased with increasing DHA production. As example, the best producer contained 50% less acetyl-CoA than the producer with the lowest efficiency. The pool of malonyl-CoA was even stronger affected. The best producer contained 80% less of the precursor than the one with the lowest DHA titer. Interestingly, similar trends also applied to the other CoA-esters, suggesting that these pools were, to some extent, actively equilibrated. This effect was obvious for the pools of acetyl-CoA and malonyl-CoA, which appeared tightly coupled among all producers (R^2 = 0.93) (Figure 19B). A linear correlation was also obtained between DHA production and intracellular malonyl-CoA availability (R^2 = 0.95), revealing that the engineered producers were not able to fully replenish the main DHA precursors pool during product synthesis (Figure 19C), pointing to a potential bottleneck in precursor supply that emerged more and more with stepwise strain improvement. On the transcriptional side, mean gene expression showed a positive trend towards higher expression (Figure 19D). Digging deeper into the link between transcription and production performance, the inspection of expression ratios between different genes of the cluster

revealed another interesting insight. Across all strains, an appropriate ratio between the expression of the genes *pfa2* plus *pfa3* to the genes *pfa1* plus *ppt*, i. e. between the inner to the outer cluster genes, seemed crucial to achieve high DHA production (Figure 19E).

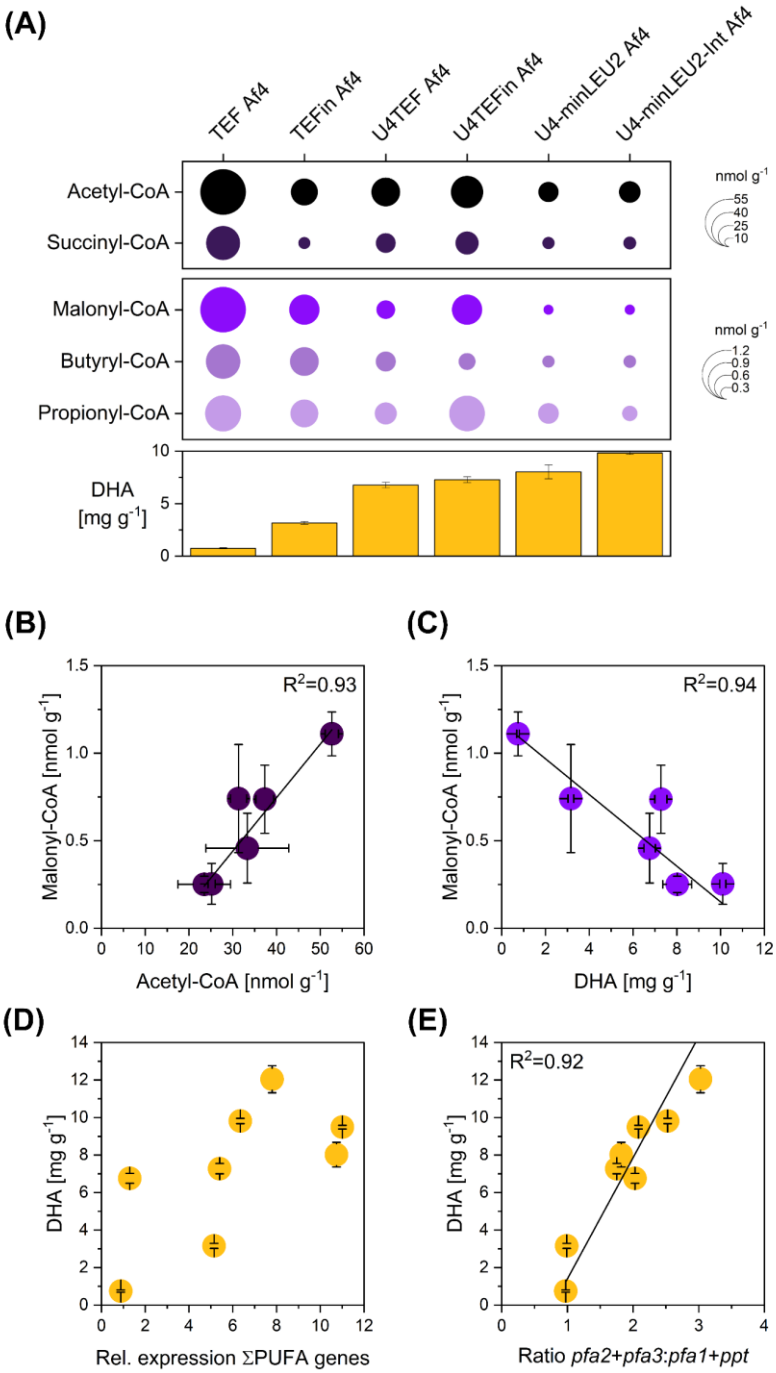

Figure 19: A systems view on heterologous DHA production in *Y. lipolytica*.

Absolute levels of intracellular CoA thioesters in different producers were determined using LC-MS/MS and internal 13C standards, sampled during the early production phase (20 h after the maximum biomass concentration had been reached). The data display mean values and standard errors from three biological replicates. In addition, the final DHA titer after 185 h of cultivation is displayed (A). Correlation between the intracellular availability of acetyl-CoA and malonyl-CoA, the two precursors for DHA biosynthesis. Each data point represents a different strain (B). Correlation of the intracellular level of the major DHA-precursor malonyl-CoA and the overall production performance. Each data point represents a different strain (C). Correlation between PUFA cluster expression and DHA production performance. The given expression strength displays the sum of expression of all four cluster genes in the different strains during the DHA production phase. The data display mean values and standard errors from three biological replicates (D). Correlation between expression balance and DHA production performance. The given value displays the expression ratio between *pfa2+pfa3* versus *pfa1+ppt* in the different strains during the DHA production phase. The data display mean values and standard errors from three biological replicates (D).

The increase of cluster expression to a certain level increased DHA formation, demonstrating that the efficiency of the initial strains was transcriptionally limited (Figure 15). Sufficient precursor availability is an important pre-requisite for efficient metabolite overproduction (Christmann et al., 2023; Gläser et al., 2021; Kind et al., 2014; Wittmann et al., 2007). The synthesis of one molecule of DHA requires the supply of one molecule of acetyl-CoA and ten molecules of malonyl-CoA, respectively. It was therefore interesting to note that strains with higher DHA production contained significantly less intracellular CoA esters (Figure 19A). The pool of malonyl-CoA, the major DHA-building block even closely correlated to the extent of overproduction: high-level producers contained six-fold less of the CoA thioester (Fig. 7C). Notably, the pools of succinyl-CoA and malonyl-CoA were also found to be coupled, indicating balancing effects between different CoA esters as also observed in other microbes (Glaser et al., 2020; Gläser et al., 2021; Kuhl et al., 2020). The findings indicate to streamline the CoA ester supply for further strain improvement, which has proven successful before to overproduce other CoA-based products in *Y. lipolytica* (Arnesen & Borodina, 2022; Huang et al., 2018; Lu et al., 2020).

4.3 Fed-batch production process for DHA

To assess performance under industrially relevant conditions, we benchmarked the DHA producer *Y. lipolytica* Po1h::Af4 in a fed-batch process (Figure 20). Glucose and glycerol were tested as carbon sources in parallel setups with a starting C/N ratio of 11 and a C/P ratio of 57, thus phosphate levels were doubled and YNB was set to 1.7 g L^{-1} accounting for the increased cell concentration in comparison to a shake flask batch culture. On both substrates, the strain grew fast during the initial batch phase and reached a biomass level of about 30 g L^{-1}. During this phase, DHA was not accumulated. Glycerol catabolism resulted in a slight accumulation of citrate, which was not observed in the glucose-based process. Both substrates were efficiently consumed during the first 48 h. Likely triggered by the limitation of phosphate, growth then stopped, and the cells switched into production mode. The DHA level increased to more than 350 mg L^{-1} on glucose after 300 h. On glycerol, the final titer was slightly lower (300 mg L^{-1}). The glucose-based process was superior in regard to the fraction of DHA formed. The DHA content gradually increased during the process and reached a final value of more than 10% of TFAs. The imposed feed rate enabled low substrate levels during the entire feed phase, which, however, were still high enough to keep cells in their producing mode. Citrate accumulated to some extent during the feed-phase, whereas it was slightly higher in glycerol. Other by-products were not detected.

The established fermentation setup enabled *Y. lipolytica* Po1h::Af4 to exceed the maximal titers in shake flask experiments by more than a factor of 3 on glucose. Intracellular DHA concentration (~12 $mg_{DHA}\ g_{CDM}^{-1}$) was similar to the best condition in the shake flask (Table 2; condition 6), thus the increased titers result from an overall higher cell concentration. As cell concentrations of over 100 $g_{CDM}\ L^{-1}$ have been reported for *Yarrowia*, even higher titers are possible (Liu et al., 2022; Marella et al., 2020; Sáez-Sáez et al., 2020). Extrapolating the DHA content to the highest reported cell densities, titers of over 1 g DHA L^{-1} could be achieved. The glycerol-based fed-batch cultivation felt short of the expectations, since it couldn't exhibit the performance increase over glucose from shake flask experiments. The intracellular DHA concentration (9.2 $mg_{DHA}\ g_{CDM}^{-1}$) did not reach the levels measured previously in shake flask cultivations (14.53 $mg_{DHA}\ g_{CDM}^{-1}$), thus further investigation of the metabolic

limitations in shake flask versus fed-batch fermentation would be needed to unlock the full potential in *Yarrowia* on glycerol. As Sabra et al. (2017) found, glycerol-based *Y. lipolytica* cultures adjust their carbon metabolism depending on the oxygen supply. Glucose-based cultures were found to be less affected, which eventually results in citrate formation (as precursor for acetyl-CoA). Looking at the results from bioreactor and shake flask comparison low dissolved oxygen levels might be beneficial and could lead especially in glycerol-based bioreactor to further performance increases. Consequently, the effect of different dissolved oxygen levels on production performance should be tested in future bioreactor experiments. Acetate as a cheap and promising carbon source funneling right into the acetyl-CoA pool might be tested in a co-substrate fed-batch fermentation to investigate the potential benefit of the high intracellular DHA content. Additionally, other acetyl-CoA supplying medium supplements should be considered (e.g. lysine, leucine, isoleucine or short chain fatty acids).

Besides the here described approach DHA production in *Y. lipolytica* was reported by researchers associated with DuPont (Damude et al., 2014). The patented process (US8685682B2, US20060115881A1) reached 5.6% DHA or 56.6% EPA of TFAs by employing several elongases and desaturases to convert the native linoleic acid to DHA (Wang et al., 2022). The novel commercialized process made PUFA production economically viable and price-competitive with EPA from marine sources (Xie et al., 2015).

In case of the here described PKS-based approach further development is needed to push titers to reach cost-effective production. The fermentation has to be optimized in regards of cell density and space time yield. Therefore, all relevant physicochemical process parameters like pH, temperature, duration, but first and foremost the production medium needs to be enhanced since the nutrient ratios and available resources stand out to influence the productivity. As shown in this work, improvements from shake flask experiments do not always translate to bioreactor fermentations at larger scale, thus further focus on process development is needed.

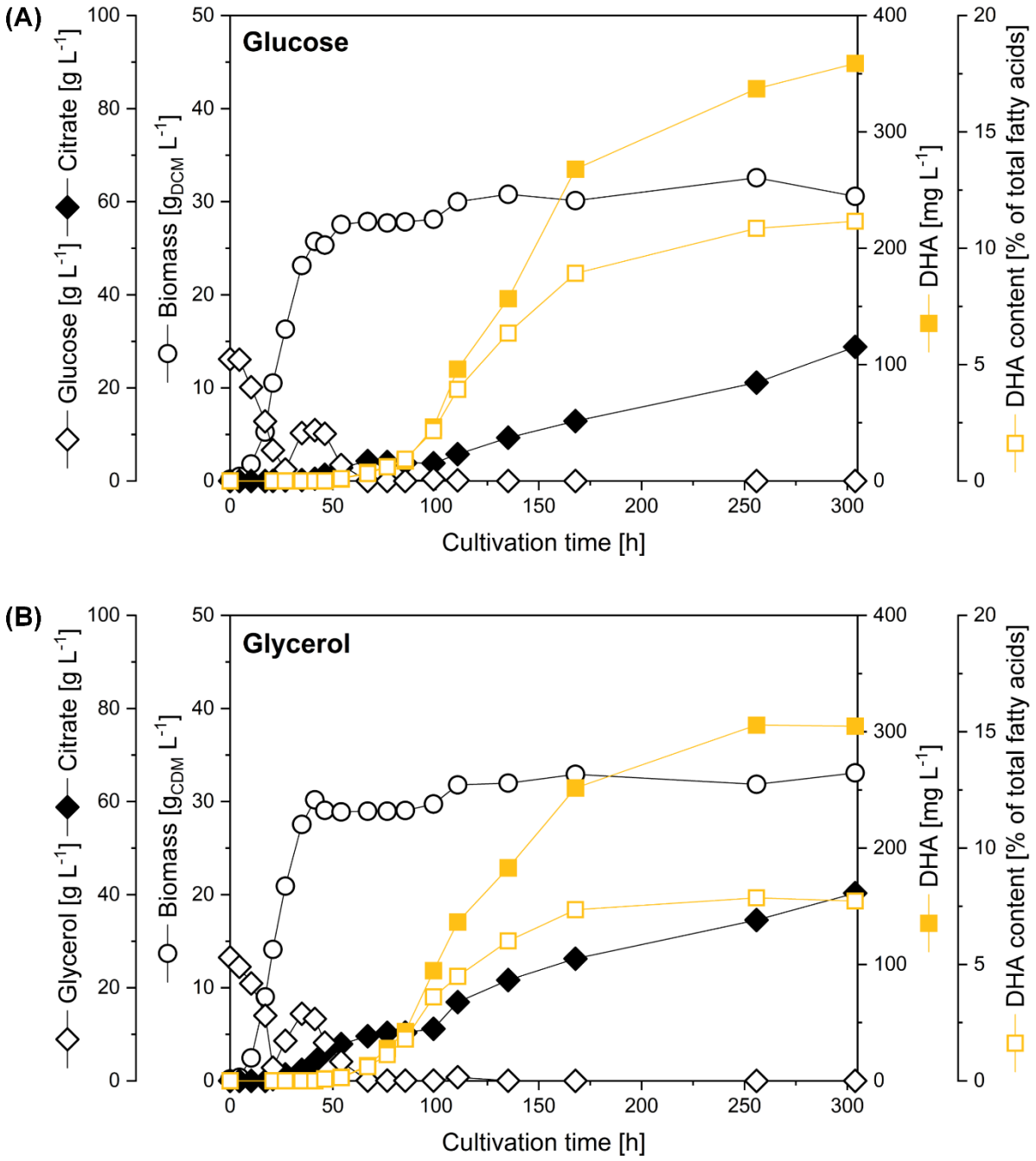

Figure 20: DHA production in fed-batch fermentation using *Y. lipolytica* Po1h::Af4.

The strain was grown in two configurations, supplying the following batch medium with either glucose or glycerol: 25 g L^{-1} carbon source, 1.7 g L^{-1} YNB, 5 g L^{-1} ammoniumsulfate, 1.0 g L^{-1} KH_2PO_4. After the depletion of the substrate, a 600 g L^{-1} carbon source solution was fed, maintaining a low carbon concentration until the end of the fermentation. pH was maintained at 5.5 with 5 M HCl and 6 M NaOH feeds. Temperature: 28 °C; Dissolved oxygen: 30% growth phase, 5% production phase. Coefficients of variation (CVs) across biological replicates were below 5% for biomass, substrate, and citrate levels, and below 10% for PUFA and native fatty acid content.

5 Conclusion and outlook

The oleaginous yeast *Y. lipolytica* has emerged as a promising host for the bioproduction of various chemicals, foods, and pharmaceuticals, owing to its inherent robustness and metabolic versatility (Park & Ledesma-Amaro, 2022). It possesses all the necessary attributes to serve as an industrial workhorse for the microbial production of valuable compounds, ranging from biofuels to pharmaceutically relevant nutraceuticals such as EPA and DHA (Wang et al., 2022). In light of global warming and ongoing issue of overfishing, the reliance on marine sources of LC-PUFAs as a crucial part of our diet has become scarce and unsustainable (Jovanovic et al., 2021).

In this work, we aimed to optimize DHA production in *Y. lipolytica* by expressing a myxobacterial PKS-like PUFA synthase. Initially, we focused on developing an improved growth medium by identifying and optimizing the key medium components that have the greatest impact on DHA production. Particularly, the replacement of phosphate buffer by MES buffer has proven to be beneficial for DHA production. The resulting phosphate restriction was even more efficient than a commonly employed nitrogen restriction. Additionally, a reduction in YNB, thus further constraining the supply of phosphate and other growth-supporting supplements, as well as unrestrictive nitrogen levels, we were able to achieve even higher levels of DHA production. Among the different carbon sources tested, glycerol proved to be superior to glucose or acetate. However, it should be noted that the transferability of results obtained in shake flasks to bioreactor-scale production was not always successful, highlighting the need for further investigation in this area.

In the second part of this work, a modular cloning approach was developed to understand and streamline the expression of the myxobacterial PUFA synthase. The best strain *Y. lipolytica* U4-*minLEU2*-Int-S expressed the cluster with compact upstream activating sequences (U4), 5'-introns (Int), and spacers (S) under control of the *minLEU2* promoter. Hereby, the different genetic control elements acted synergistically, with the UAS1B elements generally increasing expression and the intron causing gene-specific effects. The mutant achieved a 16-fold increased DHA content of 17.1% of total fatty acids as compared to a basic strain mutant that expressed a minimal cluster under control of strong

constitutive *TEF* promoter. Mutants with UAS1B16 sequences in 2-8 kb proximity were found genetically unstable, suggesting avoiding long repetitive sequence blocks in synthetic multi-gene clusters to assure genetic long-term stability of the strain. These findings have significant implications for the development of *Y. lipolytica* strains for industrial-scale production of PUFAs and related products In addition, they might provide guidance to streamline other *Y. lipolytica* cell factories based on heterologous multi-gene pathways (Arnesen et al., 2020; Huang et al., 2018; Lu et al., 2020).

As a benchmark, we carried out fed-batch fermentations of the *Y. lipolytica* Po1h::Af4 strain, which eventually led to titers of up to 350 mg DHA per liter. By strain the optimization DHA levels of 17.1 % of TFAs have been reached, displaying a further increase from previously published levels (Gemperlein et al., 2019). The combined efforts in strain engineering and bioprocess development serve as a solid foundation for future optimization and transfer to industrial scale with the aim to compete with currently established microalgae-based processes. Most promising, however, will be the application for the expression of other myxobacterial PUFA clusters and the production of other long-chain PUFA molecules such as EPA, DPA or TPA, extending the scope of their industrial applications (Gemperlein et al., 2019).

6 Supplementary

6.1 Supplementary figures

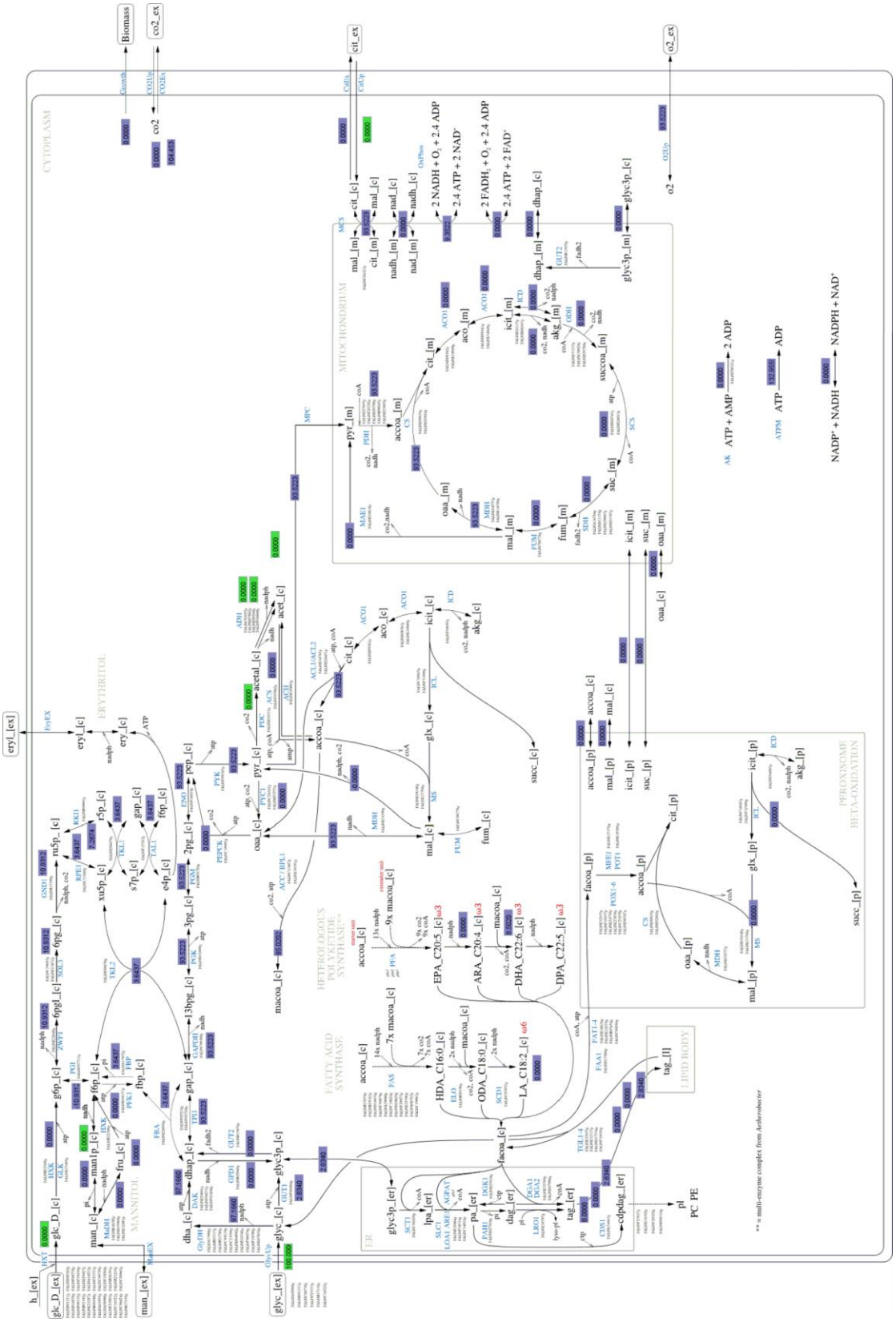

Figure S 1: Flux balance analysis for the production of DHA in *Y. lipolytica* with glycerol as C-source.

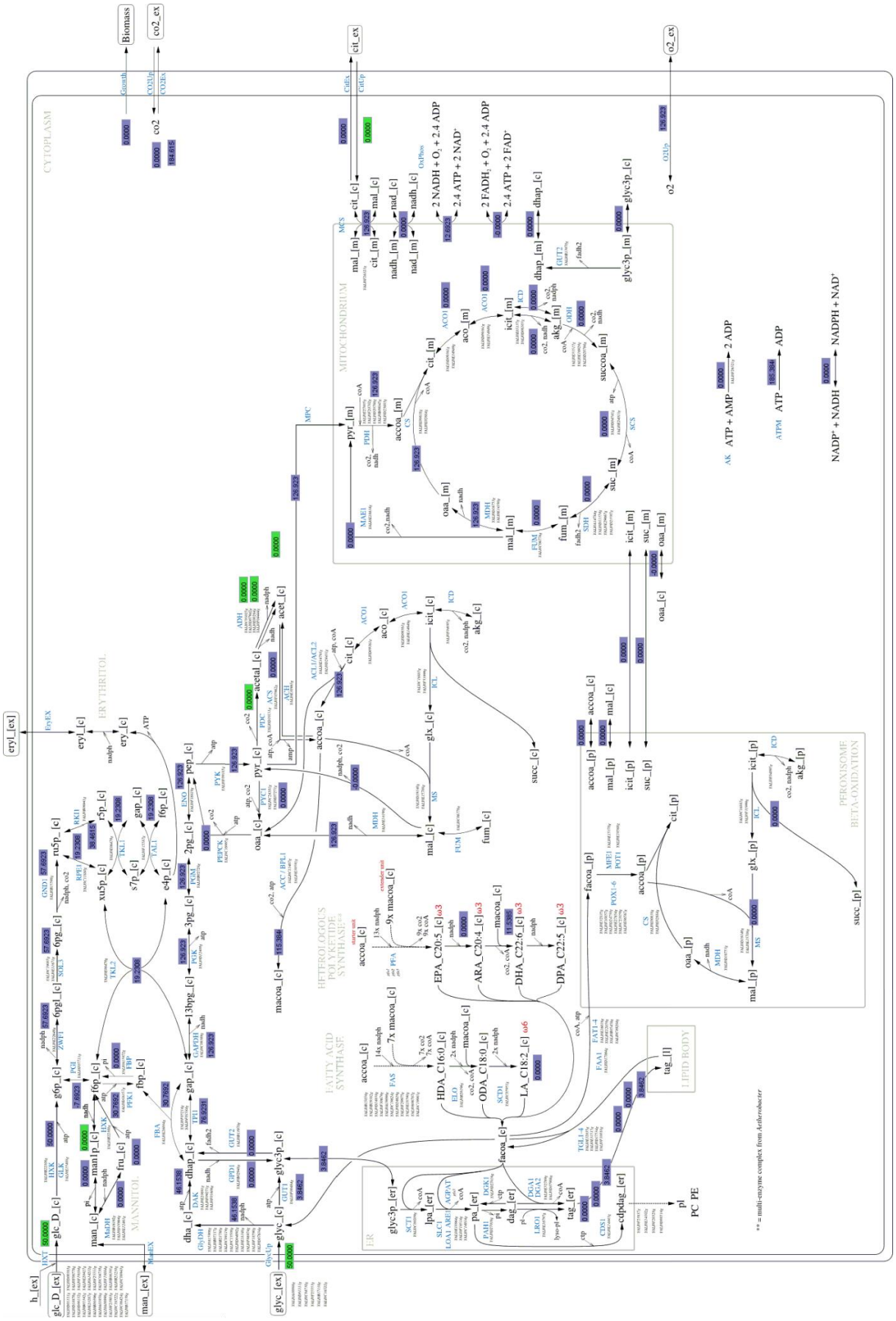

Figure S 2: Flux balance analysis for the production of DHA in *Y. lipolytica* with glycerol and glucose as C-source.

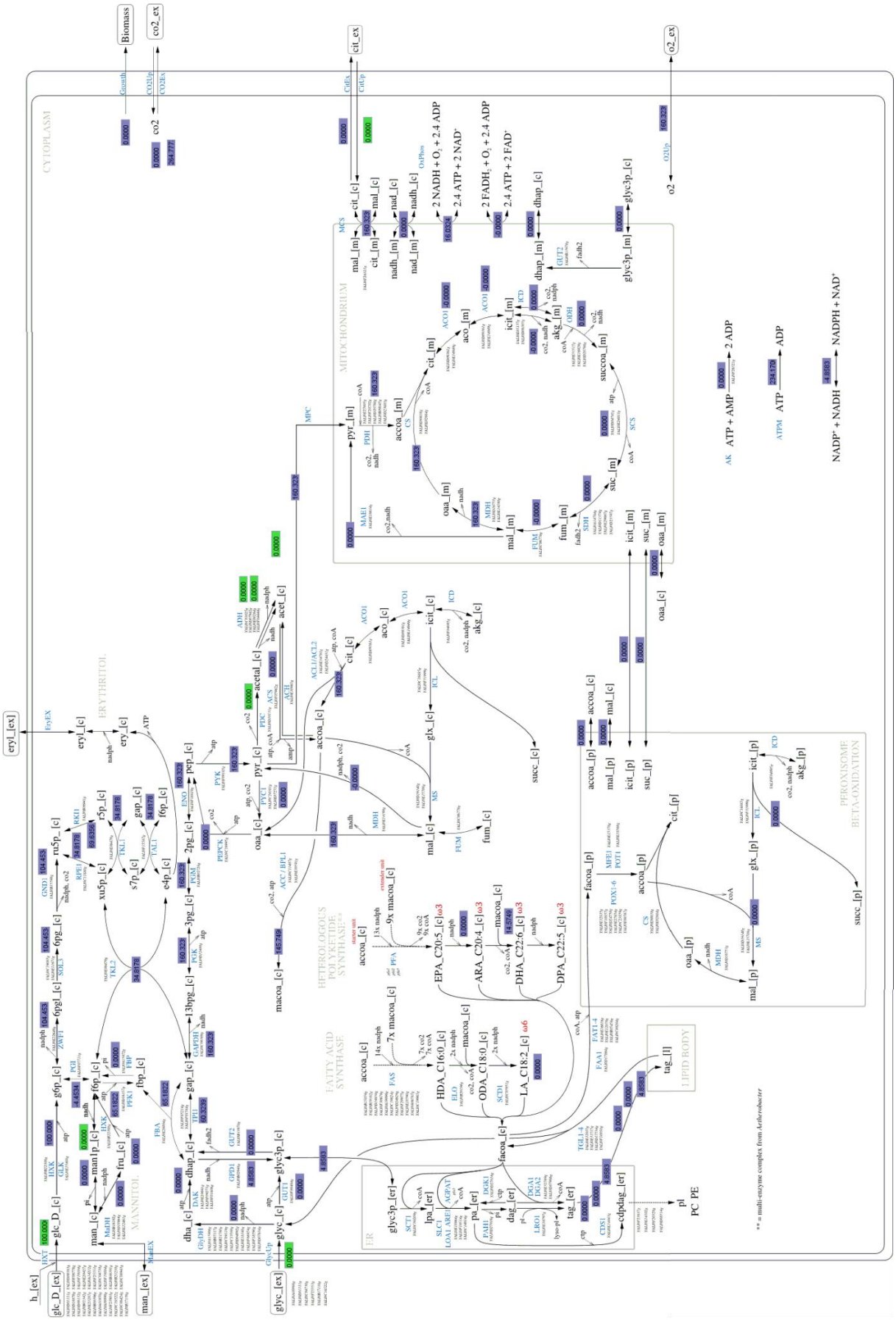

Figure S 3: Flux balance analysis for the production of DHA in *Y. lipolytica* with glucose.

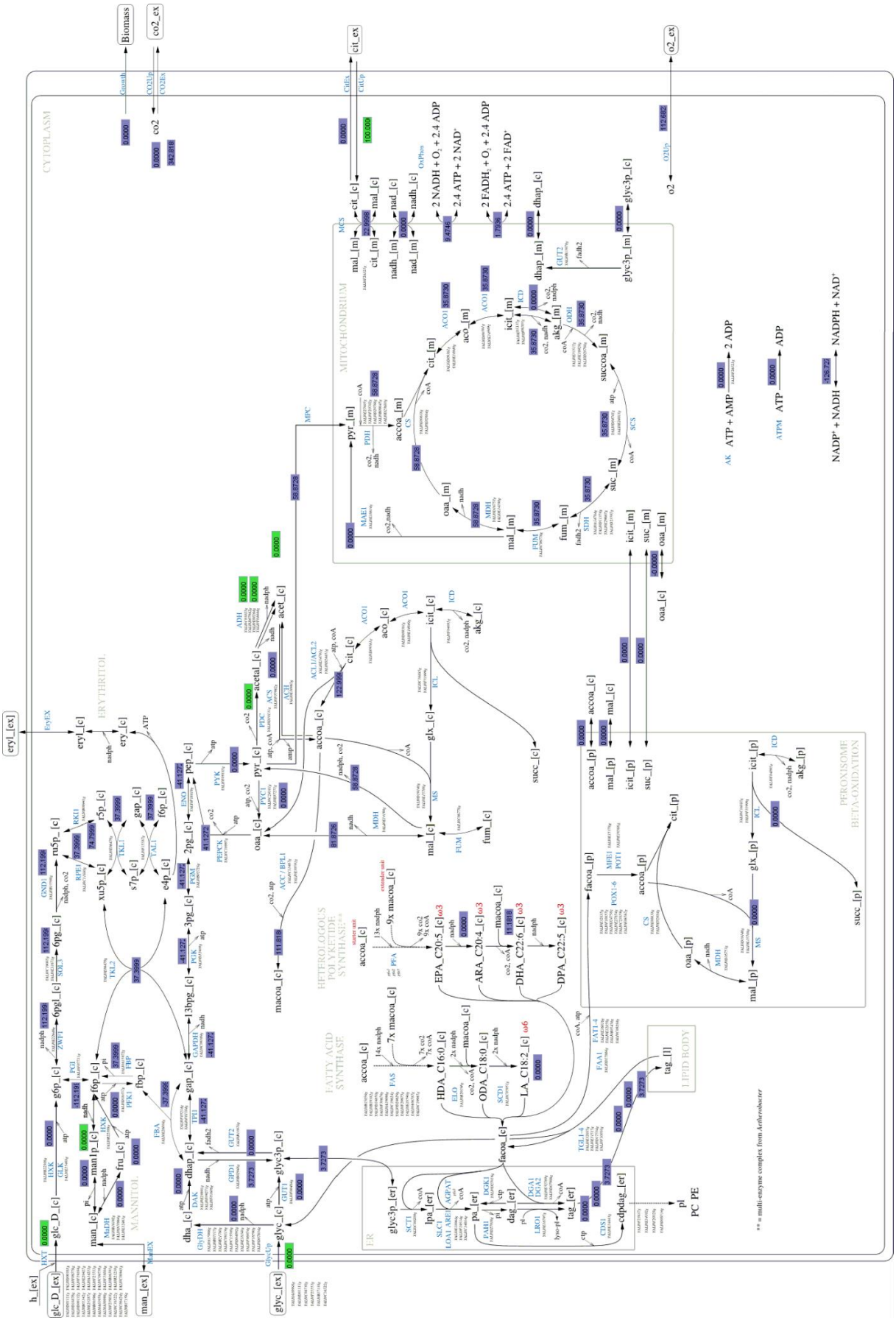

Figure S 4: Flux balance analysis for the production of DHA in *Y. lipolytica* with citrate as C-source.

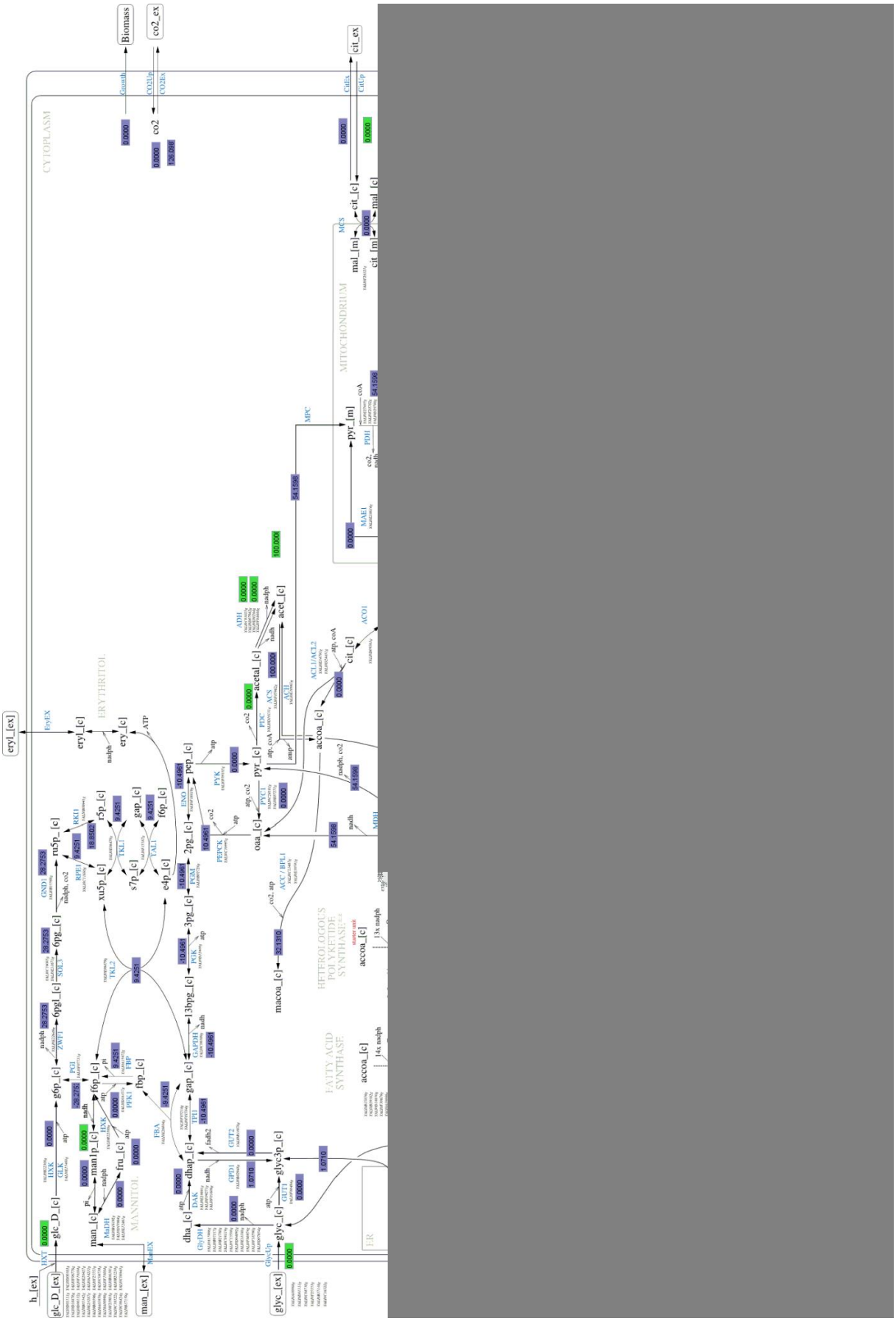

Figure S 5: Flux balance analysis for the production of DHA in *Y. lipolytica* with acetate as C-source.

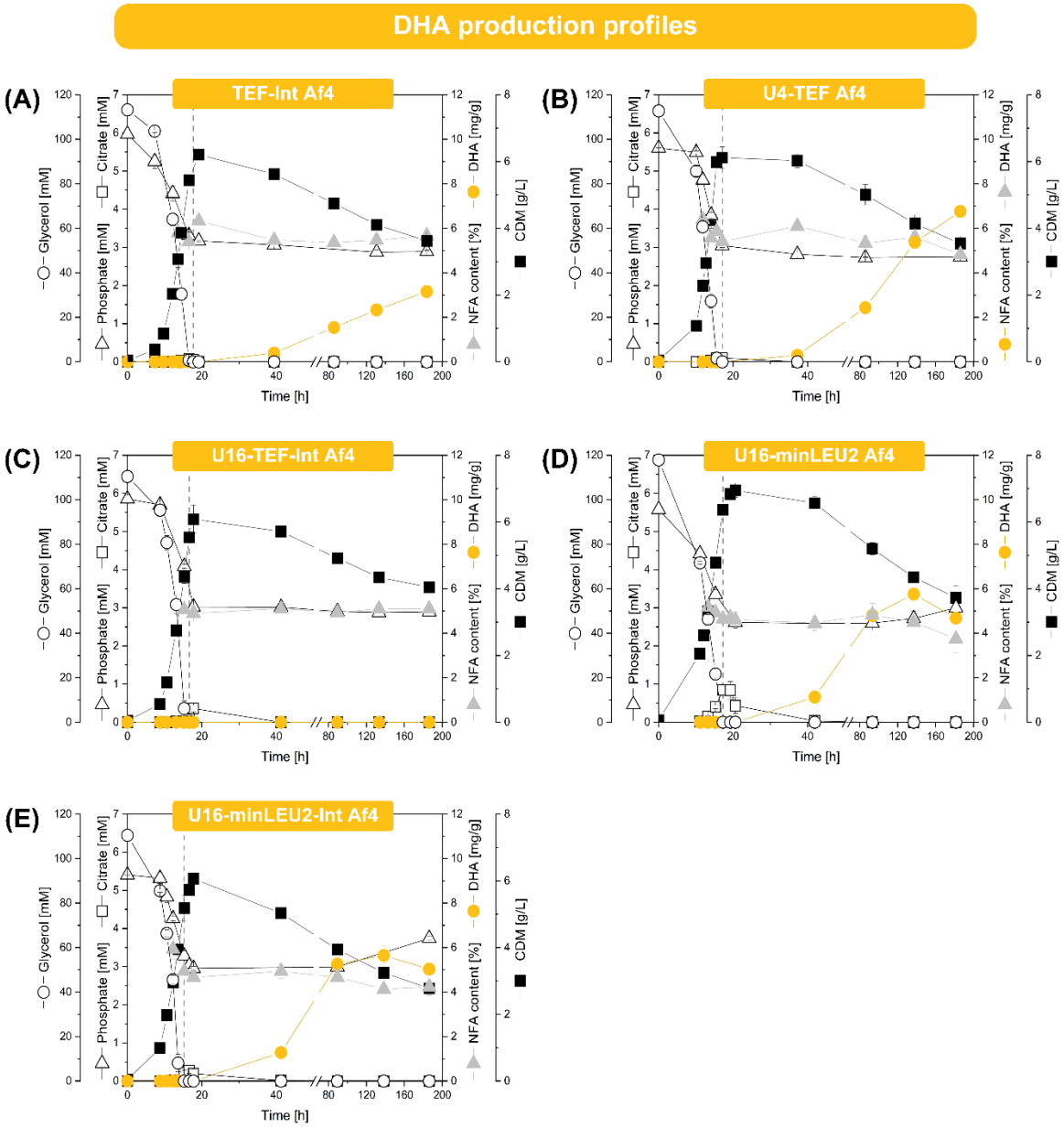

Figure S 6: DHA production profiles depending on the genetic architecture of the PUFA cluster.

The strains were cultivated in a glycerol-based minimal medium over 185 hours. The time point of glycerol depletion is indicated by a dotted line. The data display mean values and standard errors from three biological replicates. NFA = native fatty acids.

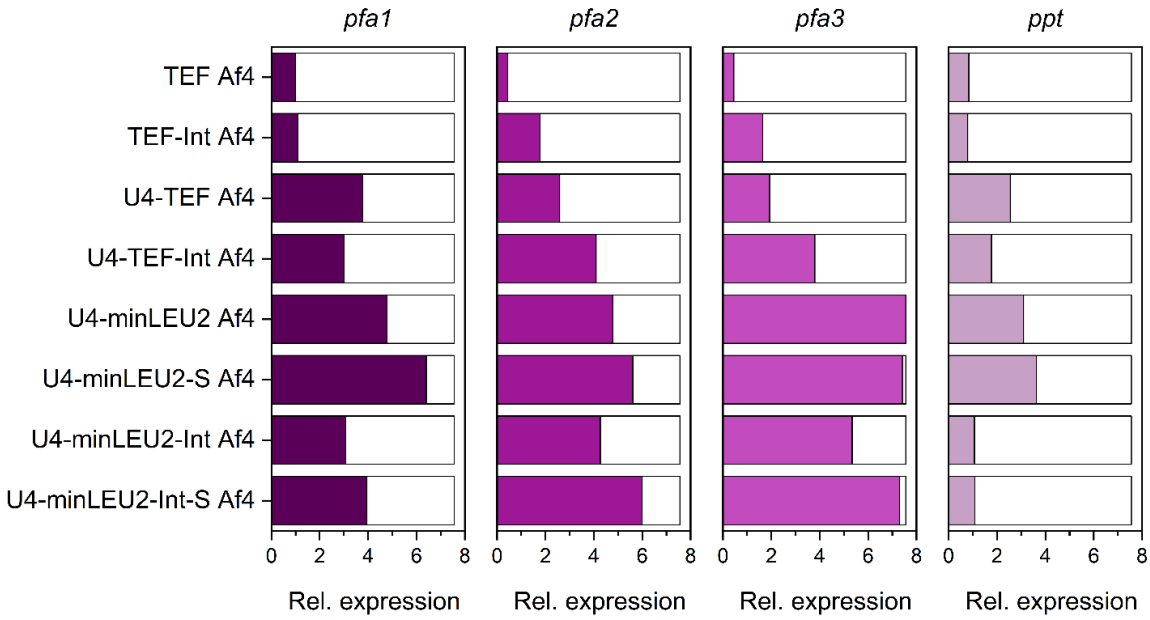

Figure S 7: Relative Expression of PUFA cluster genes.

Total expression of PUFA gene for intergenic and strain comparison with the mean relative expression towards *pfa1* of the strain *Y. lipolytica* TEF Af4. Strains were cultivated in triplicates in shake flasks for approximately 185 h. mRNA samples taken at three time points of the cultivation.

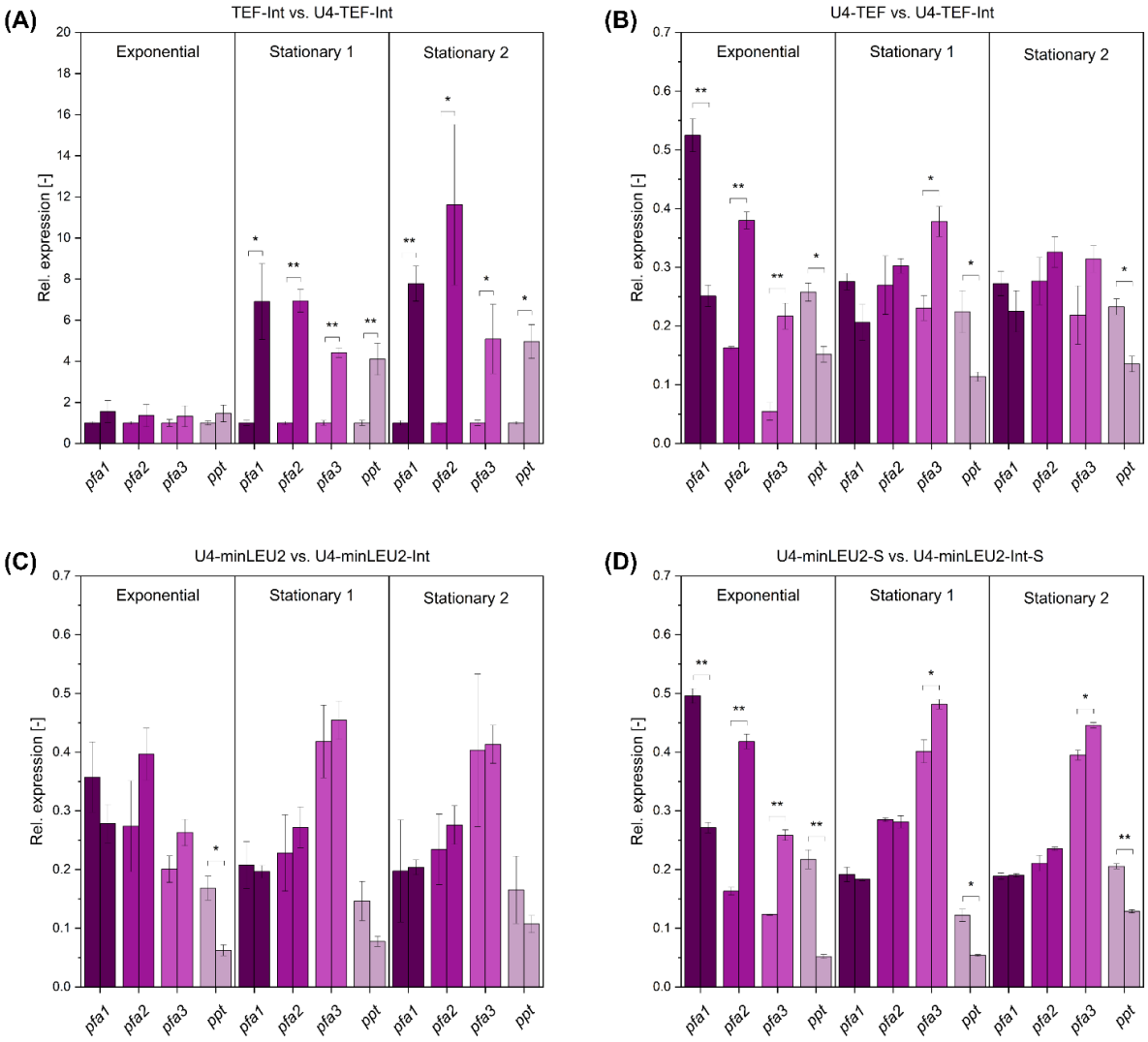

Figure S 8: Influence of genetic elements on PUFA gene expression and balance.

(A) Expression comparison of strain TEF-Int Af4 (left bars) and U4-TEF-Int Af4 (right bars) in in the exponential phase, early stationary phase (S1) and late stationary phase (S2). Expression was normalized to the expression of each gene in TEF Af4. (B) PUFA gene balance of strain U4-TEF Af4 (left bars) and U4-TEF-Int Af4 (right bars) in the exponential phase, early stationary phase (S1) and late stationary phase (S2). Relative expression is calculated by the ratio of the expression of the single gene and the total PUFA gene expression for each time point. (C) PUFA gene balance of strain U4-minLEU2 Af4 (left bars) and U4-minLEU2-Int Af4 (right bars) in the exponential phase, early stationary phase (S1) and late stationary phase (S2). Relative expression is calculated by the ratio of the expression of the single gene and the total PUFA gene expression for each time point. (D) PUFA gene balance of strain U4-minLEU2-S Af4 (left bars) and U4-minLEU2-Int-S Af4 (right bars) in the exponential phase, early stationary phase (S1) and late stationary phase (S2). Relative expression is calculated by the ratio of the expression of the single gene and the total PUFA gene expression for each time point. Significance was calculated with students t-test. *: p=0.05; **: p=0,01.

6.2 Supplementary methods

Generation of the PUFA gene cluster building blocks (BB; Table S5).

Generation of UAS and Spacer:

UAS1B4/16 sequence was cut from plasmids pUC57-Kan-UAT4 and pUC57-Kan-UAS1B16 with BseRI to create BB_U4 or BB_U16, respectively. Spacer1/2/3 were amplified from pSynPfaPptAf4 with the primer pairs Pr_Link1_FW_v2/ Pr_Link1_RW_v2, Pr_Link2_FW_v2/Pr_Link2_RW_v2, Pr_Link3_FW_v2/ Pr_Link3_RW_v2 to gain BB_S1/S2/S3, respectively.

Generation of the single gene expression units (SGUs):

SGU's consisting of a promoter, ORF and terminator sequence. PUFA genes were amplified from pSynPfaPptAf4.

PCR product with Pr_Pfa1_FW_pTEF/Pr_Lip2t_RW_ApaLI_pTEFgibson amplification was integrated by Gibson assembly into pUC19_SdaI_PrTEF_AjuI cut with AjuI and subsequentially cut with SdaI+ApaLI to create BB_T1 or cut with SmaI for the integration of BB_U4 or BB_U16 by GA and cut with SdaI+ApaLI to create BB_U4T1 and BB_U16T1. PCR product with Pr_Pfa2_FW_pTEF/Pr_Lip2t_RW_AclI_pTEFgibson amplification was integrated by Gibson assembly into pUC19_ApaLI_PrTEF_AjuI cut with AjuI and subsequentially cut with ApaLI+AclI to create BB_T2 or cut with SmaI for the integration of BB_U4 or BB_U16 by GA and cut with ApaLI+AclI to create BB_U4T2 and BB_U16T2. PCR product with Pr_Pfa3_FW_pTEF/Pr_Lip2t_RW_AvrII_pTEFgibson amplification was integrated by Gibson assembly into pUC19_AclI_PrTEF_AjuI cut with AjuI and subsequentially cut with AclI+AvrII to create BB_T3 or cut with SmaI for the integration of BB_U4 or BB_U16 by GA and cut with AclI+AvrII to create BB_U4T3 and BB_U16T3. PCR product with Pr_Ppt_FW_pTEF/Pr_Lip2t_RW_PacI_pTEFgibson amplification was integrated by Gibson assembly into pUC19_AvrII_PrTEF_AjuI cut with AjuI and subsequentially cut with AvrII+PacI to create BB_TP or cut with SmaI for the integration of BB_U4 or BB_U16 by GA and cut with AvrII+PacI to create BB_U4TP and BB_U16TP. PCR product with Pr_Pfa1_FW_pTEFin/Pr_Lip2t_RW_ApaLI amplification was integrated by Gibson assembly into pUC19_SdaI_PrTEFin(-) cut with SnaBI and subsequentially cut with SdaI+ApaLI to create BB_Tin1 or cut with SmaI for the integration of BB_U4 or BB_U16 to create BB_U4Tin1 and BB_U16Tin1.

PCR product with Pr_Pfa2_FW_pTEFin/Pr_Lip2t_RW_AclI amplification was integrated by Gibson assembly into pUC19_ApaLI_PrTEFin(-) cut with SnaBI and subsequentially cut with ApaLI+AclI to create BB_Tin2 or cut with SmaI for the integration of BB_U4 or BB_U16 to create BB_U4Tin2 and BB_U16Tin2. PCR product with Pr_Pfa3_FW_pTEFin/Pr_Lip2t_RW_AvrII amplification was integrated by Gibson assembly into pUC19_AclI_PrTEFin(-) cut with SnaBI and subsequentially cut with AclI+AvrII to create BB_Tin3 or cut with SmaI for the integration of BB_U4 or BB_U16 to create BB_U4Tin3 and BB_U16Tin3. PCR product with Pr_Ppt_FW_pTEFin/Pr_Lip2t_RW_PacI amplification was integrated by Gibson assembly into pUC19_AvrII_PrTEFin(-) cut with SnaBI and subsequentially cut with AvrII+PacI to create BB_TinP or cut with SmaI for the integration of BB_U4 or BB_U16 to create BB_U4TinP and BB_U16TinP. PCR

product with Pr_minLEU2_SdaI/Pr_Lip2t_RW_ApaLI_pTEFgibson amplification was integrated by Gibson assembly into pUC19 cut with SmaI and subsequently cut with SmaI for the integration of BB_U4 or BB_U16 by GA and cut with SdaI+ApaLI to create BB_U4M1 and BB_U16M1, respectively.

PCR product with Pr_minLEU2_ApaLI/Pr_Lip2t_RW_AclI_pTEFgibson amplification was integrated by Gibson assembly into pUC19 cut with SmaI and subsequently cut with SmaI for the integration of BB_U4 or BB_U16 by GA and cut with ApaLI+AclI to create BB_U4M2 and BB_U16M2, respectively. PCR product with Pr_minLEU2_AclI/Pr_Lip2t_RW_AvrII_pTEFgibson amplification was integrated by Gibson assembly into pUC19 cut with SmaI and subsequently cut with SmaI for the integration of BB_U4 or BB_U16 by GA and cut with AclI+AvrII to create BB_U4M3 and BB_U16M3, respectively. PCR product with Pr_minLEU2_AvrII/Pr_Lip2t_RW_PacI_pTEFgibson amplification was integrated by Gibson assembly into pUC19 cut with SmaI and subsequently cut with SmaI for the integration of BB_U4 or BB_U16 by GA and cut with AvrII+PacI to create BB_U4MP and BB_U16MP, respectively. PCR product with Pr_Pfa1_FW_pTEFin /Pr_Lip2t_RW_ApaLI amplification was integrated by Gibson assembly into pUC19_SdaI_hpNdin_cassette cut with SnaBI and subsequently cut with SmaI for the integration of BB_U4 or BB_U16 by GA and cut with SdaI+ApaLI to create BB_U4Min1 and BB_U16Min1, respectively. PCR product with Pr_Pfa2_FW_pTEFin/Pr_Lip2t_RW_AclI amplification was integrated by Gibson assembly into pUC19_ApaLI_hpNdin_cassette cut with SnaBI and subsequently cut with SmaI for the integration of BB_U4 or BB_U16 by GA and cut with ApaLI+AclI to create BB_U4Min2 and BB_U16Min2, respectively. PCR product with Pr_Pfa3_FW_pTEFin/Pr_Lip2t_RW_AvrII amplification was integrated by Gibson assembly into pUC19_AclI_hpNdin_cassette cut with SnaBI and subsequently cut with SmaI for the integration of BB_U4 or BB_U16 by GA and cut with AclI+AvrII to create BB_U4Min3 and BB_U16Min3, respectively.

PCR product with Pr_Ppt_FW_pTEFin/Pr_Lip2t_RW_PacI amplification was integrated by Gibson assembly into pUC19_AvrII_hpNdin_cassette cut with SnaBI and subsequently cut with SmaI for the integration of BB_U4 or BB_U16 by GA and cut with AvrII+PacI to create BB_U4MinP and BB_U16MinP, respectively. Based on the generated building blocks the clusters were assembled by sequential ligation into pACYC_assembly, which was cut for the integration with the respective restriction enzymes used for the liberation of the building blocks. Subsequently, the PUFA clusters (PC) liberated with SdaI+PacI (see Table S6). The finished PC's are then ligated into pKG2-PIS via SdaI+PacI to yield the integration cassette plasmid (see Table S3). For the integration the plasmids are cut with SwaI+NotI and the linearized integration cassette is integrated into Po1h to gain the respective modified strains (Table S2)

Table S1: Strain characteristics for growth and DHA production performance. Shake flask cultivations were carried out in triplicates (n=3). Performance parameters were determined after 185 h.

Strains	Cluster size [kb]	μ_{max} [h^{-1}]	Biomass yield [g_{CDM} C-mole^{-1}]	DHA [mg g_{CDM}^{-1}]	DHA [g L^{-1}]	DHA [% of TFAs]
U4-minLEU2-Int-S Af4	20.76	0.34 ± 0.00	16.78 ± 0.46	12.04 ± 0.72	48.3 ± 1.88	17.13 ± 0.40
U4-minLEU2-S Af4	20.27	0.36 ± 0.01	17.07 ± 0.19	9.49 ± 0.10	41.2 ± 4.4	13.87 ± 0.51
U16-minLEU2-Int Af4	25.28	0.28 ± 0.01	18.30 ± 0.39	5.65 ± 0.39	13.2 ± 0.93	11.67 ± 0.82
U4-minLEU2-Int Af4	20.17	0.30 ± 0.20	19.80 ± 1.06	9.82 ± 0.14	43.8 ± 0.64	16.55 ± 0.50
U16-minLEU2 Af4	24.79	0.20 ± 0.00	19.65 ± 0.59	5.76 ± 0.24	18.2 ± 1.20	10.80 ± 0.99
U4-minLEU2 Af4	19.69	0.32 ± 0.02	19.65 ± 0.84	8.02 ± 0.66	35.4 ± 1.81	14.07 ± 0.31
U16-TEF-Int Af4	26.43	0.32 ± 0.02	18.37 ± 1.27	0	0	0
U4-TEF-Int Af4	21.32	0.34 ± 0.01	16.62 ± 0.45	7.27 ± 0.28	23.1 ± 0.51	10.63 ± 0.58
TEF-Int Af4	19.62	0.35 ± 0.01	18.28 ± 0.44	3.16 ± 0.13	10.7 ± 0.67	5.10 ± 0.27
U4-TEF Af4	20.83	0.35 ± 0.02	18.09 ± 0.94	6.76 ± 0.26	23.4 ± 0.46	11.93 ± 0.55
TEF Af4	19.13	0.34 ± 0.00	18.09 ± 0.31	0.75 ± 0.06	3.1 ± 0.32	1.27 ± 0.15

Table S2: Strains used in this study.

Genomic integration of the clusters into YALI0_C05907g by homologous recombination.

Strains	Description	Source
Po1h (CLIB882)	*MatA, ura3-302, xpr2-322, axp1-2*	Madzak et al.
Po1h::Af4	Po1h with a genomic copy of SynPfaPptAf4 cluster *(*from pSynPfaPptAf4)	Gemperlein et al.
TEF-Af4	Po1h with a genomic copy of pTEF-*pfa1-LIP2t*-pTEF-*pfa2-LIP2t*-pTEF-*pfa3-LIP2t*-pTEF-*ppt-LIP2t (*from pPrTEFAf4)	This work
U4-TEF Af4	Po1h with a genomic copy of U4-pTEF-*pfa1-LIP2t*-U4-pTEF-*pfa2-LIP2t*-U4-pTEF-*pfa3-LIP2t*-U4-pTEF-*ppt-LIP2t (*from pU4PrTEFAf4)	This work
TEF-Int Af4	Po1h with a genomic copy of pTEF-Int-*pfa1-LIP2t*-pTEF-Int-*pfa2-LIP2t*-pTEF-Int-*pfa3-LIP2t*-pTEF-Int-*ppt-LIP2t (*from pPrTEFinAf4)	This work
U4-TEF-Int Af4	Po1h with a genomic copy of U4-pTEF-Int-*pfa1-LIP2t*-U4-pTEF-Int-*pfa2-LIP2t*-U4-pTEF-Int-*pfa3-LIP2t*-U4-pTEF-Int-*ppt-LIP2t (*from pU4PrTEFinAf4)	This work
U16-TEF-Int Af4	Po1h with a genomic copy of U16-pTEF-Int-*pfa1-LIP2t*-U16-pTEF-Int-*pfa2-LIP2t*-U16-pTEF-INt-*pfa3-LIP2t*-U16-pTEF-Int-*ppt-LIP2t (*from pU16PrTEFinAf4)	This work
U4-minLEU2 Af4	Po1h with a genomic copy of U4-minLEU2-*pfa1-LIP2t*-U4-minLUE2-*pfa2-LIP2t*-U4-minLEU2-*pfa3-LIP2t*-U4-minLEU2-*ppt-LIP2t* (from php4dAf4)	This work
U16-minLEU2 Af4	Po1h with a genomic copy of U16-minLEU2-*pfa1-LIP2t*-U16-minLEU2-*pfa2-LIP2t*-U16-minLEU2-*pfa3-LIP2t*-U16-minLEU2-*ppt-LIP2t* (from php16dAf4)	This work
U4-minLEU2-Int Af4	Po1h with a genomic copy of U4-minLEU2-Int-*pfa1-LIP2t*-U4-minLEU2-Int-*pfa2-LIP2t*-U4-minLEU2-Int-*pfa3-LIP2t*-U4-minLEU2-Int-*ppt-LIP2t* (from php4dinAf4)	This work
U16-minLEU2-Int Af4	Po1h with a genomic copy of U16-minLEU2-Int-*pfa1-LIP2t*-U16-minLEU2-Int-*pfa2-LIP2t*-U16-minLEU2-Int-*pfa3-LIP2t*-U16-minLEU2-Int-*ppt-LIP2t* (from php16dinAf4)	This work
U4-minLEU2-S Af4	Po1h with a genomic copy of U4-minLEU2-*pfa1-LIP2t*-linker1-U4-minLEU2-*pfa2-LIP2t*-linker2-U4-minLEU2-*pfa3-LIP2t*-linker3-U4-minLEU2-*ppt-LIP2t* (from php4dAf4_1xL)	This work
U4-minLEU2-Int-S Af4	Po1h with a genomic copy of U4-minLEU2-Int-*pfa1-LIP2t*-linker1-U4-minLEU2-Int -*pfa2-LIP2t*-linker2-U4-minLEU2-Int -*pfa3-LIP2t*-linker3-U4-minLEU2-Int -*ppt-LIP2t* (from php4dinAf4_1xL)	This work

Table S3: Plasmids used in this study.

aph(3')-IIa: kanamycin resistance gene; *cat*: chloramphenicol resistance gene; LIP2t: terminator of gene *LIP2* encoding from *Y. lipolytica*; minLEU2: minimal pLEU2 from *Y. lipolytica; oriV*: origin of replication; *ura3*: orotidine 5'-phosphate decarboxylase gene from *Y. lipolytica*; PC: PUFA Cluster from Table S6; $UAS1B_n$: upstream activating sequence 1 (UAS1) of pXPR2 from *Y. lipolytica* in tandem repeats of the count of n; U4/U16: upstream activating sequence 1 (UAS1) of pXPR2 from *Y. lipolytica* in tandem repeats of 4 or 16.

Plasmid	Description
pACYC_assembly	Derivative of pACYC177 (New England Biolabs). A fragment with *SdaI, ApaLI, NcoI, SalI, AclI, AatII, NgoMIV, AvrII*, and *PacI* restriction sites were inserted into the digested plasmid (*DraI*/*BamHI*)
pKG2-PIS	p15A *oriV* and *cat* of pACYC184 (New England Biolabs) with *ura3p-ura3-ura3t* and *SdaI-PacI* flanked by 1 kb homology regions for the integration in the preferred integration site.
pSynPfaPptAf4	Gemperlein et al.
pUC57-Kan-UAT4	Derivative of pUC57 (GenScript) with *aph(3')-Ia* kanamycin resistance gene and UAS1B2-*EcoRV*-UAS1B2 which is flanked by *BseRI* restriction sites and overlaps for the integration into *SmaI* of pUC19 by Gibson assembly.
pUC57-Kan-UAT4-ext	Derivative of pUC57 (GenScript) with *aph(3')-Ia* kanamycin resistance gene and UAS1B2-*EcoRV*-UAS1B2 which is flanked by *SchI* restriction sites and the integration into *EcoRV* of pUC57-Kan-UAT4 by ligation.
pUC57-Kan-UAS1B8	Derivative of pUC57-Kan-UAT4 with UAS1B2-*EcoRV*-UAS1B2 from pUC57-Kan-UAT4-ext integrated into *EcoRV.*
pUC57-Kan-UAS1B12	Derivative of pUC57-Kan-UAS1B8 with UAS1B2-*EcoRV*-UAS1B2 from pUC57-Kan-UAT4-ext integrated into *EcoRV.*
pUC57-Kan-UAS1B16	Derivative of pUC57-Kan-UAS1B12 with UAS1B2-*EcoRV*-UAS1B2 from pUC57-Kan-UAT4-ext integrated into *EcoRV.*
pUC19_SdaI_PrTEF_AjuI	Derivative of pUC19 (New England Biolabs) with *SdaI-pTEF-AjuI.*
pUC19_ApaLI_PrTEF_AjuI	Derivative of pUC19 (New England Biolabs) with *ApaLI-pTEF-AjuI.*
pUC19_AclI_PrTEF_AjuI	Derivative of pUC19 (New England Biolabs) with *AclI-pTEF-AjuI.*
pUC19_AvrII_PrTEF_AjuI	Derivative of pUC19 (New England Biolabs) with *AvrII-pTEF-AjuI.*
pUC19_SdaI_PrTEFin(-)	Derivative of pUC19 (New England Biolabs) with *SdaI-pTEF* with the first intron of *tef* from *Y. lipolytica* followed by *SnaBI.*
pUC19_ApaLI_PrTEFin(-)	Derivative of pUC19 (New England Biolabs) with *ApaLI-pTEF* with the first intron of *tef* from *Y. lipolytica* followed by *SnaBI.*
pUC19_AclI_PrTEFin(-)	Derivative of pUC19 (New England Biolabs) with *AclI-pTEF* with the first intron of *tef* from *Y. lipolytica* followed by *SnaBI.*
pUC19_AvrII_PrTEFin(-)	Derivative of pUC19 (New England Biolabs) with *AvrII-pTEF* with the first intron of *tef* from *Y. lipolytica* followed by *SnaBI.*
pUC19_SdaI_hpNdin_cassette	Derivative of pUC19 (New England Biolabs) with *SdaI-minLEU2* with the first intron of *tef* from *Y. lipolytica* followed by *SnaBI.*
pUC19_ApaLI_hpNdin_cassette	Derivative of pUC19 (New England Biolabs) with *ApaLI-minLEU2* with the first intron of *tef* from *Y. lipolytica* followed by *SnaBI.*
pUC19_AclI_hpNdin_cassette	Derivative of pUC19 (New England Biolabs) with *AclI-minLEU2* with the first intron of *tef* from *Y. lipolytica* followed by *SnaBI.*
pUC19_AvrII_hpNdin_cassette	Derivative of pUC19 (New England Biolabs) with *AvrII-minLEU2* with the first intron of *tef* from *Y. lipolytica* followed by *SnaBI.*
pPrTEFAf4	Derivative of pKG2-PIS with PC_T integrated into *SdaI* and *PacI*

pU4PrTEFAf4	Derivative of pKG2-PIS with PC_U4T integrated into *SdaI* and *PacI*
pPrTEFinAf4	Derivative of pKG2-PIS with PC_Ti integrated into *SdaI* and *PacI*
pU4PrTEFinAf4	Derivative of pKG2-PIS with PC_U4Ti integrated into *SdaI* and *PacI*
pU16PrTEFinAf4	Derivative of pKG2-PIS with PC_U16Ti integrated into *SdaI* and *PacI*
php4dAf4	Derivative of pKG2-PIS with PC_U4M integrated into *SdaI* and *PacI*
php16dAf4	Derivative of pKG2-PIS with PC_U16M integrated into *SdaI* and *PacI*
php4dinAf4	Derivative of pKG2-PIS with PC_U4Mi integrated into *SdaI* and *PacI*
php16dinAf4	Derivative of pKG2-PIS with PC_U16Mi integrated into *SdaI* and *PacI*
php4dAf4_1xL	Derivative of pKG2-PIS with PC_U4ML integrated into *SdaI* and *PacI*
php4dinAf4_1xL	Derivative of pKG2-PIS with PC_U4MiL integrated into *SdaI* and *PacI*

Table S4: Assembly and sequencing primers used.

Overlaps are shown in bold and restriction sites are underlined.

Type	Primer	Sequence (5'→3')
Amplification	Pr_FW_pTEFin(-)	**AGGTCGACTCTAGAGGATC**CCCGGGAGAGACCGG GTTGGCGGCGCATTTG
	Pr_RW_pTEFin(-)	**AGTGAATTCGAGCTCGG**TACGTACTGCAAAAAGTG CTGGTCGGAT
	Pr_Ver_pUC19_MCS_FW	GGTTTCGCCACCTCTGACTTGAGC
	Pr_Ver_pUC19_MCS_RW	GTGCCACCTGACGTCTAAGAAACC
	Pr_Pfa1_FW_pTEFin	**ACCAGCACTTTTTGCAGTAC**TAACCGCAGTCCGCTA TTGGCCGATGGAATGCTC
	Pr_Lip2t_RW_ApaLI	**AGTGAATTCGAGCTCGGTAC**GTGCACGGTTTCGAT TTGTCTTAGAGG
	Pr_Pfa2_FW_pTEFin	**ACCAGCACTTTTTGCAGTAC**TAACCGCAGACCCAA GTCCCCGTTGCTATTGTC
	Pr_Lip2t_RW_AclI	**AGTGAATTCGAGCTCGGTAC**AACGTTGGTTTCGATT TGTCTTAGAGG
	Pr_Pfa3_FW_pTEFin	**ACCAGCACTTTTTGCAGTAC**TAACCGCAGACCTTTG AACCTATTGCTATCGTCG
	Pr_Lip2t_RW_AvrII	**AGTGAATTCGAGCTCGGTAC**CCTAGGGGTTTCGAT TTGTCTTAGAGG
	Pr_Ppt_FW_pTEFin	**ACCAGCACTTTTTGCAGTAC**TAACCGCAGGCCCTG CTGGACCTGCCCCGAGGAG
	Pr_Lip2t_RW_PacI	**AGTGAATTCGAGCTCGGTAC**TTAATTAAGGTTTCGA TTTGTCTTAGAGG
	Pr_Pfa1_FW_pTEF	**GAGTATAAGAATCATTCAAA**ATGTCCGCTATTGGCC GATGGAATGCTC
	Pr_Lip2t_RW_ApaLI_pTEFgibson	**ACCCGAGGAGTGCGCGGATT**GTGCACGGTTTCGAT TTGTCTTAGAGG
	Pr_Pfa2_FW_pTEF	**GAGTATAAGAATCATTCAAA**ATGACCCAAGTCCCC GTTGCTATTGTC
	Pr_Lip2t_RW_AclI_pTEFgibson	**ACCCGAGGAGTGCGCGGATT**AACGTTGGTTTCGAT TTGTCTTAGAGG
	Pr_Pfa3_FW_pTEF	**GAGTATAAGAATCATTCAAA**ATGACCTTTGAACCTA TTGCTATCG
	Pr_Lip2t_RW_AvrII_pTEFgibson	**ACCCGAGGAGTGCGCGGATT**CCTAGGGGTTTCGAT TTGTCTTAGAGG
	Pr_Ppt_FW_pTEF	**GAGTATAAGAATCATTCAAA**ATGGCCCTGCTGGAC CTGCCCCGAGGAG
	Pr_Lip2t_RW_PacI_pTEFgibson	**ACCCGAGGAGTGCGCGGATT**TTAATTAAGGTTTCG ATTTGTCTTAGAGG
	Pr_UAS1BN_Syn_FW	GTCGACTCTAGAGGATCCCC
	Pr_UAS1BN_Syn_RW	CCGCCAACCCGGTCTCTCCC
	Pr_pUC19_mutMCS_FW_v4	**GCCAAGCTTGCATGCCTGCA**CCAATACGCAAACCG CCTCTCCC
	Pr_pUC19_mutMCS_ApaLI_RW_v4	**TCCTCTAGAGTCGACCTGCA**GTGCACGGGTGCCTA ATGAGTGAGCTAAC
	Pr_pUC19_mutMCS_AclI_RW_v4	**TCCTCTAGAGTCGACCTGCA**AACGTTGGGTGCCTA ATGAGTGAGCTAAC
	Pr_pUC19_mutMCS_AvrII_RW_v4	**TCCTCTAGAGTCGACCTGCA**CCTAGGGGGTGCCTA ATGAGTGAGCTAAC

	Pr_minLEU2_SdaI	CCTGCAGGGTCGACTCTAGAGGATCCCCGGGAGAGACCGGGTTGGCGGCATGCACTGATCACGGGCAAAAG
	Pr_minLEU2_ApaLI	GTGCACGTCGACTCTAGAGGATCCCCGGGAGAGACCGGGTTGGCGGCATGCACTGATCACGGGCAAAAG
	Pr_minLEU2_AclI	AACGTTGTCGACTCTAGAGGATCCCCGGGAGAGACCGGGTTGGCGGCATGCACTGATCACGGGCAAAAG
	Pr_minLEU2_AvrII	CCTAGGGTCGACTCTAGAGGATCCCCGGGAGAGACCGGGTTGGCGGCATGCACTGATCACGGGCAAAAG
	Pr_M13_pUC57_FW	CCCAGTCACGACGTTGTAAAACG
	Pr_M13_pUC57_RW	AGCGGATAACAATTTCACACAGG
	Pr_pTEF_AjuI_RW	TGAATTCGAGCTCGGTACCCGAGGAGTGCGCGGAACTGTTCCAAAATGCTTTTCTAAGTTG**TTTGAATGATTCTTATACTCAGAAGGAAATG**
	Pr_Lip2t_RW_SdaI	**AGTGAATTCGAGCTCGGTAC**CCTGCAGGGGTTTCGATTTGTCTTAGAGG
	Pr_Link1_FW_v2	TCTAAGACAAATCGAAACCGGGATCCGGCGC
	Pr_Link1_RW_v2	GGGATCCTCTAGAGTCGACGGCGAAGACCTGTCGAGT
	Pr_Link2_FW_v2	CTAAGACAAATCGAAACCAAACGCCAGCAAGACGTAGC
	Pr_Link2_RW_v2	GGATCCTCTAGAGTCGACAAGGCAGCGCTCTGGGT
	Pr_Link3_FW_v2	TCTAAGACAAATCGAAACCCGGCACCTGTCCT
	Pr_Link3_RW_v2	GGGATCCTCTAGAGTCGACCTTCCTTGCGGCGGCG
Sequencing	PR_seq_Pfa1_reverse	GCTGGCTGACAAATACGACTACAC
	PR_seq_Pfa1_1_forward	GGGTCGAGGTCGGAAATCAAAG
	PR_seq_Pfa1_2_forward	GTTGTCGGTATGACCACCAG
	PR_seq_Pfa2_reverse	ACTTTGGCGTTTCCGTTTCC
	PR_seq_Pfa2_1_forward	GACCTCAGCAGGTCGAACAATG
	PR_seq_Pfa2_2_forward	GATCCTTCGATCTCAGCGATG
	PR_seq_Pfa2_3_forward	AAGCCACAACCACAGAGGATCGAG
	PR_seq_Pfa2_4_forward	ATTTCAGAGGCCACCACCTCAG
	PR_seq_Pfa2_5_forward	CTTAATAGAGTCGATGCCCAGGTC
	PR_seq_Pfa2_6_forward	CGTGCTTTCCCTTTCGATCC
	PR_seq_Pfa2_7_forward	GGTAGAAGAGGCGGCATTCATC
	PR_seq_Pfa2_8_forward	GGCATCAGAGGCAACGATAG
	PR_seq_Pfa2_9_forward	CAGCTTCAGTCCGCCAAATTC
	PR_seq_Pfa2_10_forward	CGTTAGTGATTCGGTCACAGATTC
	PR_seq_Pfa3_reverse	TTTATTATGGTCGCTTCTGCC
	PR_seq_Pfa3_1_forward	GAATTCTCCCAGCCATCGATCC
	PR_seq_Pfa3_2_forward	GACCTGGTGGTTAGCGACATAGAG
	PR_seq_Pfa3_3_forward	GCAGTCCGACCTGATTGTCAAAG
	PR_seq_Pfa3_4_forward	ATCGACCTTAACAGAAGGAATAGG
	PR_seq_Pfa3_5_forward	AGGAGTCGGTAGACTCGTTC
	PR_seq_Pfa3_6_forward	ACGTGAGTGAACACAGGTTCGG
	PR_seq_Pfa3_7_forward	TCAGCAGTGTTAATAATGGTCAGG
	PR_seq_Pfa3_8_forward	TCCGACCCAAGGCATAGAAG
	PR_seq_Pfa3_9_forward	CAGGGTTTGCTCCAGATCTC
	PR_seq_Pfa3_10_forward	CTGGAGGGCAAAGAACACAG

	LIP2t_fwd	GCGTTCCTCTAAGACAAATCGAAACC
	Pr_PIS_genome_fwd	AATTCCCAGAGGTGTCGAGTGGC
	Pr_PIS_genome_rev	TGTTCGCTTCTCCTGTCTACATTGG
	Pr_seq_Ppt_fwd	CCGGTCTCCGATTTAACCTG
	Pr_seq_Ppt_rev	GGGAGAGAGCTGGAAAGAGAATTG
	Pr_seq_Prom_Pfa1	CGCACGACGTGCAGAGATTC
	Pr_seq_Prom_Pfa2	TCTCGGGAAGCCACAATATC
	Pr_seq_Prom_Pfa3	GGAGAGGTCACGGCAGATTC
qRT PCR	Pr_qRT_Pfa1_FW	TGATGAGGGAAAGCGAATGC
	Pr_qRT_Pfa1_RW	ACGCCGAGCTCAAACATATC
	Pr_qRT_Pfa2_FW	TCTTTTGGTTTCGGCGGTTC
	Pr_qRT_Pfa2_RW	AAGGGGCGGAAATCACAAAC
	Pr_qRT_Pfa3_FW	TTTCTTGGCTGGGCATTGAC
	Pr_qRT_Pfa3_RW	TCAGCATGTCCGTCAATGTG
	Pr_qRT_PPt_FW_v2	ACGACGACCTCGATTTTTCG
	Pr_qRT_PPt_RW_v2	TCCAGAACGGGATCAAAGGC
	Pr_qRT_rRNA_FW	TAACACCTCGATGTCGGCTTAC
	Pr_qRT_rRNA_RW	ACCGTGCTATCTCACAATGC

Table S5: Generated building blocks for the assembly of the PUFA clusters.

Type	Building block	Description
UAS	BB_U4	UAS1B4 (U4)
	BB_U16	UAS1B16 (U16)
Spacer	BB_S1	Spacer1
	BB_S2	Spacer2
	BB_S3	Spacer3
SGUs	BB_T1	*SdaI*-pTEF-*pfa1-ApaLI*
	BB_U4T1	*SdaI*-U4-pTEF-*pfa1-Lip2t-ApaLI*
	BB_T2	*ApaLI*-pTEF-*pfa2-AclI*
	BB_U4T2	*ApaLI*-U4-pTEF-*pfa2-AclI*
	BB_T3	*AclI*-pTEF-*pfa3-AvrII*
	BB_U4T3	*AclI*-U4-pTEF-*pfa3-AvrII*
	BB_TP	*AvrII*-pTEF-*ppt-PacI*
	BB_U4TP	*AvrII*-U4-pTEF-*ppt-PacI*
	BB_Ti1	*SdaI*-pTEF-Int-*pfa1-ApaLI*
	BB_U4Ti1	*SdaI*-U4-pTEF-Int-*pfa1-ApaLI*
	BB_U16Ti1	*SdaI*-U16-pTEF-Int-*pfa1-ApaLI*
	BB_Ti2	*ApaLI*-pTEF-Int-*pfa2-AclI*
	BB_U4Ti2	*ApaLI*-U4-pTEF-Int-*pfa2-AclI*
	BB_U16Ti2	*ApaLI*-U16-pTEF-Int-*pfa2-AclI*
	BB_Ti3	*AclI*-pTEF-Int-*pfa3-AvrII*
	BB_U4Ti3	*AclI*-U4-pTEF-Int-*pfa3-AvrII*
	BB_U16Ti3	*AclI*-U16-pTEF-Int-*pfa3-AvrII*
	BB_TinP	*AvrII*-pTEF-Int-*ppt-PacI*
	BB_U4TiP	*AvrII*-U4-pTEF-Int-*ppt-PacI*
	BB_U16TiP	*AvrII*-U16-pTEF-Int-*ppt-PacI*
	BB_U4M1	*SdaI*-U4-pminLEU2-*pfa1-ApaLI*
	BB_U16M1	*SdaI*-U16-pminLEU2-*pfa1-ApaLI*
	BB_U4M2	*ApaLI*-U4-pminLEU2-*pfa2-AclI*
	BB_U16M2	*ApaLI*-U16-pminLEU2-*pfa2-AclI*
	BB_U4M3	*AclI*-U4-pminLEU2-*pfa3-AvrII*
	BB_U16M3	*AclI*-U16-pminLEU2-*pfa3-AvrII*
	BB_U4MP	*AvrII*-U4-pminLEU2-*ppt-PacI*
	BB_U16MP	*AvrII*-U16-pminLEU2-*ppt-PacI*
	BB_U4Mi1	*SdaI*-U4-pminLEU2-Int-*pfa1-ApaLI*
	BB_U16Mi1	*SdaI*-U16-pminLEU2-Int-*pfa1-ApaLI*
	BB_U4Mi2	*ApaLI*-U4-pminLEU2-Int-*pfa2-AclI*
	BB_U16Mi2	*ApaLI*-U16-pminLEU2-Int-*pfa3-AclI*
	BB_U4Mi3	*AclI*-U4-pminLEU2-Int-*pfa3-AvrII*
	BB_U16Mi3	*AclI*-U16-pminLEU2-Int-*pfa3-AvrII*
	BB_U4MiP	*AvrII*-U4-pminLEU2-Int-*ppt-PacI*
	BB_U16MiP	*AvrII*-U16-pminLEU2-Int-*ppt-PacI*

Table S6: Generated PUFA cluster versions.

Clusters are flanked and cut by *SdaI* (upstream) and *PacI* (downstream). BB: building blocks; PC: PUFA cluster.

Cluster variants	Description
PC_T	BB_T1 + BB_T2 + BB_T3 + BB_TP
PC_U4T	BB_U4T1 + BB_U4T2 + BB_U4T3 + BB_U4TP
PC_Ti	BB_Ti1 + BB_Ti2 + BB_Ti3 + BB_TiP
PC_U4Ti	BB_U4Ti1 + BB_U4Ti2 + BB_U4Ti3 + BB_U4TiP
PC_U16Ti	BB_U16Ti1 + BB_U16Ti2 + BB_U16Ti3 + BB_U16TiP
PC_U4M	BB_U4M1 + BB_U4M2 + BB_U4M3 + BB_U4MP
PC_U16M	BB_U16M1 + BB_U16M2 + BB_U16M3 + BB_U16MP
PC_U4Mi	BB_U4Mi1 + BB_U4Mi2 + BB_U4Mi3 + BB_U4MiP
PC_U16Mi	BB_U16Mi1 + BB_U16Mi2 + BB_U16Mi3 + BB_U16MiP
PC_U4ML	BB_U4M1 + BB_S1 + BB_U4M2 + BB_S2 + BB_U4M3 + BB_S3 + BB_U4MP
PC_U4MiL	BB_U4Mi1 + BB_S1 + BB_U4Mi2 + BB_S2 + BB_U4Mi3 + BB_S3 + BB_U4MiP

7 References

Ahn, J., Hong, J., Lee, H., Park, M., Lee, E., Kim, C., . . . Lee, H. (2007). Translation elongation factor 1-alpha gene from Pichia pastoris: molecular cloning, sequence, and use of its promoter. *Applied Microbiology and Biotechnology, 74*(3), 601-608. doi:10.1007/s00253-006-0698-6

Amiri-Jami, M., & Griffiths, M. W. (2010). Recombinant production of omega-3 fatty acids in *Escherichia coli* using a gene cluster isolated from *Shewanella baltica* MAC1. *Journal of Applied Microbiology, 109*(6), 1897-1905. doi:10.1111/j.1365-2672.2010.04817.x

Amiri-Jami, M., LaPointe, G., & Griffiths, M. W. (2014). Engineering of EPA/DHA omega-3 fatty acid production by *Lactococcus lactis* subsp. *cremoris* MG1363. *Applied Microbiology and Biotechnology, 98*(7), 3071-3080. doi:10.1007/s00253-013-5381-0

Arbter, P., Sinha, A., Troesch, J., Utesch, T., & Zeng, A.-P. (2019). Redox governed electro-fermentation improves lipid production by the oleaginous yeast *Rhodosporidium toruloides*. *Bioresource Technology, 294*, 122122. doi:10.1016/j.biortech.2019.122122

Arnesen, J. A., & Borodina, I. (2022). Engineering of Yarrowia lipolytica for terpenoid production. *Metabolic engineering communications, 15*, e00213. doi:https://doi.org/10.1016/j.mec.2022.e00213

Arnesen, J. A., Kildegaard, K. R., Cernuda Pastor, M., Jayachandran, S., Kristensen, M., & Borodina, I. (2020). Yarrowia lipolytica Strains Engineered for the Production of Terpenoids. *Frontiers in Bioengineering and Biotechnology, 8*, 945. doi:10.3389/fbioe.2020.00945

Bagul, V. P., & Annapure, U. S. (2020). Effect of sequential recycling of spent media wastewater on docosahexaenoic acid production by newly isolated strain *Aurantiochytrium* sp. ICTFD5. *Bioresource Technology, 306*, 123153. doi:10.1016/j.biortech.2020.123153

Bankar, A. V., Kumar, A. R., & Zinjarde, S. S. (2009). Environmental and industrial applications of *Yarrowia lipolytica*. *Applied Microbiology and Biotechnology, 84*(5), 847-865. doi:10.1007/s00253-009-2156-8

Barescut, J., Lariviere, D., Stocki, T., Zotina, T., Trofimova, E., & Bolsunovsky, A. (2011). Artificial radionuclides in fish fauna of the Yenisei River in the vicinity of the Mining-and-Chemical Combine (Siberia, Russia). *Radioprotection, 46*(6), S75-S78. doi:10.1051/radiopro/20116649s

Barth, G., & Gaillardin, C. (1996). *Yarrowia lipolytica*. In K. Wolf (Ed.), *Nonconventional Yeasts in Biotechnology: A Handbook* (pp. 313-388). Berlin, Heidelberg: Springer Berlin Heidelberg.

Bati, N., Hammond, E. G., & Glatz, B. A. (1984). Biomodification of fats and oils: Trials with *Candida lipolytica*. *Journal of the American Oil Chemists' Society, 61*(11), 1743-1746. doi:10.1007/BF02582139

Bellou, S., Triantaphyllidou, I. E., Mizerakis, P., & Aggelis, G. (2016). High lipid accumulation in Yarrowia lipolytica cultivated under double limitation of nitrogen and magnesium. *Journal of Biotechnology, 234*, 116-126. doi:10.1016/j.jbiotec.2016.08.001

Belo, I. (2010). *Yarrowia lipolytica: an industrial workhorse*.

Beopoulos, A., Cescut, J., Haddouche, R., Uribelarrea, J.-L., Molina-Jouve, C., & Nicaud, J.-M. (2009a). *Yarrowia lipolytica* as a model for bio-oil production. *Progress in lipid research, 48*(6), 375-387. doi:10.1016/j.plipres.2009.08.005

Beopoulos, A., Chardot, T., & Nicaud, J.-M. (2009b). *Yarrowia lipolytica*: A model and a tool to understand the mechanisms implicated in lipid accumulation. *Biochimie, 91*(6), 692-696. doi:10.1016/j.biochi.2009.02.004

Beopoulos, A., Chardot, T., & Nicaud, J. M. (2009c). Yarrowia lipolytica: A model and a tool to understand the mechanisms implicated in lipid accumulation. *Biochimie, 91*(6), 692-696. doi:10.1016/j.biochi.2009.02.004

Beopoulos, A., Haddouche, R., Kabran, P., Dulermo, T., Chardot, T., & Nicaud, J.-M. (2012). Identification and characterization of DGA2, an acyltransferase of the DGAT1 acyl-CoA:diacylglycerol acyltransferase family in the oleaginous yeast *Yarrowia lipolytica*. New insights into the storage lipid metabolism of oleaginous yeasts. *Applied Microbiology and Biotechnology, 93*(4), 1523-1537. doi:10.1007/s00253-011-3506-x

Birchler, J. A., & Veitia, R. A. (2010). The gene balance hypothesis: implications for gene regulation, quantitative traits and evolution. *New Phytol, 186*(1), 54-62. doi:10.1111/j.1469-8137.2009.03087.x

Bjerregaard, P., & Dyerberg, J. (1988). Mortality from ischaemic heart disease and cerebrovascular disease in Greenland. *Int J Epidemiol, 17*(3), 514-519. doi:10.1093/ije/17.3.514

Blanchin-Roland, S., Cordero Otero, R. R., & Gaillardin, C. (1994). Two upstream activation sequences control the expression of the XPR2 gene in the yeast Yarrowia lipolytica. *Molecular and Cellular Biology, 14*(1), 327-338. doi:10.1128/mcb.14.1.327-338.1994

Blazeck, J., Hill, A., Liu, L., Knight, R., Miller, J., Pan, A., . . . Alper, H. S. (2014). Harnessing *Yarrowia lipolytica* lipogenesis to create a platform for lipid and biofuel production. *Nat Commun, 5*, 3131. doi:10.1038/ncomms4131

Blazeck, J., Liu, L., Redden, H., & Alper, H. (2011a). Tuning gene expression in Yarrowia lipolytica by a hybrid promoter approach. *Applied and Environmental Microbiology, 77*(22), 7905-7914. doi:10.1128/AEM.05763-11

Blazeck, J., Liu, L., Redden, H., & Alper, H. (2011b). Tuning Gene Expression in *Yarrowia lipolytica* by a Hybrid Promoter Approach. *Applied and Environmental Microbiology, 77*(22), 7905. doi:10.1128/AEM.05763-11

Blazeck, J., Reed, B., Garg, R., Gerstner, R., Pan, A., Agarwala, V., & Alper, H. S. (2013). Generalizing a hybrid synthetic promoter approach in Yarrowia lipolytica. *Applied Microbiology and Biotechnology, 97*(7), 3037-3052. doi:10.1007/s00253-012-4421-5

Bornscheuer, U. T. (2018). The fourth wave of biocatalysis is approaching. *Philos Trans A Math Phys Eng Sci, 376*(2110). doi:10.1098/rsta.2017.0063

Brain, R. A., & Prosser, R. S. (2022). Human induced fish declines in North America, how do agricultural pesticides compare to other drivers?

Environ Sci Pollut Res Int, 29(44), 66010-66040. doi:10.1007/s11356-022-22102-z

Breslow, J. L. (2006). n-3 fatty acids and cardiovascular disease. *Am J Clin Nutr, 83*(6 Suppl), 1477s-1482s. doi:10.1093/ajcn/83.6.1477S

Calder, P. C. (2004). n-3 Fatty acids and cardiovascular disease: evidence explained and mechanisms explored. *Clin Sci (Lond), 107*(1), 1-11. doi:10.1042/cs20040119

Calder, P. C. (2006). n-3 polyunsaturated fatty acids, inflammation, and inflammatory diseases. *Am J Clin Nutr, 83*(6 Suppl), 1505s-1519s. doi:10.1093/ajcn/83.6.1505S

Calder, P. C. (2009). Fatty acids and immune function: relevance to inflammatory bowel diseases. *Int Rev Immunol, 28*(6), 506-534. doi:10.3109/08830180903197480

Calder, P. C. (2018). Very long-chain n-3 fatty acids and human health: fact, fiction and the future. *Proc Nutr Soc, 77*(1), 52-72. doi:10.1017/s0029665117003950

Calero, P., & Nikel, P. I. (2019). Chasing bacterial chassis for metabolic engineering: a perspective review from classical to non-traditional microorganisms. *Microb Biotechnol, 12*(1), 98-124. doi:10.1111/1751-7915.13292

Christen, S., & Sauer, U. (2011). Intracellular characterization of aerobic glucose metabolism in seven yeast species by 13C flux analysis and metabolomics. *FEMS yeast research, 11*(3), 263-272. doi:10.1111/j.1567-1364.2010.00713.x

Christie, W. W., & Han, X. (2012). Chapter 1 - Lipids: their structures and occurrence. In W. W. Christie & X. Han (Eds.), *Lipid Analysis (Fourth Edition)* (pp. 3-19): Woodhead Publishing.

Christmann, J., Cao, P., Becker, J., Desiderato, C. K., Goldbeck, O., Riedel, C. U., . . . Wittmann, C. (2023). High-efficiency production of the antimicrobial peptide pediocin PA-1 in metabolically engineered Corynebacterium glutamicum using a microaerobic process at acidic pH and elevated levels of bivalent calcium ions. *Microbial Cell Factories, 22*(1), 41. doi:10.1186/s12934-023-02044-y

Cohen, Z., Norman, H. A., & Heimer, Y. M. (1995). Microalgae as a source of omega 3 fatty acids. *World Rev Nutr Diet, 77*, 1-31. doi:10.1159/000424462

Colombo, S. M., Rodgers, T. F. M., Diamond, M. L., Bazinet, R. P., & Arts, M. T. (2020). Projected declines in global DHA availability for human consumption as a result of global warming. *Ambio, 49*(4), 865-880. doi:10.1007/s13280-019-01234-6

Cui, Z., Zheng, H., Jiang, Z., Wang, Z., Hou, J., Wang, Q., . . . Qi, Q. (2021a). Identification and Characterization of the Mitochondrial Replication Origin for Stable and Episomal Expression in *Yarrowia lipolytica*. *ACS synthetic biology, 10*(4), 826-835. doi:10.1021/acssynbio.0c00619

Cui, Z., Zheng, H., Zhang, J., Jiang, Z., Zhu, Z., Liu, X., . . . Hou, J. (2021b). A CRISPR/Cas9-Mediated, Homology-Independent Tool Developed for Targeted Genome Integration in *Yarrowia lipolytica*. *Applied and environmental microbiology, 87*(6). doi:10.1128/aem.02666-20

Curran, K. A., Morse, N. J., Markham, K. A., Wagman, A. M., Gupta, A., & Alper, H. S. (2015). Short Synthetic Terminators for Improved Heterologous Gene Expression in Yeast. *ACS synthetic biology, 4*(7), 824-832. doi:10.1021/sb5003357

Damude, H. G., Gillies, P. J., Macool, D. J., Picataggio, S. K., Ragghianti, J. J., Seip, J. E., . . . Zhu, Q. Q. (2014).

Das, U. N. (2006). Essential fatty acids: biochemistry, physiology and pathology. *Biotechnology Journal, 1*(4), 420-439. doi:10.1002/biot.200600012

Del Gobbo, L. C., Imamura, F., Aslibekyan, S., Marklund, M., Virtanen, J. K., Wennberg, M., . . . Mozaffarian, D. (2016). ω-3 Polyunsaturated Fatty Acid Biomarkers and Coronary Heart Disease: Pooling Project of 19 Cohort Studies. *JAMA Intern Med, 176*(8), 1155-1166. doi:10.1001/jamainternmed.2016.2925

Drover, J. R., Hoffman, D. R., Castañeda, Y. S., Morale, S. E., & Birch, E. E. (2009). Three randomized controlled trials of early long-chain polyunsaturated Fatty Acid supplementation on means-end problem solving in 9-month-olds. *Child Dev, 80*(5), 1376-1384. doi:10.1111/j.1467-8624.2009.01339.x

Drover, J. R., Hoffman, D. R., Castañeda, Y. S., Morale, S. E., Garfield, S., Wheaton, D. H., & Birch, E. E. (2011). Cognitive function in 18-month-old term infants of the DIAMOND study: a randomized, controlled clinical trial with multiple dietary levels of docosahexaenoic acid. *Early Hum Dev, 87*(3), 223-230. doi:10.1016/j.earlhumdev.2010.12.047

Du, F., Wang, Y. Z., Xu, Y. S., Shi, T. Q., Liu, W. Z., Sun, X. M., & Huang, H. (2021). Biotechnological production of lipid and terpenoid from thraustochytrids. *Biotechnol Adv, 48*, 107725. doi:10.1016/j.biotechadv.2021.107725

Dulermo, R., Brunel, F., Dulermo, T., Ledesma-Amaro, R., Vion, J., Trassaert, M., . . . Leplat, C. (2017a). Using a vector pool containing variable-strength promoters to optimize protein production in Yarrowia lipolytica. *Microbial cell factories, 16*(1), 31. doi:10.1186/s12934-017-0647-3

Dulermo, R., Brunel, F., Dulermo, T., Ledesma-Amaro, R., Vion, J., Trassaert, M., . . . Leplat, C. (2017b). Using a vector pool containing variable-strength promoters to optimize protein production in Yarrowia lipolytica. *Microbial cell factories, 16*(1), 31. doi:10.1186/s12934-017-0647-3

Dulermo, T., & Nicaud, J. M. (2011). Involvement of the G3P shuttle and β-oxidation pathway in the control of TAG synthesis and lipid accumulation in *Yarrowia lipolytica*. *Metabolic Engineering, 13*(5), 482-491. doi:10.1016/j.ymben.2011.05.002

Dunstan, J. A., Simmer, K., Dixon, G., & Prescott, S. L. (2008). Cognitive assessment of children at age 2(1/2) years after maternal fish oil supplementation in pregnancy: a randomised controlled trial. *Arch Dis Child Fetal Neonatal Ed, 93*(1), F45-50. doi:10.1136/adc.2006.099085

Dyerberg, J., Bang, H. O., Stoffersen, E., Moncada, S., & Vane, J. R. (1978). Eicosapentaenoic acid and prevention of thrombosis and atherosclerosis? *Lancet, 2*(8081), 117-119. doi:10.1016/s0140-6736(78)91505-2

Erb, I., & van Nimwegen, E. (2011). Transcription factor binding site positioning in yeast: proximal promoter motifs characterize TATA-less promoters. *PloS One, 6*(9), e24279. doi:10.1371/journal.pone.0024279

Erian, A. M., Egermeier, M., Marx, H., & Sauer, M. (2022). Insights into the glycerol transport of *Yarrowia lipolytica*. *Yeast, 39*(5), 323-336. doi:10.1002/yea.3702

Estupiñán, M., Hernández, I., Saitua, E., Bilbao, M. E., Mendibil, I., Ferrer, J., & Alonso-Sáez, L. (2020). Novel *Vibrio* spp. Strains Producing Omega-3 Fatty Acids Isolated from Coastal Seawater. *Marine Drugs, 18*(2), 99. doi:10.3390/md18020099

FAO. (2022). *The State of World Fisheries and Aquaculture 2022*. Rome, Italy: FAO.

Fedorova-Dahms, I., Thorsrud, B. A., Bailey, E., & Salem, N. (2014). A 3-week dietary bioequivalence study in preweaning farm piglets of two sources of docosahexaenoic acid produced from two different organisms. *Food and Chemical Toxicology, 65*, 43-51. doi:10.1016/j.fct.2013.12.008

Foran, J. A., Good, D. H., Carpenter, D. O., Hamilton, M. C., Knuth, B. A., & Schwager, S. J. (2005). Quantitative analysis of the benefits and risks of consuming farmed and wild salmon. *J Nutr, 135*(11), 2639-2643. doi:10.1093/jn/135.11.2639

Fournier, P., Abbas, A., Chasles, M., Kudla, B., Ogrydziak, D. M., Yaver, D., . . . Feynerol, C. (1993). Colocalization of centromeric and replicative functions on autonomously replicating sequences isolated from the yeast *Yarrowia lipolytica*. *Proceedings of the National Academy of Sciences, 90*(11), 4912-4916. doi:10.1073/pnas.90.11.4912

Fröhlich-Wyder, M.-T., Arias-Roth, E., & Jakob, E. (2019). Cheese yeasts. *Yeast, 36*(3), 129-141. doi:10.1002/yea.3368

Furger, A., O'Sullivan, J. M., Binnie, A., Lee, B. A., & Proudfoot, N. J. (2002). Promoter proximal splice sites enhance transcription. *Genes Dev, 16*(21), 2792-2799. doi:10.1101/gad.983602

Gaillardin, C., Mekouar, M., & Neuvéglise, C. (2013). Comparative Genomics of Yarrowia lipolytica. In G. Barth (Ed.), *Yarrowia lipolytica: Genetics, Genomics, and Physiology* (pp. 1-30). Berlin, Heidelberg: Springer Berlin Heidelberg.

Gao, C., Yang, X., Wang, H., Rivero, C. P., Li, C., Cui, Z., . . . Lin, C. S. K. (2016). Robust succinic acid production from crude glycerol using engineered Yarrowia lipolytica. *Biotechnology for biofuels, 9*(1), 179. doi:10.1186/s13068-016-0597-8

Gao, Q., Cao, X., Huang, Y.-Y., Yang, J.-L., Chen, J., Wei, L.-J., & Hua, Q. (2018). Overproduction of Fatty Acid Ethyl Esters by the Oleaginous Yeast Yarrowia lipolytica through Metabolic Engineering and Process Optimization. *ACS synthetic biology, 7*(5), 1371-1380. doi:10.1021/acssynbio.7b00453

Garcia, R., Stadler, M., Gemperlein, K., & Müller, R. (2016). *Aetherobacter fasciculatus* gen. nov., sp. nov. and *Aetherobacter rufus* sp. nov., novel myxobacteria with promising biotechnological applications. *International Journal of Systematic and Evolutionary Microbiology, 66*(2), 928-938. doi:10.1099/ijsem.0.000813

Garland, M. R., Hallahan, B., McNamara, M., Carney, P. A., Grimes, H., Hibbeln, J. R., . . . Conroy, R. M. (2007). Lipids and essential fatty acids in patients presenting with self-harm. *Br J Psychiatry, 190*, 112-117. doi:10.1192/bjp.bp.105.019562

Geisberg, J. V., Moqtaderi, Z., Fan, X., Ozsolak, F., & Struhl, K. (2014). Global analysis of mRNA isoform half-lives reveals stabilizing and destabilizing elements in yeast. *Cell, 156*(4), 812-824. doi:10.1016/j.cell.2013.12.026

Gemperlein, K., Dietrich, D., Kohlstedt, M., Zipf, G., Bernauer, H. S., Wittmann, C., . . . Müller, R. (2019). Polyunsaturated fatty acid production by *Yarrowia lipolytica* employing designed myxobacterial PUFA synthases. *Nature Communications, 10*(1), 4055. doi:10.1038/s41467-019-12025-8

Gemperlein, K., Rachid, S., Garcia, R. O., Wenzel, S. C., & Müller, R. (2014). Polyunsaturated fatty acid biosynthesis in myxobacteria: different PUFA synthases and their product diversity. *Chemical Science, 5*(5), 1733-1741. doi:10.1039/C3SC53163E

Gemperlein, K., Zipf, G., Bernauer, H. S., Müller, R., & Wenzel, S. C. (2016). Metabolic engineering of Pseudomonas putida for production of docosahexaenoic acid based on a myxobacterial PUFA synthase. *Metabolic Engineering, 33*, 98-108. doi:https://doi.org/10.1016/j.ymben.2015.11.001

Gerster, H. (1998). Can adults adequately convert alpha-linolenic acid (18:3n-3) to eicosapentaenoic acid (20:5n-3) and docosahexaenoic acid (22:6n-3)? *Int J Vitam Nutr Res, 68*(3), 159-173.

Gießelmann, G., Dietrich, D., Jungmann, L., Kohlstedt, M., Jeon, E. J., Yim, S. S., . . . Wittmann, C. (2019). Metabolic Engineering of *Corynebacterium glutamicum* for High-Level Ectoine Production: Design, Combinatorial Assembly, and Implementation of a Transcriptionally Balanced Heterologous Ectoine Pathway. *Biotechnology Journal, 14*(9), 1800417. doi:10.1002/biot.201800417

Gladyshev, M. I., Anishchenko, O. V., Sushchnik, N. N., Kalacheva, G. S., Gribovskaya, I. V., & Ageev, A. V. (2012). Influence of anthropogenic pollution on content of essential polyunsaturated fatty acids in links of food chain of river ecosystem. *Contemporary Problems of Ecology, 5*(4), 376-385. doi:10.1134/S1995425512040051

Gladyshev, M. I., Arts, M. T., & Sushchik, N. N. (2009a). Preliminary estimates of the export of omega-3 highly unsaturated fatty acids (EPA+DHA) from aquatic to terrestrial ecosystems. In M. Kainz, M. T. Brett, & M. T. Arts (Eds.), *Lipids in Aquatic Ecosystems* (pp. 179-210). New York, NY: Springer New York.

Gladyshev, M. I., Gribovskaya, I. V., Moskvicheva, A. V., Muchkina, E. Y., Chuprov, S. M., & Ivanova, E. A. (2001). Content of metals in compartments of ecosystem of a siberian pond. *Arch Environ Contam Toxicol, 41*(2), 157-162. doi:10.1007/s002440010233

Gladyshev, M. I., Sushchik, N. N., Anishchenko, O. V., Makhutova, O. N., Kalachova, G. S., & Gribovskaya, I. V. (2009b). Benefit-risk ratio of food fish intake as the source of essential fatty acids vs. heavy metals: A case study of Siberian grayling from the Yenisei River. *Food Chemistry, 115*(2), 545-550. doi:10.1016/j.foodchem.2008.12.062

Gladyshev, M. I., Sushchik, N. N., & Makhutova, O. N. (2013). Production of EPA and DHA in aquatic ecosystems and their transfer to the land. *Prostaglandins Other Lipid Mediat, 107*, 117-126. doi:10.1016/j.prostaglandins.2013.03.002

Glaser, L., Kuhl, M., Jovanovic, S., Fritz, M., Vogeli, B., Erb, T. J., . . . Wittmann, C. (2020). A common approach for absolute quantification of short chain CoA thioesters in prokaryotic and eukaryotic microbes. *Microbial cell factories, 19*(1), 160. doi:10.1186/s12934-020-01413-1

Gläser, L., Kuhl, M., Jovanovic, S., Fritz, M., Vögeli, B., Erb, T. J., . . . Wittmann, C. (2020). A common approach for absolute quantification of short chain CoA thioesters in prokaryotic and eukaryotic microbes. *Microbial cell factories, 19*(1), 160. doi:10.1186/s12934-020-01413-1

Gläser, L., Kuhl, M., Stegmuller, J., Ruckert, C., Myronovskyi, M., Kalinowski, J., . . . Wittmann, C. (2021). Superior production of heavy pamamycin derivatives using a bkdR deletion mutant of Streptomyces albus J1074/R2. *Microbial Cell Factories, 20*(1), 111. doi:10.1186/s12934-021-01602-6

Good, N. E., Winget, G. D., Winter, W., Connolly, T. N., Izawa, S., & Singh, R. M. M. (1966). Hydrogen Ion Buffers for Biological Research*. *Biochemistry, 5*(2), 467-477. doi:10.1021/bi00866a011

Groenewald, M., Boekhout, T., Neuvéglise, C., Gaillardin, C., van Dijck, P. W. M., & Wyss, M. (2014). *Yarrowia lipolytica*: Safety assessment of an oleaginous yeast with a great industrial potential. *Critical Reviews in Microbiology, 40*(3), 187-206. doi:10.3109/1040841X.2013.770386

Gruchattka, E., Hädicke, O., Klamt, S., Schütz, V., & Kayser, O. (2013). In silico profiling of Escherichia coli and Saccharomyces cerevisiae as terpenoid factories. *Microbial cell factories, 12*(1), 84. doi:10.1186/1475-2859-12-84

Gu, W., Kavanagh, J. M., & McClure, D. D. (2022). Towards a sustainable supply of omega-3 fatty acids: Screening microalgae for scalable production of eicosapentaenoic acid (EPA). *Algal Research, 61*, 102564. doi:10.1016/j.algal.2021.102564

Guo, M., Chen, G., Chen, J., & Zheng, M. (2019). Identification of a Long-Chain Fatty Acid Elongase from Nannochloropsis sp. Involved in the Biosynthesis of Fatty Acids by Heterologous Expression in *Saccharomyces cerevisiae*. *Journal of Ocean University of China, 18*(5), 1199-1206. doi:10.1007/s11802-019-3946-y

Guo, Z.-p., Borsenberger, V., Croux, C., Duquesne, S., Truan, G., Marty, A., & Bordes, F. (2020). An artificial chromosome ylAC enables efficient assembly of multiple genes in *Yarrowia lipolytica* for biomanufacturing. *Communications Biology, 3*(1), 199. doi:10.1038/s42003-020-0936-y

Gurr, M., Harwood, J. L., & Frayn, K. N. (2002). Fatty Acid Structure and Metabolism. In *Lipid Biochemistry* (5th ed., pp. 13-92). Wiley Online Library.

Guschina, I. A., & Harwood, J. L. (2009a). *Algal lipids and effect of the environment on their biochemistry*.

Guschina, I. A., & Harwood, J. L. (2009b). Algal lipids and effect of the environment on their biochemistry. In M. Kainz, M. T. Brett, & M. T. Arts

(Eds.), *Lipids in Aquatic Ecosystems* (pp. 1-24). New York, NY: Springer New York.

Haag, M. (2003). Essential fatty acids and the brain. *Can J Psychiatry, 48*(3), 195-203. doi:10.1177/070674370304800308

Hallahan, B., Hibbeln, J. R., Davis, J. M., & Garland, M. R. (2007). Omega-3 fatty acid supplementation in patients with recurrent self-harm. Single-centre double-blind randomised controlled trial. *Br J Psychiatry, 190*, 118-122. doi:10.1192/bjp.bp.106.022707

Harris, M. A., Reece, M. S., McGregor, J. A., Wilson, J. W., Burke, S. M., Wheeler, M., . . . Allen, K. G. (2015). The Effect of Omega-3 Docosahexaenoic Acid Supplementation on Gestational Length: Randomized Trial of Supplementation Compared to Nutrition Education for Increasing n-3 Intake from Foods. *Biomed Res Int, 2015*, 123078. doi:10.1155/2015/123078

Harris, W. S. (1996). n-3 fatty acids and lipoproteins: comparison of results from human and animal studies. *Lipids, 31*(3), 243-252. doi:10.1007/bf02529870

Hibbeln, J. R., Davis, J. M., Steer, C., Emmett, P., Rogers, I., Williams, C., & Golding, J. (2007). Maternal seafood consumption in pregnancy and neurodevelopmental outcomes in childhood (ALSPAC study): an observational cohort study. *Lancet, 369*(9561), 578-585. doi:10.1016/s0140-6736(07)60277-3

Holkenbrink, C., Dam, M. I., Kildegaard, K. R., Beder, J., Dahlin, J., Domenech Belda, D., & Borodina, I. (2018a). EasyCloneYALI: CRISPR/Cas9-Based Synthetic Toolbox for Engineering of the Yeast *Yarrowia lipolytica*. *Biotechnol J, 13*(9), e1700543. doi:10.1002/biot.201700543

Holkenbrink, C., Dam, M. I., Kildegaard, K. R., Beder, J., Dahlin, J., Doménech Belda, D., & Borodina, I. (2018b). EasyCloneYALI: CRISPR/Cas9-Based Synthetic Toolbox for Engineering of the Yeast *Yarrowia lipolytica*. *Biotechnology Journal, 13*(9), 1700543. doi:10.1002/biot.201700543

Howlett, N. G., & Avery, S. V. (1997). Induction of lipid peroxidation during heavy metal stress in Saccharomyces cerevisiae and influence of plasma membrane fatty acid unsaturation. *Applied and Environmental Microbiology, 63*(8), 2971-2976. doi:10.1128/aem.63.8.2971-2976.1997

Huang, Y.-Y., Jian, X.-X., Lv, Y.-B., Nian, K.-Q., Gao, Q., Chen, J., . . . Hua, Q. (2018). Enhanced squalene biosynthesis in Yarrowia lipolytica based on metabolically engineered acetyl-CoA metabolism. *Journal of Biotechnology, 281*, 106-114. doi:https://doi.org/10.1016/j.jbiotec.2018.07.001

Humhal, T., Kastanek, P., Jezkova, Z., Cadkova, A., Kohoutkova, J., & Branyik, T. (2017). Use of saline waste water from demineralization of cheese whey for cultivation of *Schizochytrium limacinum* PA-968 and *Japonochytrium marinum* AN-4. *Bioprocess and Biosystems Engineering, 40*(3), 395-402. doi:10.1007/s00449-016-1707-5

Hussein, N., Ah-Sing, E., Wilkinson, P., Leach, C., Griffin, B. A., & Millward, D. J. (2005). Long-chain conversion of [13C]linoleic acid and α-linolenic acid in response to marked changes in their dietary intake in men. *Journal of Lipid Research, 46*(2), 269-280. doi:10.1194/jlr.M400225-JLR200

Inoue, H., Nojima, H., & Okayama, H. (1990). High efficiency transformation of *Escherichia coli* with plasmids. *Gene, 96*(1), 23-28. doi:10.1016/0378-1119(90)90336-P

Jach, M. E., & Malm, A. (2022). *Yarrowia lipolytica* as an Alternative and Valuable Source of Nutritional and Bioactive Compounds for Humans. *Molecules, 27*(7), 2300. doi:10.3390/molecules27072300

Jain, N., Vergish, S., & Khurana, J. P. (2018). Validation of house-keeping genes for normalization of gene expression data during diurnal/circadian studies in rice by RT-qPCR. *Sci Rep, 8*(1), 3203. doi:10.1038/s41598-018-21374-1

Jang, I.-S., Yu, B. J., Jang, J. Y., Jegal, J., & Lee, J. Y. (2018). Improving the efficiency of homologous recombination by chemical and biological approaches in *Yarrowia lipolytica*. *PloS One, 13*(3), e0194954. doi:10.1371/journal.pone.0194954

Johansson, M., Chen, X., Milanova, S., Santos, C., & Petranovic, D. (2016). PUFA-induced cell death is mediated by Yca1p-dependent and -independent pathways, and is reduced by vitamin C in yeast. *FEMS yeast research, 16*(2). doi:10.1093/femsyr/fow007

Jones, P. R. (2014). Genetic instability in cyanobacteria - an elephant in the room? *Frontiers in Bioengineering and Biotechnology, 2*, 12. doi:10.3389/fbioe.2014.00012

Jovanovic, S., Dietrich, D., Becker, J., Kohlstedt, M., & Wittmann, C. (2021). Microbial production of polyunsaturated fatty acids - high-value ingredients for aquafeed, superfoods, and pharmaceuticals. *Curr Opin Biotechnol, 69*, 199-211. doi:10.1016/j.copbio.2021.01.009

Kar, S., Wong, M., Rogozinska, E., & Thangaratinam, S. (2016). Effects of omega-3 fatty acids in prevention of early preterm delivery: a systematic review and meta-analysis of randomized studies. *Eur J Obstet Gynecol Reprod Biol, 198*, 40-46. doi:10.1016/j.ejogrb.2015.11.033

Kaštovská, K., Stibal, M., Šabacká, M., Černá, B., Šantrůčková, H., & Elster, J. (2007). Microbial community structure and ecology of subglacial sediments in two polythermal Svalbard glaciers characterized by epifluorescence microscopy and PLFA. *Polar Biology, 30*(3), 277-287. doi:10.1007/s00300-006-0181-y

Kavšček, M., Bhutada, G., Madl, T., & Natter, K. (2015). Optimization of lipid production with a genome-scale model of *Yarrowia lipolytica*. *BMC Systems Biology, 9*(1), 72. doi:10.1186/s12918-015-0217-4

Kerkhoven, E. J., Pomraning, K. R., Baker, S. E., & Nielsen, J. (2016). Regulation of amino-acid metabolism controls flux to lipid accumulation in *Yarrowia lipolytica*. *NPJ systems biology and applications, 2*, 16005. doi:10.1038/npjsba.2016.5

Kessler, R. C., Berglund, P., Demler, O., Jin, R., Merikangas, K. R., & Walters, E. E. (2005). Lifetime prevalence and age-of-onset distributions of DSM-IV disorders in the National Comorbidity Survey Replication. *Arch Gen Psychiatry, 62*(6), 593-602. doi:10.1001/archpsyc.62.6.593

Khozin-Goldberg, I., Iskandarov, U., & Cohen, Z. (2011). LC-PUFA from photosynthetic microalgae: occurrence, biosynthesis, and prospects in biotechnology. *Applied Microbiology and Biotechnology, 91*(4), 905-915. doi:10.1007/s00253-011-3441-x

Kibbe, W. A. (2007). OligoCalc: an online oligonucleotide properties calculator. *Nucleic acids research, 35*(Web Server issue), W43-46. doi:10.1093/nar/gkm234

Kieling, C., Baker-Henningham, H., Belfer, M., Conti, G., Ertem, I., Omigbodun, O., . . . Rahman, A. (2011). Child and adolescent mental health worldwide: evidence for action. *The Lancet, 378*(9801), 1515-1525. doi:10.1016/S0140-6736(11)60827-1

Kind, S., Neubauer, S., Becker, J., Yamamoto, M., Völkert, M., Abendroth, G. V., . . . Wittmann, C. (2014). From zero to hero - Production of bio-based nylon from renewable resources using engineered *Corynebacterium glutamicum*. *Metabolic Engineering, 25*, 113-123. doi:10.1016/j.ymben.2014.05.007

Klamt, S., Saez-Rodriguez, J., & Gilles, E. D. (2007). Structural and functional analysis of cellular networks with CellNetAnalyzer. *BMC Systems Biology, 1*(1), 2. doi:10.1186/1752-0509-1-2

Koletzko, B., Beblo, S., Demmelmair, H., & Hanebutt, F. L. (2009). Omega-3 LC-PUFA Supply and Neurological Outcomes in Children With Phenylketonuria (PKU). *Journal of Pediatric Gastroenterology and Nutrition, 48*. doi:10.1097/MPG.0b013e3181977399

Kolouchová, I., Maťátková, O., Sigler, K., Masák, J., & Řezanka, T. (2016). Lipid accumulation by oleaginous and non-oleaginous yeast strains in nitrogen and phosphate limitation. *Folia Microbiologica, 61*(5), 431-438. doi:10.1007/s12223-016-0454-y

Kozera, B., & Rapacz, M. (2013). Reference genes in real-time PCR. *J Appl Genet, 54*(4), 391-406. doi:10.1007/s13353-013-0173-x

Kris-Etherton, P. M., Harris, M. A., & Appel, L. J. (2002). Fish Consumption, Fish Oil, Omega-3 Fatty Acids, and Cardiovascular Disease. *Circulation, 106*(21), 2747-2757. doi:10.1161/01.CIR.0000038493.65177.94

Kuhl, M., Glaser, L., Rebets, Y., Ruckert, C., Sarkar, N., Hartsch, T., . . . Wittmann, C. (2020). Microparticles globally reprogram *Streptomyces albus* toward accelerated morphogenesis, streamlined carbon core metabolism, and enhanced production of the antituberculosis polyketide pamamycin. *Biotechnology and Bioengineering, 117*(12), 3858-3875. doi:10.1002/bit.27537

Kusube, M., Kyaw, T. S., Tanikawa, K., Chastain, R. A., Hardy, K. M., Cameron, J., & Bartlett, D. H. (2017). *Colwellia marinimaniae* sp. nov., a hyperpiezophilic species isolated from an amphipod within the Challenger Deep, Mariana Trench. *International Journal of Systematic and Evolutionary Microbiology, 67*(4), 824-831. doi:10.1099/ijsem.0.001671

Kwek, K. Y., Murphy, S., Furger, A., Thomas, B., O'Gorman, W., Kimura, H., . . . Akoulitchev, A. (2002). U1 snRNA associates with TFIIH and regulates transcriptional initiation. *Nat Struct Biol, 9*(11), 800-805. doi:10.1038/nsb862

Kyle, D. J., & Ratledge, C. (1992). Microbial Lipids: Commercial Realities or Academic Curiosities. In *Industrial Applications of Single Cell Oils* (1 ed., pp. 15). AOCS AOCS Publishing.

Lands, W. E. M. (2009). Human life: caught in the food web. In M. Kainz, M. T. Brett, & M. T. Arts (Eds.), *Lipids in Aquatic Ecosystems* (pp. 327-354). New York, NY: Springer New York.

Larroude, M., Rossignol, T., Nicaud, J. M., & Ledesma-Amaro, R. (2018). Synthetic biology tools for engineering *Yarrowia lipolytica*. *Biotechnol Adv, 36*(8), 2150-2164. doi:10.1016/j.biotechadv.2018.10.004

Lazar, Z., Liu, N., & Stephanopoulos, G. (2018). Holistic Approaches in Lipid Production by *Yarrowia lipolytica*. *Trends in Biotechnology, 36*(11), 1157-1170. doi:10.1016/j.tibtech.2018.06.007

Le Hir, H., Nott, A., & Moore, M. J. (2003a). How introns influence and enhance eukaryotic gene expression. *Trends Biochem Sci, 28*(4), 215-220. doi:10.1016/s0968-0004(03)00052-5

Le Hir, H., Nott, A., & Moore, M. J. (2003b). How introns influence and enhance eukaryotic gene expression. *Trends in Biochemical Sciences, 28*(4), 215-220. doi:10.1016/S0968-0004(03)00052-5

Ledesma-Amaro, R., & Nicaud, J. M. (2016). Metabolic Engineering for Expanding the Substrate Range of *Yarrowia lipolytica*. *Trends Biotechnol, 34*(10), 798-809. doi:10.1016/j.tibtech.2016.04.010

Leslie, M. A., Cohen, D. J., Liddle, D. M., Robinson, L. E., & Ma, D. W. (2015). A review of the effect of omega-3 polyunsaturated fatty acids on blood triacylglycerol levels in normolipidemic and borderline hyperlipidemic individuals. *Lipids Health Dis, 14*, 53. doi:10.1186/s12944-015-0049-7

Li, J., Pora, B. L. R., Dong, K., & Hasjim, J. (2021a). Health benefits of docosahexaenoic acid and its bioavailability: A review. *Food Sci Nutr, 9*(9), 5229-5243. doi:10.1002/fsn3.2299

Li, L., Maclntyre, L. W., & Brady, S. F. (2021b). Refactoring biosynthetic gene clusters for heterologous production of microbial natural products. *Current opinion in biotechnology, 69*, 145-152. doi:10.1016/j.copbio.2020.12.011

Liu, H.-H., Ji, X.-J., & Huang, H. (2015). Biotechnological applications of Yarrowia lipolytica: Past, present and future. *Biotechnology Advances, 33*(8), 1522-1546. doi:10.1016/j.biotechadv.2015.07.010

Liu, H., Song, Y., Fan, X., Wang, C., Lu, X., & Tian, Y. (2021). *Yarrowia lipolytica* as an Oleaginous Platform for the Production of Value-Added Fatty Acid-Based Bioproducts. *Frontiers in microbiology, 11*. doi:10.3389/fmicb.2020.608662

Liu, M., Wang, C., Ren, X., Gao, S., Yu, S., & Zhou, J. (2022). Remodelling metabolism for high-level resveratrol production in Yarrowia lipolytica. *Bioresource Technology, 365*, 128178. doi:10.1016/j.biortech.2022.128178

Liu, N., Qiao, K., & Stephanopoulos, G. (2016). (13)C Metabolic Flux Analysis of acetate conversion to lipids by *Yarrowia lipolytica*. *Metabolic Engineering, 38*, 86-97. doi:10.1016/j.ymben.2016.06.006

Lopes, M., Gomes, N., Mota, M., & Belo, I. (2009). Yarrowia lipolytica Growth Under Increased Air Pressure: Influence on Enzyme Production. *Applied Biochemistry and Biotechnology, 159*(1), 46-53. doi:10.1007/s12010-008-8359-0

Lu, Y., Yang, Q., Lin, Z., & Yang, X. (2020). A modular pathway engineering strategy for the high-level production of β-ionone in Yarrowia lipolytica. *Microbial Cell Factories, 19*(1), 49. doi:10.1186/s12934-020-01309-0

Lubliner, S., Keren, L., & Segal, E. (2013). Sequence features of yeast and human core promoters that are predictive of maximal promoter activity. *Nucleic acids research, 41*(11), 5569-5581. doi:10.1093/nar/gkt256

Lung, Y.-T., Tan, C. H., Show, P. L., Ling, T. C., Lan, J. C.-W., Lam, H. L., & Chang, J.-S. (2016). Docosahexaenoic acid production from crude glycerol by *Schizochytrium limacinum* SR21. *Clean Technologies and Environmental Policy, 18*(7), 2209-2216. doi:10.1007/s10098-016-1126-y

Lustig, A. J. (1999). The Kudos of non-homologous end-joining. *Nature Genetics, 23*(2), 130-131. doi:10.1038/13755

Ma, J., Gu, Y., Marsafari, M., & Xu, P. (2020). Synthetic biology, systems biology, and metabolic engineering of Yarrowia lipolytica toward a sustainable biorefinery platform. *J Ind Microbiol Biotechnol, 47*(9-10), 845-862. doi:10.1007/s10295-020-02290-8

Madzak, C. (2021). *Yarrowia lipolytica* Strains and Their Biotechnological Applications: How Natural Biodiversity and Metabolic Engineering Could Contribute to Cell Factories Improvement. *Journal of Fungi, 7*(7), 548. doi:10.3390/jof7070548

Madzak, C., Blanchin-Roland, S., Cordero Otero, R. R., & Gaillardin, C. (1999). Functional analysis of upstream regulating regions from the Yarrowia lipolytica XPR2 promoter. *Microbiology (Reading), 145 (Pt 1)*, 75-87. doi:10.1099/13500872-145-1-75

Madzak, C., Gaillardin, C., & Beckerich, J. M. (2004). Heterologous protein expression and secretion in the non-conventional yeast *Yarrowia lipolytica*: a review. *J Biotechnol, 109*(1-2), 63-81. doi:10.1016/j.jbiotec.2003.10.027

Madzak, C., Treton, B., & Blanchin-Roland, S. (2000). Strong hybrid promoters and integrative expression/secretion vectors for quasi-constitutive expression of heterologous proteins in the yeast *Yarrowia lipolytica*. *J Mol Microbiol Biotechnol, 2*(2), 207-216. Retrieved from https://www.ncbi.nlm.nih.gov/pubmed/10939246

Makri, A., Fakas, S., & Aggelis, G. (2010). Metabolic activities of biotechnological interest in *Yarrowia lipolytica* grown on glycerol in repeated batch cultures. *Bioresource Technology, 101*(7), 2351-2358. doi:10.1016/j.biortech.2009.11.024

Makrides, M., Neumann, M. A., Byard, R. W., Simmer, K., & Gibson, R. A. (1994). Fatty acid composition of brain, retina, and erythrocytes in breast- and formula-fed infants. *Am J Clin Nutr, 60*(2), 189-194. doi:10.1093/ajcn/60.2.189

Mamaev, D., & Zvyagilskaya, R. (2021). *Yarrowia lipolytica*: a multitalented yeast species of ecological significance. *FEMS yeast research, 21*(2). doi:10.1093/femsyr/foab008

Marella, E. R., Dahlin, J., Dam, M. I., ter Horst, J., Christensen, H. B., Sudarsan, S., . . . Borodina, I. (2020). A single-host fermentation process for the production of flavor lactones from non-hydroxylated fatty acids. *Metabolic Engineering, 61*, 427-436. doi:10.1016/j.ymben.2019.08.009

Markham, K. A., & Alper, H. S. (2018). Synthetic Biology Expands the Industrial Potential of Yarrowia lipolytica. *Trends in Biotechnology, 36*(10), 1085-1095. doi:10.1016/j.tibtech.2018.05.004

Mathew, G. M., Raina, D., Narisetty, V., Kumar, V., Saran, S., Pugazhendi, A., . . . Binod, P. (2021). Recent advances in biodiesel production: Challenges and solutions. *Sci Total Environ, 794*, 148751. doi:10.1016/j.scitotenv.2021.148751

Matsuoka, M., Matsubara, M., Daidoh, H., Imanaka, T., Uchida, K., & Aiba, S. (1993). Analysis of regions essential for the function of chromosomal replicator sequences from *Yarrowia lipolytica*. *Molecular and General Genetics MGG, 237*(3), 327-333. doi:10.1007/BF00279435

Mekouar, M., Blanc-Lenfle, I., Ozanne, C., Silva, C., Cruaud, C., Wincker, P., . . . Neuvéglise, C. (2010). Detection and analysis of alternative splicing in Yarrowia lipolytica reveal structural constraints facilitating nonsense-mediated decay of intron-retaining transcripts. *Genome Biology, 11*, R65. doi:10.1186/gb-2010-11-6-r65

Mendes, A., Reis, A., Vasconcelos, R., Guerra, P., & Lopes da Silva, T. (2009). *Crypthecodinium cohnii* with emphasis on DHA production: a review. *Journal of Applied Phycology, 21*(2), 199-214. doi:10.1007/s10811-008-9351-3

Metherel, A. H., & Bazinet, R. P. (2019). Updates to the n-3 polyunsaturated fatty acid biosynthesis pathway: DHA synthesis rates, tetracosahexaenoic acid and (minimal) retroconversion. *Progress in Lipid Research, 76*, 101008. doi:10.1016/j.plipres.2019.101008

Metz, J. G., Roessler, P., Facciotti, D., Levering, C., Dittrich, F., Lassner, M., . . . Browse, J. (2001). Production of Polyunsaturated Fatty Acids by Polyketide Synthases in Both Prokaryotes and Eukaryotes. *Science, 293*(5528), 290-293. doi:10.1126/science.1059593

Miles, E. A., & Calder, P. C. (2012). Influence of marine n-3 polyunsaturated fatty acids on immune function and a systematic review of their effects on clinical outcomes in rheumatoid arthritis. *Br J Nutr, 107 Suppl 2*, S171-184. doi:10.1017/s0007114512001560

Miller, K. K., & Alper, H. S. (2019). *Yarrowia lipolytica*: more than an oleaginous workhorse. *Applied Microbiology and Biotechnology, 103*(23), 9251-9262. doi:10.1007/s00253-019-10200-x

Mischo, H. E., & Proudfoot, N. J. (2013). Disengaging polymerase: terminating RNA polymerase II transcription in budding yeast. *Biochimica et biophysica acta, 1829*(1), 174-185. doi:10.1016/j.bbagrm.2012.10.003

Montiel, D., Kang, H. S., Chang, F. Y., Charlop-Powers, Z., & Brady, S. F. (2015). Yeast homologous recombination-based promoter engineering for the activation of silent natural product biosynthetic gene clusters. *Proc Natl Acad Sci U S A, 112*(29), 8953-8958. doi:10.1073/pnas.1507606112

Moore, J. C., Ramos, I., & Van Dien, S. (2022). Practical genetic control strategies for industrial bioprocesses. *Journal of Industrial Microbiology & Biotechnology, 49*(2). doi:10.1093/jimb/kuab088

Müller, S., Sandal, T., Kamp-Hansen, P., & Dalbøge, H. (1998). Comparison of expression systems in the yeasts *Saccharomyces cerevisiae*, *Hansenula polymorpha, Klyveromyces lactis, Schizosaccharomyces pombe* and

Yarrowia lipolytica. Cloning of two novel promoters from *Yarrowia lipolytica*. *Yeast, 14*(14), 1267-1283. doi:10.1002/(sici)1097-0061(1998100)14:14<1267::Aid-yea327>3.0.Co;2-2

Newman, W. P., Middaugh, J. P., Propst, M. T., & Rogers, D. R. (1993). Atherosclerosis in Alaska Natives and non-natives. *Lancet, 341*(8852), 1056-1057. doi:10.1016/0140-6736(93)92413-n

Nicaud, J.-M., Madzak, C., van den Broek, P., Gysler, C., Duboc, P., Niederberger, P., & Gaillardin, C. (2002). Protein expression and secretion in the yeast *Yarrowia lipolytica*. *FEMS yeast research, 2*(3), 371-379. doi:10.1016/S1567-1356(02)00082-X

Nicaud, J. M. (2012). *Yarrowia lipolytica*. *Yeast, 29*(10), 409-418. doi:10.1002/yea.2921

Nielsen, J. (2019). Yeast Systems Biology: Model Organism and Cell Factory. *Biotechnology Journal, 14*(9), 1800421. doi:10.1002/biot.201800421

Noweck, K., & Grafahrend, W. (2006). Fatty Alcohols. In *Ullmann's Encyclopedia of Industrial Chemistry*.

Ochsenreither, K., Glück, C., Stressler, T., Fischer, L., & Syldatk, C. (2016). Production Strategies and Applications of Microbial Single Cell Oils. *Frontiers in microbiology, 7*. doi:10.3389/fmicb.2016.01539

Papanikolaou, S., & Aggelis, G. (2011). Lipids of oleaginous yeasts. Part I: Biochemistry of single cell oil production. *European Journal of Lipid Science and Technology, 113*(8), 1031-1051. doi:10.1002/ejlt.201100014

Park, Y.-K., & Ledesma-Amaro, R. (2022). What makes *Yarrowia lipolytica* well suited for industry? *Trends in Biotechnology*. doi:10.1016/j.tibtech.2022.07.006

Park, Y.-K., Ledesma-Amaro, R., & Nicaud, J.-M. (2020). De novo Biosynthesis of Odd-Chain Fatty Acids in *Yarrowia lipolytica* Enabled by Modular Pathway Engineering. *Frontiers in Bioengineering and Biotechnology, 7*. doi:10.3389/fbioe.2019.00484

Patel, A., Rova, U., Christakopoulos, P., & Matsakas, L. (2019). Simultaneous production of DHA and squalene from *Aurantiochytrium* sp. grown on forest biomass hydrolysates. *Biotechnology for biofuels, 12*(1), 255. doi:10.1186/s13068-019-1593-6

Pauli, S., Kohlstedt, M., Lamber, J., Weiland, F., Becker, J., & Wittmann, C. (2023). Systems metabolic engineering upgrades Corynebacterium glutamicum for selective high-level production of the chiral drug precursor and cell-protective extremolyte L-pipecolic acid. *Metabolic Engineering, 77*, 100-117. doi:10.1016/j.ymben.2023.03.006

Pauly, D., Christensen, V., Guénette, S., Pitcher, T. J., Sumaila, U. R., Walters, C. J., . . . Zeller, D. (2002). Towards sustainability in world fisheries. *Nature, 418*(6898), 689-695. doi:10.1038/nature01017

Portela, R. M., Vogl, T., Kniely, C., Fischer, J. E., Oliveira, R., & Glieder, A. (2017). Synthetic Core Promoters as Universal Parts for Fine-Tuning Expression in Different Yeast Species. *ACS synthetic biology, 6*(3), 471-484. doi:10.1021/acssynbio.6b00178

Pyle, D. J., Garcia, R. A., & Wen, Z. (2008). Producing Docosahexaenoic Acid (DHA)-Rich Algae from Biodiesel-Derived Crude Glycerol: Effects of Impurities on DHA Production and Algal Biomass Composition. *Journal*

of Agricultural and Food Chemistry, 56(11), 3933-3939. doi:10.1021/jf800602s

Qiao, K., Imam Abidi, S. H., Liu, H., Zhang, H., Chakraborty, S., Watson, N., . . . Stephanopoulos, G. (2015). Engineering lipid overproduction in the oleaginous yeast *Yarrowia lipolytica*. *Metabolic Engineering, 29*, 56-65. doi:10.1016/j.ymben.2015.02.005

Ratledge, C. (1976). Food from Waste, edited by G.G. Birch, K.J. Parker, and J.T. Worgan. *Applied Science Publishers*, 98-113. doi:10.1017/S0014479700007845

Reynolds, L. A., & Finlay, B. B. (2017). Early life factors that affect allergy development. *Nature Reviews Immunology, 17*(8), 518-528. doi:10.1038/nri.2017.39

Richard, G.-F., Kerrest, A., Lafontaine, I., & Dujon, B. (2005). Comparative Genomics of Hemiascomycete Yeasts: Genes Involved in DNA Replication, Repair, and Recombination. *Molecular Biology and Evolution, 22*(4), 1011-1023. doi:10.1093/molbev/msi083

Rohles, C., Pauli, S., Giesselmann, G., Kohlstedt, M., Becker, J., & Wittmann, C. (2022). Systems metabolic engineering of Corynebacterium glutamicum eliminates all by-products for selective and high-yield production of the platform chemical 5-aminovalerate. *Metabolic Engineering, 73*, 168-181. doi:10.1016/j.ymben.2022.07.005

Rohles, C. M., Gläser, L., Kohlstedt, M., Gießelmann, G., Pearson, S., del Campo, A., . . . Wittmann, C. (2018). A bio-based route to the carbon-5 chemical glutaric acid and to bionylon-6,5 using metabolically engineered Corynebacterium glutamicum. *Green Chemistry, 20*(20), 4662-4674. doi:10.1039/C8GC01901K

Ruiz-Herrera, J., & Sentandreu, R. (2002). Different effectors of dimorphism in *Yarrowia lipolytica*. *Archives of microbiology, 178*(6), 477-483. doi:10.1007/s00203-002-0478-3

Rutter, C. D., Zhang, S., & Rao, C. V. (2015). Engineering *Yarrowia lipolytica* for production of medium-chain fatty acids. *Applied Microbiology and Biotechnology, 99*(17), 7359-7368. doi:10.1007/s00253-015-6764-1

Rywińska, A., Juszczyk, P., Wojtatowicz, M., Robak, M., Lazar, Z., Tomaszewska, L., & Rymowicz, W. (2013). Glycerol as a promising substrate for *Yarrowia lipolytica* biotechnological applications. *Biomass and Bioenergy, 48*, 148-166. doi:10.1016/j.biombioe.2012.11.021

Sabra, W., Bommareddy, R. R., Maheshwari, G., Papanikolaou, S., & Zeng, A. P. (2017). Substrates and oxygen dependent citric acid production by Yarrowia lipolytica: insights through transcriptome and fluxome analyses. *Microbial cell factories, 16*(1), 78. doi:10.1186/s12934-017-0690-0

Sáez-Sáez, J., Wang, G., Marella, E. R., Sudarsan, S., Cernuda Pastor, M., & Borodina, I. (2020). Engineering the oleaginous yeast Yarrowia lipolytica for high-level resveratrol production. *Metabolic Engineering, 62*, 51-61. doi:10.1016/j.ymben.2020.08.009

Saravanan, P., Davidson, N. C., Schmidt, E. B., & Calder, P. C. (2010). Cardiovascular effects of marine omega-3 fatty acids. *Lancet, 376*(9740), 540-550. doi:10.1016/s0140-6736(10)60445-x

Sayanova, O. V., & Napier, J. A. (2004). Eicosapentaenoic acid: biosynthetic routes and the potential for synthesis in transgenic plants. *Phytochemistry, 65*(2), 147-158. doi:10.1016/j.phytochem.2003.10.017

Schwartz, C., Frogue, K., Ramesh, A., Misa, J., & Wheeldon, I. (2017). CRISPRi repression of nonhomologous end-joining for enhanced genome engineering via homologous recombination in *Yarrowia lipolytica*. *Biotechnology and Bioengineering, 114*(12), 2896-2906. doi:10.1002/bit.26404

Seddon, J. M., George, S., & Rosner, B. (2006). Cigarette smoking, fish consumption, omega-3 fatty acid intake, and associations with age-related macular degeneration: the US Twin Study of Age-Related Macular Degeneration. *Arch Ophthalmol, 124*(7), 995-1001. doi:10.1001/archopht.124.7.995

Shabbir Hussain, M., Gambill, L., Smith, S., & Blenner, M. A. (2016). Engineering Promoter Architecture in Oleaginous Yeast Yarrowia lipolytica. *ACS synthetic biology, 5*(3), 213-223. doi:10.1021/acssynbio.5b00100

Shao, Z., Rao, G., Li, C., Abil, Z., Luo, Y., & Zhao, H. (2013). Refactoring the silent spectinabilin gene cluster using a plug-and-play scaffold. *ACS synthetic biology, 2*(11), 662-669. doi:10.1021/sb400058n

Shearwin, K. E., Callen, B. P., & Egan, J. B. (2005). Transcriptional interference--a crash course. *Trends Genet, 21*(6), 339-345. doi:10.1016/j.tig.2005.04.009

Sijtsma, L., & de Swaaf, M. E. (2004). Biotechnological production and applications of the ω-3 polyunsaturated fatty acid docosahexaenoic acid. *Applied Microbiology and Biotechnology, 64*(2), 146-153. doi:10.1007/s00253-003-1525-y

Simopoulos, A. P., Leaf, A., & Salem, N. (2000). Workshop Statement on the Essentiality of and Recommended Dietary Intakes for Omega-6 and Omega-3 Fatty Acids. *PROSTAGLANDINS LEUKOTRIENES AND ESSENTIAL FATTY ACIDS, 63*(3), 119-121. doi:10.1054/plef.2000.0176

Singh, V., Haque, S., Niwas, R., Srivastava, A., Pasupuleti, M., & Tripathi, C. K. M. (2017). Strategies for Fermentation Medium Optimization: An In-Depth Review. *Frontiers in microbiology, 7*. doi:10.3389/fmicb.2016.02087

Skinner, E. R., Watt, C., Besson, J. A., & Best, P. V. (1993). Differences in the fatty acid composition of the grey and white matter of different regions of the brains of patients with Alzheimer's disease and control subjects. *Brain, 116 (Pt 3)*, 717-725. doi:10.1093/brain/116.3.717

Song, W., Li, J., Liang, Q., & Marchisio, M. A. (2016). Can terminators be used as insulators into yeast synthetic gene circuits? *J Biol Eng, 10*, 19. doi:10.1186/s13036-016-0040-5

Spagnuolo, M., Shabbir Hussain, M., Gambill, L., & Blenner, M. (2018). Alternative Substrate Metabolism in *Yarrowia lipolytica*. *Frontiers in microbiology, 9*, 1077. doi:10.3389/fmicb.2018.01077

Steen, E. J., Kang, Y., Bokinsky, G., Hu, Z., Schirmer, A., McClure, A., . . . Keasling, J. D. (2010). Microbial production of fatty-acid-derived fuels and chemicals from plant biomass. *Nature, 463*(7280), 559-562. doi:10.1038/nature08721

Sublette, M. E., Hibbeln, J. R., Galfalvy, H., Oquendo, M. A., & Mann, J. J. (2006). Omega-3 polyunsaturated essential fatty acid status as a predictor of future suicide risk. *Am J Psychiatry, 163*(6), 1100-1102. doi:10.1176/ajp.2006.163.6.1100

Sun, M. L., Shi, T. Q., Lin, L., Ledesma-Amaro, R., & Ji, X. J. (2022). Advancing Yarrowia lipolytica as a superior biomanufacturing platform by tuning gene expression using promoter engineering. *Bioresource Technology, 347*, 126717. doi:10.1016/j.biortech.2022.126717

Sutherland, J. B., Cornelison, C., & Crow, S. A. (2014). Candida | *Yarrowia lipolytica (Candida lipolytica)*. In C. A. Batt & M. L. Tortorello (Eds.), *Encyclopedia of Food Microbiology (Second Edition)* (pp. 374-378). Oxford: Academic Press.

Tai, M., & Stephanopoulos, G. (2013). Engineering the push and pull of lipid biosynthesis in oleaginous yeast *Yarrowia lipolytica* for biofuel production. *Metabolic Engineering, 15*, 1-9. doi:10.1016/j.ymben.2012.08.007

Timoumi, A., Cleret, M., Bideaux, C., Guillouet, S. E., Allouche, Y., Molina-Jouve, C., . . . Gorret, N. (2017). Dynamic behavior of *Yarrowia lipolytica* in response to pH perturbations: dependence of the stress response on the culture mode. *Applied Microbiology and Biotechnology, 101*(1), 351-366. doi:10.1007/s00253-016-7856-2

Tocher, D., Betancor, M., Sprague, M., Olsen, R. E., & Napier, J. A. (2019). Omega-3 Long-Chain Polyunsaturated Fatty Acids, EPA and DHA: Bridging the Gap between Supply and Demand. *Nutrients, 11*(1), 89. doi:10.3390/nu11010089

Tsigie, Y. A., Wang, C.-Y., Truong, C.-T., & Ju, Y.-H. (2011). Lipid production from *Yarrowia lipolytica* Po1g grown in sugarcane bagasse hydrolysate. *Bioresource Technology, 102*(19), 9216-9222. doi:10.1016/j.biortech.2011.06.047

Tsirigka, A., Theodosiou, E., Patsios, S. I., Tsoureki, A., Andreadelli, A., Papa, E., . . . Makris, A. M. (2023). Novel evolved Yarrowia lipolytica strains for enhanced growth and lipid content under high concentrations of crude glycerol. *Microbial Cell Factories, 22*(1), 62. doi:10.1186/s12934-023-02072-8

Untergasser, A., Cutcutache, I., Koressaar, T., Ye, J., Faircloth, B. C., Remm, M., & Rozen, S. G. (2012). Primer3--new capabilities and interfaces. *Nucleic acids research, 40*(15), e115. doi:10.1093/nar/gks596

Uttaro, A. D. (2006). Biosynthesis of polyunsaturated fatty acids in lower eukaryotes. *IUBMB Life, 58*(10), 563-571. doi:10.1080/15216540600920899

Vagelos, P. R. (1974). 3 - Biosynthesis of Saturated Fatty Acids. In T. W. Goodwin (Ed.), *Biochemistry of Lipids* (pp. 99-140): Butterworth-Heinemann.

van der Walt, J. P., & von Arx, J. A. (1980). The yeast genus Yarrowia gen. nov. *Antonie van Leeuwenhoek, 46*(6), 517-521. doi:10.1007/bf00394008

Verbeke, J., Beopoulos, A., & Nicaud, J. M. (2013). Efficient homologous recombination with short length flanking fragments in Ku70 deficient *Yarrowia lipolytica* strains. *Biotechnology letters, 35*(4), 571-576. doi:10.1007/s10529-012-1107-0

Vernis, L., Abbas, A., Chasles, M., Gaillardin, C. M., Brun, C., Huberman, J. A., & Fournier, P. (1997). An origin of replication and a centromere are both needed to establish a replicative plasmid in the yeast *Yarrowia lipolytica*. *Mol Cell Biol, 17*(4), 1995-2004. doi:10.1128/mcb.17.4.1995

Villarroel Hipp, M. P., & Silva Rodríguez, D. (2018). Bioremediation of piggery slaughterhouse wastewater using the marine protist, *Thraustochytrium kinney* VAL-B1. *Journal of Advanced Research, 12*, 21-26. doi:10.1016/j.jare.2018.01.010

Wan, X., Peng, Y.-F., Zhou, X.-R., Gong, Y.-M., Huang, F.-H., & Moncalián, G. (2016). Effect of cerulenin on fatty acid composition and gene expression pattern of DHA-producing strain *Colwellia psychrerythraea* strain 34H. *Microbial cell factories, 15*(1), 30. doi:10.1186/s12934-016-0431-9

Wang, K., Shi, T.-Q., Lin, L., Wei, P., Ledesma-Amaro, R., & Ji, X.-J. (2022). Engineering *Yarrowia lipolytica* to Produce Tailored Chain-Length Fatty Acids and Their Derivatives. *ACS synthetic biology, 11*(8), 2564-2577. doi:10.1021/acssynbio.2c00305

Wasylenko, T. M., Ahn, W. S., & Stephanopoulos, G. (2015). The oxidative pentose phosphate pathway is the primary source of NADPH for lipid overproduction from glucose in Yarrowia lipolytica. *Metabolic Engineering, 30*, 27-39. doi:10.1016/j.ymben.2015.02.007

Watanabe, K., Yazawa, K., Kondo, K., & Kawaguchi, A. (1997). Fatty Acid Synthesis of an Eicosapentaenoic Acid-Producing Bacterium: De Novo Synthesis, Chain Elongation, and Desaturation Systems. *The Journal of Biochemistry, 122*(2), 467-473. doi:10.1093/oxfordjournals.jbchem.a021775

Webster, N., Jin, J. R., Green, S., Hollis, M., & Chambon, P. (1988). The yeast UASG is a transcriptional enhancer in human hela cells in the presence of the GAL4 trans-activator. *Cell, 52*(2), 169-178. doi:https://doi.org/10.1016/0092-8674(88)90505-3

Weingarten-Gabbay, S., & Segal, E. (2014). The grammar of transcriptional regulation. *Human Genetics, 133*(6), 701-711. doi:10.1007/s00439-013-1413-1

Wickerham, L. J. (1946). A Critical Evaluation of the Nitrogen Assimilation Tests Commonly Used in the Classification of Yeasts. *J Bacteriol, 52*(3), 293-301.

Widlund, P. O., & Davis, T. N. (2005). A high-efficiency method to replace essential genes with mutant alleles in yeast. *Yeast, 22*(10), 769-774. doi:10.1002/yea.1244

Wierzchowska, K., Zieniuk, B., Nowak, D., & Fabiszewska, A. (2021). Phosphorus and Nitrogen Limitation as a Part of the Strategy to Stimulate Microbial Lipid Biosynthesis. *Applied Sciences, 11*(24), 11819. doi:10.3390/app112411819

Wijendran, V., & Hayes, K. C. (2004). Dietary n-6 and n-3 fatty acid balance and cardiovascular health. *Annual Review of Nutrition, 24*(1), 597-615. doi:10.1146/annurev.nutr.24.012003.132106

Wittmann, C., Weber, J., Betiku, E., Krömer, J., Bohm, D., & Rinas, U. (2007). Response of fluxome and metabolome to temperature-induced recombinant protein synthesis in *Escherichia coli*. *Journal of Biotechnology, 132*(4), 375-384. doi:10.1016/j.jbiotec.2007.07.495

Wong, L., Engel, J., Jin, E., Holdridge, B., & Xu, P. (2017a). YaliBricks, a versatile genetic toolkit for streamlined and rapid pathway engineering in *Yarrowia lipolytica*. *Metabolic Engineering Communications, 5*, 68-77. doi:10.1016/j.meteno.2017.09.001

Wong, L., Engel, J., Jin, E., Holdridge, B., & Xu, P. (2017b). YaliBricks, a versatile genetic toolkit for streamlined and rapid pathway engineering in Yarrowia lipolytica. *Metabolic engineering communications, 5*, 68-77. doi:10.1016/j.meteno.2017.09.001

Workman, M., Holt, P., & Thykaer, J. (2013). Comparing cellular performance of *Yarrowia lipolytica* during growth on glucose and glycerol in submerged cultivations. *AMB Express, 3*(1), 58. doi:10.1186/2191-0855-3-58

Xie, D., Jackson, E. N., & Zhu, Q. (2015). Sustainable source of omega-3 eicosapentaenoic acid from metabolically engineered *Yarrowia lipolytica*: from fundamental research to commercial production. *Applied Microbiology and Biotechnology, 99*(4), 1599-1610. doi:10.1007/s00253-014-6318-y

Xue, Z., Sharpe, P. L., Hong, S.-P., Yadav, N. S., Xie, D., Short, D. R., . . . Zhu, Q. (2013a). Production of omega-3 eicosapentaenoic acid by metabolic engineering of *Yarrowia lipolytica*. *Nature Biotechnology, 31*(8), 734-740. doi:10.1038/nbt.2622

Xue, Z., Sharpe, P. L., Hong, S. P., Yadav, N. S., Xie, D., Short, D. R., . . . Zhu, Q. (2013b). Production of omega-3 eicosapentaenoic acid by metabolic engineering of *Yarrowia lipolytica*. *Nature Biotechnology, 31*(8), 734-740. doi:10.1038/nbt.2622

Yarrow, D. (1972). Four new combinations in yeasts. *Antonie van Leeuwenhoek, 38*(1), 357-360. doi:10.1007/BF02328105

Ye, C., Qiao, W., Yu, X., Ji, X., Huang, H., Collier, J. L., & Liu, L. (2015). Reconstruction and analysis of the genome-scale metabolic model of schizochytrium limacinum SR21 for docosahexaenoic acid production. *BMC Genomics, 16*, 799. doi:10.1186/s12864-015-2042-y

Ye, J., Coulouris, G., Zaretskaya, I., Cutcutache, I., Rozen, S., & Madden, T. L. (2012). Primer-BLAST: A tool to design target-specific primers for polymerase chain reaction. *BMC Bioinformatics, 13*(1), 134. doi:10.1186/1471-2105-13-134

Yeung, E., Dy, A. J., Martin, K. B., Ng, A. H., Del Vecchio, D., Beck, J. L., . . . Murray, R. M. (2017). Biophysical Constraints Arising from Compositional Context in Synthetic Gene Networks. *Cell Syst, 5*(1), 11-24 e12. doi:10.1016/j.cels.2017.06.001

Yuzbasheva, E. Y., Mostova, E. B., Andreeva, N. I., Yuzbashev, T. V., Fedorov, A. S., Konova, I. A., & Sineoky, S. P. (2018). A metabolic engineering strategy for producing free fatty acids by the *Yarrowia lipolytica* yeast based on impairment of glycerol metabolism. *Biotechnology and Bioengineering, 115*(2), 433-443. doi:10.1002/bit.26402

Zárate, R., el Jaber-Vazdekis, N., Tejera, N., Pérez, J. A., & Rodríguez, C. (2017). Significance of long chain polyunsaturated fatty acids in human health. *Clinical and Translational Medicine, 6*(1), 25. doi:10.1186/s40169-017-0153-6

Zhang, J., & Burgess, J. G. (2017). Enhanced eicosapentaenoic acid production by a new deep-sea marine bacterium *Shewanella electrodiphila* MAR441T. *PloS One, 12*(11), e0188081. doi:10.1371/journal.pone.0188081

Zhou, Q., Jiao, L., Li, W., Hu, Z., Li, Y., Zhang, H., . . . Yan, Y. (2021). A Novel Cre/lox-Based Genetic Tool for Repeated, Targeted and Markerless Gene Integration in *Yarrowia lipolytica*. *Int J Mol Sci, 22*(19). doi:10.3390/ijms221910739